

# Tensor network approximation of Koopman operators

Dimitrios Giannakis<sup>a</sup>, Mohammad Javad Latifi Jebelli<sup>a</sup>, Michael Montgomery<sup>a</sup>, Philipp Pfeffer<sup>b</sup>, Jörg Schumacher<sup>b,c</sup>, Joanna Slawinska<sup>a</sup>

<sup>a</sup>*Department of Mathematics, Dartmouth College, 29 N. Main St., Hanover, 03755, New Hampshire, USA*

<sup>b</sup>*Department of Mechanical Engineering, TU Ilmenau, P.O. Box 100565, Ilmenau, D-98693, Germany*

<sup>c</sup>*Tandon School of Engineering, New York University, New York, 11201, New York, USA*

---

## Abstract

We propose a tensor network framework for approximating the evolution of observables of measure-preserving ergodic systems. Our approach is based on a spectrally-convergent approximation of the skew-adjoint Koopman generator by a diagonalizable, skew-adjoint operator  $W_\tau$  that acts on a reproducing kernel Hilbert space  $\mathcal{H}_\tau$  with coalgebra structure and Banach algebra structure under the pointwise product of functions. Leveraging this structure, we lift the unitary evolution operators  $e^{tW_\tau}$  (which can be thought of as regularized Koopman operators) to a unitary evolution group on the Fock space  $F(\mathcal{H}_\tau)$  generated by  $\mathcal{H}_\tau$  that acts multiplicatively with respect to the tensor product. Our scheme also employs a representation of classical observables ( $L^\infty$  functions of the state) by quantum observables (self-adjoint operators) acting on the Fock space, and a representation of probability densities in  $L^1$  by quantum states. Combining these constructions leads to an approximation of the Koopman evolution of observables that is representable as evaluation of a tree tensor network built on a tensor product subspace  $\mathcal{H}_\tau^{\otimes n} \subset F(\mathcal{H}_\tau)$  of arbitrarily high grading  $n \in \mathbb{N}$ . A key feature of this quantum-inspired approximation is that it captures information from a tensor product space of dimension  $(2d+1)^n$ , generated from a collection of  $2d+1$  eigenfunctions of  $W_\tau$ . Furthermore, the approximation is positivity preserving. The paper contains a theoretical convergence analysis of the method and numerical applications to two dynamical systems on the 2-torus: an ergodic torus rotation as an example with pure point Koopman spectrum and a Stepanoff flow as an example with topological weak mixing. The examples demonstrate improved consistency and prediction skill over conventional subspace projection methods, while also highlighting challenges stemming from numerical discretization of high-dimensional tensor product spaces.

*Keywords:*

Koopman operators, transfer operators, reproducing Kernel Hilbert spaces, coalgebras, Fock spaces, tensor networks, quantum mechanics

---

## 1. Introduction

In recent years, there has been considerable interest in the development of operator-theoretic techniques for computational analysis and modeling of dynamical systems. These methods leverage the linearity of the induced action of (nonlinear) state space dynamics on linear spaces of observables or measures, implemented through the Koopman and transfer operators, respectively, to carry out tasks such as mode decomposition, forecasting, uncertainty quantification, and control using linear-operator techniques. From an analytical standpoint, the operator-theoretic approach to dynamics dates back to classical work of Koopman and von Neumann from the 1930s [1, 2], and has since become central to modern ergodic theory [3, 4]. Starting from the late 1990s [5–7], there has been a surge of research in this area from the perspective of data-driven computational techniques. Popular examples include set-theoretic methods, [8], Fourier analytical methods [9], and subspace projection methods; see, e.g., [10–13] for comprehensive surveys.

Among subspace projection methods, the dynamic mode decomposition (DMD) [14–16] and the extended DMD (EDMD) [17] are some of the most popular approaches that build finite-rank approximations of

the Koopman operator on spaces spanned by dictionaries of linear and possibly nonlinear observables, respectively. These methods are related to linear inverse modeling techniques [18] introduced in the 1980s, and have since been modified and generalized in various ways; e.g., by combining them with delay-embedding approaches [19–21], methods for dictionary learning [22], and Laplace transform techniques [23]. Extensions of (E)DMD that impose physics-informed constraints such as unitarity of the Koopman/transfer operator under measure-preserving dynamics have also been developed [24, 25]. Other approaches have focused on approximating the generator of Koopman/transfer semigroups in continuous time [26–31], also known as the Liouville operator [32, 33].

While many data-driven methods perform approximation of Koopman operators in  $L^p$  spaces, some approaches have explored approximations in reproducing kernel Hilbert spaces (RKHSs) [34–37] or reproducing kernel Banach spaces [38], making connections with aspects of statistical learning theory. Yet another approach has been to build approximations of spectral measures [39–41], which allows approximation of functions of the operators via the functional calculus. In the setting of non-autonomous dynamics, there is a rich literature on techniques based on the theory of operator cocycles [42–44] and dynamic Laplace operators [45, 46] for detecting coherent sets under time-dependent dynamics.

*Connections with quantum information science.* Besides data-driven computational analysis and modeling, a more recent impetus for the development of operator methods for dynamical systems has been the prospect of practical quantum computing and the advances in information processing capabilities that it promises to deliver. Since the early 2000s [47–49], efforts have been underway for designing quantum algorithms for simulation of classical systems that have led to a growing body of methodological approaches [50–56], along with applications in diverse domains dealing with complex systems [57–67]. Here, a primary challenge is that classical dynamical systems are described by generally nonlinear maps (flows) on state space, whereas quantum algorithms proceed by unitary linear operators acting on quantum states and observables. Being firmly rooted in linear operator theory, the formulation of dynamics based on Koopman and transfer operators provides a natural bridge between classical and quantum systems that can serve as a foundation for building quantum algorithms. Efforts in this direction include [52, 56], which utilize different types of so-called Koopman–von Neumann embeddings to represent classical states and probability densities as quantum states evolving under the induced action of Koopman/transfer operators. Other works have developed “quantum-inspired” computational techniques [68–70] that employ properties of operator algebras to perform structure-preserving (e.g., positivity-preserving) approximations, implemented using classical numerical methods.

In a different context from dynamical systems, tensor networks [71, 72] were originally introduced for calculations in statistical mechanics and many-body quantum physics [73–75], and have since found applications in machine learning [76, 77] as a framework for expressing computations in high-dimensional vector spaces. Tensor networks describe factorizations of such computations in terms of basic algebraic operations such as operator compositions and tensor products which can be carried out at a feasible computational cost when brute-force approaches would have been intractable. Using tensor networks to express operator-theoretic computations for classical dynamical systems will be a primary focus of this work.

*Our contributions.* Leveraging mathematical connections between operator-theoretic formulations of classical dynamics and quantum theory, we introduce an approach for approximating the Koopman evolution of observables in continuous-time systems through tensor networks. Our approach begins by a spectrally consistent approximation of the generator of a unitary Koopman group by skew-adjoint, diagonalizable operators  $W_\tau$  with discrete spectra [30, 31, 35], acting on a one-parameter family of RKHSs  $\mathcal{H}_\tau$ ,  $\tau > 0$ . In this work, we build the spaces  $\mathcal{H}_\tau$  so as to have reproducing kernel Hilbert algebra (RKHA) structure [78–80]—this means that  $\mathcal{H}_\tau$  admits a bounded operator  $\Delta: \mathcal{H}_\tau \rightarrow \mathcal{H}_\tau \otimes \mathcal{H}_\tau$  mapping into its two-fold tensor product, whose adjoint implements pointwise multiplication. In other words,  $\mathcal{H}_\tau$  is a commutative Banach algebra with respect to pointwise multiplication that has additional coalgebra structure with  $\Delta$  as the comultiplication operator. We lift the unitary group generated by  $\mathcal{H}_\tau$  to a unitary group acting multiplicatively with respect to the tensor product on the Fock space,  $F(\mathcal{H}_\tau)$ , generated by  $\mathcal{H}_\tau$ . The Fock space  $F(\mathcal{H}_\tau)$  plays the role of the Hilbert space of a many-body quantum system [81] that allows us to represent (i) pointwise evaluation

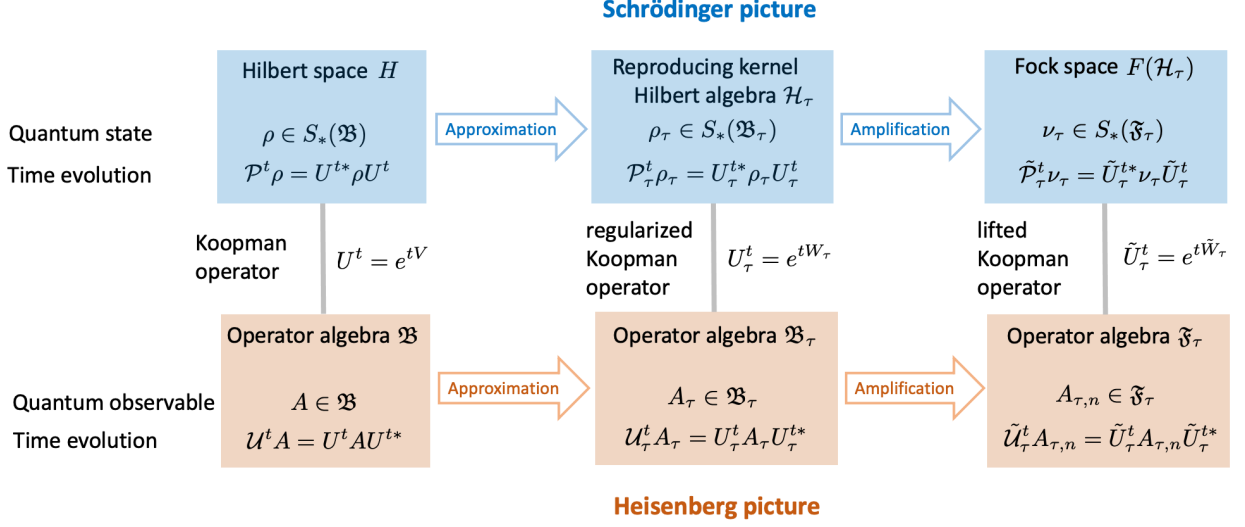


Figure 1: Evolution of quantum states (Schrödinger picture) and observables (Heisenberg picture) under the tensor network approximation framework described in this paper. Given a classical probability density  $p \in \mathfrak{S}_*(\mathfrak{A})$ , our scheme approximates the evolution of a vector state  $\rho = \langle p^{1/2}, \cdot \rangle_{\mathcal{H}} p^{1/2} \in S_*(\mathfrak{B})$  under the induced transfer operator  $\mathcal{P}^t$  by a vector state  $\rho_\tau = \langle \xi_\tau, \cdot \rangle_{\mathcal{H}_\tau} \xi_\tau$  on an RKHA  $\mathcal{H}_\tau$  under an evolution operator  $\mathcal{P}_\tau^t$  induced from a regularized Koopman operator  $U_\tau^t$  on  $\mathcal{H}_\tau$  with pure point spectrum. Similarly, the evolution of quantum observables  $A \in \mathfrak{B}$  under the induced Koopman operator  $U^t$  is approximated by a regularized operator  $U_\tau^t$  induced from  $U_\tau^t$  acting on smoothed quantum observables  $A_\tau = K_\tau A K_\tau^*$ , where  $K_\tau: H \rightarrow \mathcal{H}_\tau$  is a kernel integral operator associated with  $\mathcal{H}_\tau$ . Our scheme then dilates the regularized Koopman dynamics on  $\mathcal{H}_\tau$  to unitary dynamics  $\tilde{U}^t: F(\mathcal{H}_\tau) \rightarrow F(\mathcal{H}_\tau)$  on the Fock space generated by  $\mathcal{H}_\tau$ , such that  $\tilde{U}^t$  acts multiplicatively (tensorially) on the tensor algebra  $T(\mathcal{H}_\tau) \subset F(\mathcal{H}_\tau)$ . Furthermore, the quantum observables  $A_\tau$  are amplified using the coalgebra structure of  $\mathcal{H}_\tau$  to quantum observables  $A_{\tau,n}$  that act on any grading  $\mathcal{H}_\tau^{\otimes(n+1)} \subset F(\mathcal{H}_\tau)$ . The state vector  $\xi_\tau$  is also diluted to a vector  $\eta_\tau \in F(\mathcal{H}_\tau)$  that projects non-trivially on  $\mathcal{H}_\tau^{\otimes n}$  for every  $n \in \mathbb{N}$ , with an associated quantum state  $\nu_\tau = \langle \eta_\tau, \cdot \rangle_{F(\mathcal{H}_\tau)} \eta_\tau$ . The expectation of  $A_{\tau,n}$  with respect to the time-evolved quantum state  $\tilde{\rho}_\tau$  under the transfer operator  $\tilde{\mathcal{P}}_\tau^t$  induced by  $\tilde{U}_\tau^t$  is then used to approximate the corresponding evolution under the true dynamics on  $\mathfrak{B}$  using a tree tensor network construction (see Fig. 3).

functionals of  $\mathcal{H}_\tau$  as pure quantum states on  $F(\mathcal{H}_\tau)$  with state vectors that project non-trivially to every tensor power  $\mathcal{H}_\tau^{\otimes n} \subset F(\mathcal{H}_\tau)$ ,  $n \in \mathbb{N}$ ; (ii) classical observables in  $\mathcal{H}_\tau$  by quantum observables (self-adjoint operators) acting on any given grading  $\mathcal{H}_\tau^{\otimes n}$  as amplifications of multiplication operators. See Fig. 1 for a schematic illustration of these constructions.

Through this approach, we approximate the Koopman evolution of observables by a tree tensor network on  $F(\mathcal{H}_\tau)$  that can be implemented efficiently using functional programming techniques. Effectively, the tensor network approximates Koopman evolution on a  $(2d+1)^n$ -dimensional tensor product subspace of  $\mathcal{H}_\tau^{\otimes n}$  generated by a collection of  $d$  complex-conjugate pairs of eigenfunctions of  $W_\tau$  together with a constant eigenfunction. This allows devoting resources to compute a modest number  $(2d+1)$  of eigenfunctions of  $W_\tau$ , and algebraically amplifying these eigenfunctions to capture information from a high-dimensional tensor product space (vs. brute-force computation of large dictionaries of Koopman eigenfunctions). Moreover, the tensor network scheme is positivity-preserving and is asymptotically consistent in a suitable joint limit of  $n \rightarrow \infty$  and  $\tau \rightarrow 0$ .

The plan of the paper is as follows. Section 2 contains background on operator methods for classical dynamics and their connection with quantum theory. This is followed by a high-level overview of our tensor network approximation approach in Section 3, along with relevant definitions and constructions of RKHAs in Section 4. In Section 5, we give a precise description of our approximation scheme and in Section 6 we study its convergence properties. Section 7 presents applications to two dynamical systems on the 2-torus: an ergodic rotation with pure point Koopman spectrum and a Stepanoff flow [82] with weak topological mixing (absence of non-constant continuous Koopman eigenfunctions). Concluding remarks and perspectives on

future work are included in Section 8. Appendix A contains technical details on numerical implementation and pseudocode.

## 2. Background on operator methods and quantum theory

### 2.1. Feature extraction and prediction by spectral decomposition of evolution operators

A common aspect of many operator methods is computation of spectral data. As a concrete example, consider a measure-preserving flow  $\Phi^t: X \rightarrow X$  on a state space  $X$  in continuous time  $t \in \mathbb{R}$ , with an invariant probability measure  $\mu$ . The time- $t$  Koopman operator,

$$U^t: L^p(\mu) \rightarrow L^p(\mu), \quad U^t f = f \circ \Phi^t,$$

acts as an isometric isomorphism of the  $L^p(\mu)$  spaces with  $p \in [1, \infty]$  and its spectrum  $\sigma(U^t)$  is a subset of the unit circle in the complex plane. Moreover, for  $p \in [1, \infty)$ ,  $\{U^t\}_{t \in \mathbb{R}}$  is strongly continuous on  $L^p(\mu)$  and, by the Hille-Yosida theorem, completely characterized by its generator. The latter, is a closed (typically unbounded) operator  $V: D(V) \rightarrow L^p(\mu)$  defined on a dense subspace  $D(V) \subseteq L^p(\mu)$  via the norm limit

$$Vf = \lim_{t \rightarrow 0} \frac{U^t f - f}{t}. \quad (1)$$

The generator reconstructs the Koopman operator at any time  $t \in \mathbb{R}$  through the functional calculus,  $U^t = e^{tV}$ . As a result, every eigenfunction  $h$  of  $U^t$  has periodic evolution with period  $2\pi/\omega$ , where  $\omega \in \mathbb{R}$  is an eigenfrequency satisfying  $U^t h = e^{i\omega t} h$ .

A collection  $\{h_1, \dots, h_N\}$  of such eigenfunctions with corresponding eigenfrequencies  $\omega_1, \dots, \omega_N$  defines, for an appropriate normalization, a feature map  $\vec{h}: X \rightarrow \mathbb{C}^N$  whose range is a subset of the  $N$ -dimensional torus  $\mathbb{T}^N \subset \mathbb{C}^N$ . This map intertwines  $\Phi^t$  with a rotation system  $R_\alpha^t: \mathbb{T}^N \rightarrow \mathbb{T}^N$ . That is, we have

$$\vec{h} \circ \Phi^t = R_\alpha^t \circ \vec{h}, \quad (2)$$

$\mu$ -a.e., where  $R_\alpha^t(x) = (x + \alpha t) \bmod 2\pi$  and  $\alpha = (\omega_1, \dots, \omega_N)$ . In other words,  $\vec{h}$  has the property of rectifying the evolution of state space dynamics to a rotation with constant frequency parameters  $\omega_j$  in feature space  $\mathbb{C}^N$ ; see, e.g., [83, Fig. 4] for an illustration. This dynamical rectification property likely contributes to the physical interpretability of features based on eigenfunctions or approximate eigenfunctions of Koopman and transfer operators found in application domains spanning molecular dynamics [84], fluid dynamics [85], climate dynamics [83], neuroscience [86, 87], and energy system science [88], among other fields. In addition, observables  $f \in L^p(\mu)$  that are well-represented by linear combination of Koopman eigenfunctions,  $f \approx \sum_{j=0}^J c_j h_j$  for some  $J \in \mathbb{N}$  and  $c_j \in \mathbb{C}$ , are amenable to prediction by leveraging the known evolution of the eigenfunctions,

$$U^t f \approx \sum_{j=0}^J c_j e^{i\omega_j t} h_j. \quad (3)$$

See, e.g., [29] for numerical examples and [89] for a recent study that explores connections between the Wiener filter for least-squares prediction and Koopman eigenfunctions. Eigenfunctions of the transfer operator  $P^t: L^p(\mu) \rightarrow L^p(\mu)$ , where  $P^t f = f \circ \Phi^{-t}$  under invertible dynamics, are similarly useful for feature extraction and for approximating the evolution of measures  $\nu$  with densities  $\frac{d\nu}{d\mu} \in L^p(\mu)$ .

### 2.2. Practical challenges

The useful properties of Koopman and transfer operator eigenfunctions for feature extraction and prediction tasks outlined above provides ample motivation for developing algorithms and devoting computational resources for their computation. Still, in practical applications there is a number of challenges that prevent a straightforward implementation of this program.

*Continuous spectrum.* At a fundamental level, Koopman operators associated with complex dynamics seldom possess sufficiently rich sets of eigenfunctions in function spaces such as  $L^p(\mu)$  which are typically targeted by data-driven algorithms. Indeed, by a fundamental result in ergodic theory (e.g., Mixing Theorem in [90, p. 39]), the measure-preserving flow  $\Phi^t$  is weak mixing if and only if the Koopman operator  $U^t$  on  $L^2(\mu)$  has a simple eigenvalue equal to 1, with  $\mu$ -a.e. constant corresponding eigenfunctions, and no other eigenvalues. It follows that for weak-mixing systems there are no non-trivial analogs of the feature map from (2) and the prediction model (3). Thinking, intuitively, of weak mixing as a hallmark of dynamical complexity in a measure-theoretic sense, it consequently follows that in many real-world applications one has to seek generalizations of schemes based on pure Koopman/transfer operator eigenfunctions.

In response, a major focus of recent methodologies for Koopman operator approximation has been to consistently approximate the spectral measures of the operators, which typically have both atomic and continuous components, by discrete spectral measures that are amenable to numerical approximation, e.g., [30, 31, 33, 35, 39, 41]. In broad terms, these methods yield versions of (2) and (3) that are based on eigenfunctions of regularized approximations of  $U^t$  (or the generator  $V$ ) that possess non-trivial eigenfunctions and converge spectrally to  $U^t$  in a suitable asymptotic limit. In the transfer operator literature, a popular approach has been to perform approximations in Banach spaces where the operator is quasi-compact [5, 91, 92], allowing one to extract eigenvalues isolated from the essential spectrum.

*Bias–variance tradeoff.* Even if the system possesses a sufficiently rich set of eigenfunctions to well-represent the observables of interest, expansions such as (3) may require a large number,  $J$ , of eigenfunctions  $h_j$  to achieve the desired approximation accuracy. In practical applications, these eigenfunctions are seldom known analytically, and have to be numerically approximated, usually via data-driven algorithms. Given fixed computational and data resources, the quality of these approximations invariably decreases with  $J$ , which means that the predictive skill of a model utilizing (3) may actually decrease as  $J$  increases. This is a manifestation of the usual bias–variance tradeoff in statistical learning (e.g., [93]) that involves balancing bias errors due to using finitely many terms in the eigenfunction expansion for  $U^t f$  (which become smaller as  $J$  increases) against sampling errors associated with data-driven approximation of these eigenfunctions (which become larger as  $J$  increases). Methods for improving the quality of computed eigenfunctions include smoothing by integral operators [83, 94], learning of well-conditioned approximation dictionaries [22, 27, 29], usage of delay-coordinate maps [19–21, 95], and residual computations to detect spurious eigenvalues [41].

### 2.3. Structure-preserving approximations

Koopman and transfer operators exhibit important structural properties inherited from the underlying dynamical flow, which distinguish them from general operator (semi)groups. In applications, it is desirable (and sometimes essential) that the regularized operators preserve as many of these properties as possible. Below, we list a few examples that will concern us in this paper:

1. *Unitarity under measure-preserving, invertible dynamics.* In both discrete and continuous time, the Koopman operator  $U: L^2(\mu) \rightarrow L^2(\mu)$ ,  $Uf = f \circ \Phi$  associated with a measure-preserving, invertible transformation  $\Phi: X \rightarrow X$  is unitary. In continuous time, the generator  $V$  of the Koopman group  $\{U^t\}_{t \in \mathbb{R}}$  on  $L^2(\mu)$ , is skew-adjoint,  $V^* = -V$ , by the Stone theorem on one-parameter unitary groups.

2. *Multiplicativity.* Being a composition operator, the Koopman operator is multiplicative on spaces of observables that are closed under pointwise multiplication. As a concrete example, the Koopman operator  $U$  on  $L^\infty(\mu)$  satisfies

$$U(fg) = (Uf)(Ug), \quad \forall f, g \in L^\infty(\mu). \quad (4)$$

In continuous time, a necessary and sufficient condition for a skew-adjoint operator  $V$  on  $L^2(\mu)$  to be the generator of a unitary Koopman group  $\{U^t\}_{t \in \mathbb{R}}$  is that it satisfies the Leibniz rule on a suitable subspace of its domain [96],

$$V(fg) = (Vf)g + f(Vg), \quad \forall f, g \in D(V) \cap L^\infty(\mu). \quad (5)$$

An important consequence of (4) and (5) is that the point spectrum of  $U^t$  is a multiplicative subgroup of the unit circle and the point spectrum of  $V$  is an additive subgroup of the imaginary line.

3. *Positivity preservation.* A related property to multiplicativity is that the Koopman operator is positivity-preserving. That is, for every  $f \in L^p(\mu)$  such that  $f \geq 0$   $\mu$ -a.e., we have  $Uf \geq 0$   $\mu$ -a.e. Analogous results hold for continuous-time systems as well as the transfer operator.

In continuous-time systems, unitarity-preserving approximation techniques include smoothing the generator [35] or its resolvent [30, 31] by Markovian kernel integral operators. For example, given a family of symmetric kernel functions  $k_\tau: X \times X \rightarrow \mathbb{R}_+$  of sufficient regularity, parameterized by  $\tau > 0$ , and a corresponding family of self-adjoint kernel integral operators  $\mathcal{K}_\tau: L^2(\mu) \rightarrow L^2(\mu)$ ,  $\mathcal{K}_\tau f = \int_X k_\tau(\cdot, x)f(x) d\mu(x)$ , we have that  $V_\tau := \mathcal{K}_\tau V \mathcal{K}_\tau$  is a compact operator [35]. This operator is automatically skew-adjoint, and thus generates a strongly continuous unitary evolution group  $\{U_\tau^t = e^{tV_\tau}\}_{t \in \mathbb{R}}$  on  $L^2(\mu)$ . For suitable kernel constructions, the unitaries  $U_\tau^t$  converge to  $U^t$  strongly as  $\tau \rightarrow 0$ , and the corresponding spectral measures also converge in a suitable sense. In discrete-time systems, recently developed variants of DMD [24, 25] also preserve unitarity of the Koopman operator under measure-preserving invertible dynamics.

To our knowledge, there are no DMD-type Koopman operator approximation methods that are positivity preserving (but see below for non-commutative formulations) while offering convergence guarantees. In essence, failure to preserve positivity stems from the fact that orthogonal projections of positive observables onto the DMD approximation subspace are not necessarily positive. Similarly, no practical methods are known to us that preserve the Leibniz rule for the generator in continuous-time systems. Very recently, multiplicative dynamic mode decomposition (MultDMD) was introduced as a method that preserves the multiplicative structure on the Koopman operator on spaces of finitely-sampled observables using constrained optimization methods [97]. In the setting of transfer operators, the Ulam method [98] is a commonly employed scheme that is automatically positivity preserving by virtue of employing characteristic functions as basis elements. However, convergence results for Ulam-type schemes (e.g., [92, 99–101]) are generally limited to specific classes of dynamical systems such as expanding interval maps, and involve spaces such as  $L^1(\mu)$  or anisotropic Banach spaces that do not have Hilbert space structure (the latter being highly useful in numerical applications).

#### 2.4. Operator methods from the perspective of quantum theory

The operator-theoretic formulation of ergodic theory has close mathematical connections with quantum theory. To illustrate this, it is useful to associate to a given dynamical system abelian and non-abelian algebras of observables that we will consider as being “classical” and “quantum” respectively.

In the context of the measure-preserving flow  $\Phi^t: X \rightarrow X$  from Section 2.1, a natural abelian algebra is the space  $\mathfrak{A} := L^\infty(\mu)$  of essentially bounded observables with respect to the invariant measure  $\mu$ . This space is a von-Neumann algebra [102] with respect to pointwise function multiplication and complex conjugation; that is, it is a unital  $C^*$ -algebra,

$$\|fg\|_{\mathfrak{A}} \leq \|f\|_{\mathfrak{A}} \|g\|_{\mathfrak{A}}, \quad \|f^*f\|_{\mathfrak{A}} = \|f\|_{\mathfrak{A}}^2,$$

with unit given by the constant function  $\mathbf{1}$  equal to 1  $\mu$ -a.e., and has a Banach space predual,  $\mathfrak{A}_* := L^1(\mu)$ . The state space of  $\mathfrak{A}$ , which we denote as  $S(\mathfrak{A})$ , is the set of (automatically continuous) positive, unital functionals, i.e., functionals  $\omega: \mathfrak{A} \rightarrow \mathbb{C}$  satisfying  $\omega \mathbf{1} = 1$  and  $\omega(f^*f) \geq 0$  for every  $f \in \mathfrak{A}$ . Every probability density  $p \in \mathfrak{A}_*$  induces a state  $\mathbb{E}_p \in S(\mathfrak{A})$  that acts by expectation,  $\mathbb{E}_p f = \int_X fp d\mu$ . Such states  $\mathbb{E}_p$  are called normal states, and we denote the set of probability densities  $p$  that induce them by  $S_*(\mathfrak{A}) \subset \mathfrak{A}_*$ . For any  $t \in \mathbb{R}$ , the Koopman operator acts as an isomorphism of  $\mathfrak{A}$ ; in particular,

$$U^t(fg) = (U^t f)(U^t g), \quad U^t(f^*) = (U^t f)^*, \quad \|U^t f\|_{\mathfrak{A}} = \|f\|_{\mathfrak{A}}.$$

Moreover, by duality with the transfer operators  $P^t: \mathfrak{A}_* \rightarrow \mathfrak{A}_*$ , we have

$$\mathbb{E}_p(U^t f) = \mathbb{E}_{P^t p} f, \quad \forall f \in \mathfrak{A}, \quad \forall p \in S_*(\mathfrak{A}). \quad (6)$$

Next, as a non-abelian algebra, we consider the space  $\mathfrak{B} := B(H)$  of bounded linear operators on  $H := L^2(\mu)$ , equipped with the operator norm. This space is a von Neumann algebra with respect to operator composition and adjunction,

$$\|AB\|_{\mathfrak{B}} \leq \|A\|_{\mathfrak{B}} \|B\|_{\mathfrak{B}}, \quad \|A^*A\|_{\mathfrak{B}} = \|A\|_{\mathfrak{B}}^2,$$

and has the space of trace class operators on  $H$ ,  $\mathfrak{B}_* := B_1(H)$ , as its predual. We define the state space  $S(\mathfrak{B})$  analogously to  $S(\mathfrak{A})$ . Every positive element  $\rho \in \mathfrak{B}_*$  of unit trace induces a normal state  $\mathbb{E}_\rho \in S_*(\mathfrak{B})$  such that  $\mathbb{E}_\rho A = \text{tr}(\rho A)$ . Such elements  $\rho$  are known as density operators, and can be viewed as analogs of the classical probability densities in  $S_*(\mathfrak{A})$ . We denote the set of density operators on  $H$  as  $S_*(\mathfrak{B}) \subset \mathfrak{B}_*$ . The group of unitary Koopman operators  $U^t H \rightarrow H$  acts on  $\mathfrak{B}$  through the adjoint representation,  $\mathcal{U}^t: \mathfrak{B} \rightarrow \mathfrak{B}$  where  $\mathcal{U}^t A = U^t A U^{t*}$ . This action is an isomorphism of the von Neumann algebra  $\mathfrak{B}$ ,

$$\mathcal{U}^t(AB) = (\mathcal{U}^t A)(\mathcal{U}^t B), \quad \mathcal{U}^t(A^*) = (\mathcal{U}^t A)^*, \quad \|\mathcal{U}^t A\|_{\mathfrak{B}} = \|A\|_{\mathfrak{B}}.$$

Defining  $\mathcal{P}^t: \mathfrak{B}_* \rightarrow \mathfrak{B}_*$ ,  $\mathcal{P}^t \rho = U^{t*} \rho U^t$ , as a non-abelian version of the transfer operator on  $\mathfrak{A}_*$ , we have  $\mathbb{E}_\rho(\mathcal{U}^t A) = \mathbb{E}_{\mathcal{P}^t \rho} A$  for every density operator  $\rho \in S_*(\mathfrak{B})$ . This duality relation is a non-abelian analog of (6). In quantum mechanics, the evolution of states under  $\mathcal{P}^t$  and the evolution of observables under  $\mathcal{U}^t$  are known as the Schrödinger and Heisenberg pictures, respectively. From a more abstract point of view, we can view a Koopman operator as an element of the automorphism group of a von Neumann algebra, here either  $\mathfrak{A}$  or  $\mathfrak{B}$ , with a natural embedding  $\text{Aut}(\mathfrak{A}) \hookrightarrow \text{Aut}(\mathfrak{B})$  given by the adjoint representation.

To establish a correspondence between the evolution of classical observables in  $\mathfrak{A}$  with the evolution of quantum observables in  $\mathfrak{B}$ , we introduce the multiplier representation  $\pi: \mathfrak{A} \rightarrow \mathfrak{B}$  that maps  $f \in \mathfrak{A}$  to the multiplication operator in  $\mathfrak{B}$  that multiplies by that element,

$$(\pi f)g = fg, \quad \forall g \in H.$$

We also introduce the map  $\Gamma: S_*(\mathfrak{A}) \rightarrow S_*(\mathfrak{B})$  such that

$$\Gamma(p) = \langle p^{1/2}, \cdot \rangle_H p^{1/2}. \quad (7)$$

Note that  $\Gamma(p)$  above is a rank-1 operator that projects along the unit vector  $p^{1/2} \in H$ ; this unit vector plays an analogous role to a quantum mechanical wavefunction and is an example of a Koopman–von Neumann wave [103]. The associated state  $\mathbb{E}_{\Gamma(p)} \in S(\mathfrak{B})$  is an example of a vector state.

With these definitions, one can verify the following classical–quantum compatibility relations:

$$\mathbb{E}_p(U^t f) = \mathbb{E}_{\mathcal{P}^t p} f = \mathbb{E}_{\Gamma(p)}(\mathcal{U}^t(\pi f)) = \mathbb{E}_{\mathcal{P}^t(\Gamma(p))}(\pi f), \quad \forall f \in \mathfrak{A}, \quad \forall p \in S_*(\mathfrak{B}). \quad (8)$$

The above, describes an embedding of the statistical evolution of classical observables in the algebra  $\mathfrak{A}$  into an evolution of quantum observables in the operator algebra  $\mathfrak{B}$  induced by the unitary Koopman operators on the Hilbert space  $H$ .

The mathematical connection between operator-theoretic methods for classical dynamics and quantum mechanics was already alluded to in Koopman’s 1931 paper [1] and has since been an actively studied topic, e.g., [103–107]. As noted in Section 1, in recent years development of these connections was further stimulated by the advent of quantum computing and the prospect of simulation of (nonlinear) classical dynamics using (linear, unitary) quantum algorithms [52, 56, 65].

Besides the specific context of quantum computing, recent work [68–70] has put forward the perspective that quantum-inspired algorithms may provide opportunities for structure-preserving approximations that are implemented using classical numerical methods. For example, [68, 69] developed a quantum mechanical formulation of Bayesian sequential data assimilation (filtering) that is automatically positivity preserving. In more detail, given a sequence  $\Pi_L: H \rightarrow H$  of finite-rank orthogonal projections converging, as  $L \rightarrow \infty$ , strongly to the identity, they approximate the dynamical evolution (8) by approximating the quantum observable  $\pi f$  and density operator  $\Gamma(p)$  by finite-rank compressions,

$$\pi_L f := \Pi_L(\pi f)\Pi_L, \quad \Gamma_L(p) := \frac{\Pi_L \Gamma(p) \Pi_L}{\text{tr}(\Pi_L \Gamma(p) \Pi_L)},$$

respectively. Note that  $\pi_L f$  is a positive operator whenever  $f$  is a positive element of  $\mathfrak{A}$ , whereas a “classical” approximation  $\pi_L f$  of  $f$  by Hilbert subspace projection may not be positive. The resulting evolution,  $\mathbb{E}_{\Gamma_L(p)}(\mathcal{U}^t(\pi_L f))$ , can be implemented using numerical linear algebra methods and converges to the true evolution  $\mathbb{E}_p(U^t f)$  as  $L \rightarrow \infty$ . In essence, embedding the classical evolution into a quantum one provides access to numerical approximation algorithms that are positivity preserving while enjoying the benefits of Hilbert space structure of the underlying space  $H$ .

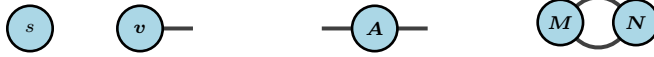


Figure 2: Simple examples of tensor networks. From left to right: A scalar,  $s$ ; a rank-1 tensor (vector),  $\mathbf{v}$ ; a rank-2 tensor (matrix),  $\mathbf{A}$ ; the contraction between two rank-2 tensors,  $\mathbf{M}$  and  $\mathbf{N}$ .

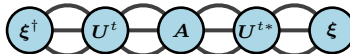
### 2.5. Tensor networks

Tensor networks provide a powerful diagrammatic framework for expressing computations involving multilinear maps on vector spaces, including operations on quantum mechanical states. In this subsection, we give a brief outline of the basic constructions that are relevant for the Koopman operator approximation scheme described in this paper. Further details can be found in one of the many surveys in the literature; e.g., [71, 72] and references therein.

The fundamental objects in a tensor network are multidimensional arrays of finite rank,  $\mathbf{A} = [A_{i_1 \dots i_r}]$ , where the indices  $i_1, \dots, i_r$  run over specified ranges,  $1 \leq i_1 \leq D_i$ . Note that the term “rank” here corresponds to the number of indices  $r$  of  $\mathbf{A}$  and not the rank of  $\mathbf{A}$  as a linear operator. Diagrammatically, a rank- $r$  tensor is represented by a node in a graph with  $r$  (optionally labeled) edges, sometimes referred to as “legs”. Scalars (rank-0 tensors) are depicted by nodes with no edges. See Fig. 2 for examples.

A tensor  $\mathbf{A}$  represents a multilinear map  $A: \mathbb{C}^{D_1} \times \dots \times \mathbb{C}^{D_r} \rightarrow \mathbb{C}$  in the standard bases of  $\mathbb{C}^{D_1}, \dots, \mathbb{C}^{D_r}$ . Given a collection of  $k \leq r$  vectors  $\mathbf{v}^{(1)}, \dots, \mathbf{v}^{(k)}$  with  $\mathbf{v}^{(j)} = [v_m^{(j)}] \in \mathbb{C}^{D_j}$ , we can form the multilinear map  $B = A(\mathbf{v}_1, \dots, \mathbf{v}_k, \cdot, \dots, \cdot): \mathbb{C}^{D_{k+1}} \times \dots \times \mathbb{C}^{D_r} \rightarrow \mathbb{C}$ . This map is represented by a rank  $r - k$  tensor  $\mathbf{B} = [B_{j_1 \dots j_{r-k}}]$  obtained by contraction (pairing) of the first  $k$  indices of  $\mathbf{A}$  with the indices of  $\mathbf{v}^{(1)}, \dots, \mathbf{v}^{(k)}$ , i.e.,  $B_{j_1 \dots j_{r-k}} = \sum_{i_1=1}^{D_1} \dots \sum_{i_k=1}^{D_k} A_{i_1 \dots i_k j_1 \dots j_{r-k}} v_{i_1}^{(1)} \dots v_{i_k}^{(k)}$ . Diagrammatically,  $\mathbf{B}$  is represented by joining the first  $k$  edges of  $\mathbf{A}$  with the edges of  $\mathbf{v}^{(1)}, \dots, \mathbf{v}^{(k)}$ . More general contractions involving different combinations of indices and/or contractions with rank  $> 1$  tensors are represented similarly. For example, joining the legs of two rank-2 tensors  $\mathbf{M}$  and  $\mathbf{N}$  yields the scalar  $\text{tr}(\mathbf{M}^\top \mathbf{N})$ . See again Fig. 2.

As noted in Section 1, a major application of tensor networks is representation of states of many-body quantum systems and operations on such states. Given  $n$  distinguishable quantum systems with associated Hilbert spaces  $\mathbb{H}_1, \dots, \mathbb{H}_n$  the composite ( $n$ -body) quantum system is defined on the tensor product Hilbert space  $\mathbb{H} := \mathbb{H}_1 \otimes \dots \otimes \mathbb{H}_n$ . When the Hilbert spaces  $\mathbb{H}_i$  have finite dimension, the state vector  $\xi$  associated with a density operator  $\rho = \langle \xi, \cdot \rangle_{\mathbb{H}} \xi$  on  $\mathbb{H}$  can be represented by a rank- $n$  tensor  $\xi$  storing the components of  $\xi$  in a tensor product basis of  $\mathbb{H}$ . Similarly, unitary evolution operators,  $U^t$ , and quantum observables,  $A$ , on  $\mathbb{H}$  can be represented by rank- $2n$  tensors,  $U^t$  and  $\mathbf{A}$ , respectively. Letting  $\xi^\dagger$  denote the elementwise complex conjugate of  $\xi$  and setting  $n = 3$  for illustration, the time-evolved quantum expectation  $\mathbb{E}_{\mathcal{P}^t \rho} A = \langle U^{t*} \xi, A U^t \xi \rangle_{\mathbb{H}}$  is implemented by the tensor network:



Note that this network utilizes rank- $n$  and rank- $(2n)$  tensors even though the density operator  $\rho$  has rank 1 as a linear operator.

While tensor networks can express arbitrary multilinear maps on tensor product Hilbert spaces, applications are typically based on architectures that exhibit different types of network locality, motivated by the local nature of interactions in physical systems of interest. Examples include matrix product states (MPSs), where the tensors are arranged in one-dimensional lattices, projected entangled pairs states (PEPs), which are higher-dimensional generalizations of MPSs, and tree tensor networks (TTN) which exhibit tree network topologies. See, e.g., [72, Figure 1] for illustrations. The class of tensor networks that we will build for Koopman operator approximation lie in the TTN family (see Fig. 3).

Based on notions from perturbative calculations in interacting quantum field theories, the dangling (open) legs in a tensor network can be thought of as representing physical degrees of freedom (particles), whereas the internal (contracted) legs are interpreted as virtual particles. Since one can insert a product  $\mathbf{A}\mathbf{A}^{-1}$  of an arbitrary invertible matrix  $\mathbf{A}$  and its inverse at any internal edge without changing the state represented



by the open edges, it follows that a given tensor network has infinitely many equivalent representations corresponding to different configurations of virtual particles. This form of “gauge freedom” has enabled the development of approaches for efficient evaluation and/or approximation of tensor networks. Examples include renormalization group techniques for coarsening MPSs and TTNs [108, 109].

### 3. Overview of tensor network approximation approach

Having surveyed the relevant notions from operator methods and quantum theory, in this section we give a high-level overview of our tensor network approximation framework for Koopman evolution of observables. This includes spectral approximation of the Koopman generator (Section 3.1), dilation of the regularized Koopman dynamics to a Fock space with an associated many-body quantum system (Sections 3.2 and 3.3), and finite-rank compression leading to a tensor network approximation of that quantum system (Section 3.4). In addition, we touch upon briefly on aspects of numerical implementation (Section 3.5). Throughout, we consider the case of measure-preserving, ergodic dynamics in continuous time, and use the same notation as in Section 2. Further mathematical and computational details will be taken up in Sections 4–6.

#### 3.1. Spectral approximation of the generator

We approximate the skew-adjoint generator  $V: D(V) \rightarrow H$  on  $H = L^2(\mu)$  by a family of skew-adjoint, diagonalizable operators  $W_\tau: D(W_\tau) \rightarrow \mathcal{H}_\tau$ ,  $\tau > 0$ , acting on RKHSs  $\mathcal{H}_\tau$  of complex-valued, continuous functions on the state space  $X$ . The operators  $W_\tau$  converge spectrally to  $V$  as  $\tau \rightarrow 0$  in a suitable sense. Moreover, the spaces  $\mathcal{H}_\tau$  are chosen so as to have so-called reproducing kernel Hilbert algebra (RKHA) structure [80]. As we elaborate in more detail in Section 4, this means that for any  $\tau > 0$ ,  $\mathcal{H}_\tau$  has a bounded multiplication operator  $\Delta: \mathcal{H}_\tau \rightarrow \mathcal{H}_\tau \otimes \mathcal{H}_\tau$  mapping into the tensor product with itself, and the adjoint  $\Delta^*: \mathcal{H}_\tau \otimes \mathcal{H}_\tau \rightarrow \mathcal{H}_\tau$  is a bounded operator implementing pointwise multiplication,  $\Delta^*(f \otimes g) = fg$ . As a result,  $\mathcal{H}_\tau$  has both RKHS and Banach algebra structure; the latter, with respect to pointwise multiplication. For each  $\tau > 0$ , the skew-adjoint operator  $W_\tau$  admits an eigendecomposition

$$W_\tau \zeta_{j,\tau} = i\omega_{j,\tau} \zeta_{j,\tau}, \quad j \in \mathbb{N}_0, \quad (9)$$

where  $\omega_{j,\tau}$  are real eigenfrequencies and the corresponding eigenfunctions  $\zeta_{j,\tau}$  form an orthonormal basis of  $\mathcal{H}_\tau$  restricted on the support of  $\mu$ . The eigenfrequencies satisfy  $\omega_{0,\tau} = 0$  and  $\omega_{2j,\tau} = -\omega_{2j-1,\tau}$  for  $j \in \mathbb{N}$ , and are ordered in increasing order of a Dirichlet energy associated with  $\mathcal{H}_\tau$ . Moreover, we have  $\zeta_{0,\tau} = \mathbf{1}$ , and the eigenvectors corresponding to nonzero eigenvalues form complex-conjugate pairs,  $\zeta_{2j,\tau}^* = -\zeta_{2j-1,\tau}$ . We denote the unitary evolution operators on  $\mathcal{H}_\tau$  generated by  $W_\tau$  as  $U_\tau^t := e^{tW_\tau}$ ,  $t \in \mathbb{R}$ .

#### 3.2. Dilation to Fock space

We consider the parameter  $\tau$  in the interval  $(0, 1]$  and build the spaces  $\mathcal{H}_\tau$  as a nested family so that  $\mathcal{H}_1 = \bigcap_{\tau \in (0,1]} \mathcal{H}_\tau$ . Let  $\iota: \mathcal{H}_1 \rightarrow L^r(\mu)$ ,  $r \in [1, \infty]$ , be the corresponding restriction map into any of the  $L^r$  spaces associated with the invariant measure. By our choice of reproducing kernels for  $\mathcal{H}_\tau$ ,  $\iota\mathcal{H}_1$  lies dense in  $L^r(\mu)$  for all  $r \in [1, \infty)$ . In particular, with  $\mathfrak{A} = L^\infty(\mu)$  as in Section 2.4, and assuming that  $\mu$  has compact support, for any probability density  $q \in S_*(\mathfrak{A})$  and tolerance  $\epsilon > 0$ , there exists a strictly positive function  $\varrho \in \mathcal{H}_1$  such that (i)  $p = \iota\varrho$  is a probability density in  $S_*(\mathfrak{A})$ ;  $\varrho$  is bounded away from zero on the support of  $\mu$ ; and (iii) for every  $t \in \mathbb{R}$  and  $f \in \mathfrak{A}$ ,  $|\mathbb{E}_p(U^t f) - \mathbb{E}_q(U^t f)| < \epsilon \|f\|_{\mathfrak{A}}$ . Our approach builds an approximation of the statistical evolution  $f^{(t)} := \mathbb{E}_p(U^t f)$  as a TTN on a Fock space generated by  $\mathcal{H}_\tau$  with a dynamical evolution induced from  $U_\tau^t$ .

First, using standard constructions from many-body quantum theory [81], we build the Fock space  $F(\mathcal{H}_\tau)$  as a Hilbert space closure of the tensor algebra  $T(\mathcal{H}_\tau)$ , i.e.,

$$F(\mathcal{H}_\tau) = \overline{T(\mathcal{H}_\tau)} \quad \text{with} \quad T(\mathcal{H}_\tau) := \mathbb{C} \oplus \mathcal{H}_\tau \oplus (\mathcal{H}_\tau \otimes \mathcal{H}_\tau) \oplus (\mathcal{H}_\tau \otimes \mathcal{H}_\tau \otimes \mathcal{H}_\tau) \oplus \dots$$

Intuitively, elements of an orthonormal basis of  $\mathcal{H}_\tau \subset F(\mathcal{H}_\tau)$  represent quantum states associated with individual “particles” of different types, and the elements of the corresponding tensor product basis of

$F(\mathcal{H}_\tau)$  represent states of potentially multiple such particles (with the particle number corresponding to the grading  $n \in \mathbb{N}$  of  $\mathcal{H}_\tau^{\otimes n} \subset F(\mathcal{H}_\tau)$ ). Meanwhile, the unit complex number  $1_{\mathbb{C}} \subset F(\mathcal{H}_\tau)$  represents the ‘‘vacuum’’ state with no particles.

By virtue of the RKHA structure of  $\mathcal{H}_\tau$ , the function  $\varrho$  introduced above has a well-defined square root  $\xi = \varrho^{1/2} \in \mathcal{H}_\tau$  for all  $\tau \in (0, 1]$ , and the  $n$ -th roots  $\xi^{1/n} \in \mathcal{H}_\tau$  are also well-defined for every  $n \in \mathbb{N}$ . We use the roots  $\xi^{1/n}$  to dilate  $\varrho$  to a unit vector  $\eta_\tau$  in the Fock space  $F(\mathcal{H}_\tau)$  generated by  $\mathcal{H}_\tau$ . In particular, the component of  $\eta_\tau$  in the  $n$ -th grading  $\mathcal{H}_\tau^{\otimes n} \subset F(\mathcal{H}_\tau)$  of the Fock space is equal to

$$\eta_{\tau,n} := w_n \frac{\xi^{1/n} \otimes \dots \otimes \xi^{1/n}}{\|\xi^{1/n}\|_{\mathcal{H}_\tau}^n}, \quad (10)$$

where  $w_n$  is a strictly positive weight. Intuitively,  $\eta_{\tau,n}$  distributes a localized density function,  $\varrho$ , into an  $n$ -fold tensor product of coarser functions,  $\xi^{1/n}$ .

Next, we lift the unitary evolution operators  $U_\tau^t: \mathcal{H}_\tau \rightarrow \mathcal{H}_\tau$  to unitaries  $\tilde{U}_\tau^t: F(\mathcal{H}_\tau) \rightarrow F(\mathcal{H}_\tau)$  that act multiplicatively on the tensor algebra  $T(\mathcal{H}_\tau)$ ,

$$\tilde{U}_\tau^t 1_{\mathbb{C}} = 1_{\mathbb{C}}, \quad \tilde{U}_\tau^t (g_1 \otimes \dots \otimes g_n) = (U_\tau^t g_1) \otimes \dots \otimes (U_\tau^t g_n), \quad (11)$$

where  $1_{\mathbb{C}}$  is the unit vacuum vector in  $F(\mathcal{H}_\tau)$  and  $g_1, \dots, g_n$  are vectors in  $\mathcal{H}_\tau$ . Note that by (9) the point spectrum of  $U_\tau^t$ , denoted by  $\sigma_p(U_\tau^t)$ , is a countable subset of the unit circle, but since, in general, the regularized generator  $W_\tau$  does not satisfy the Leibniz rule (cf. (5)),  $\sigma_p(U_\tau^t)$  does not have group structure. On the other hand, by multiplicativity of  $\tilde{U}_\tau^t$ , the point spectrum  $\sigma_p(\tilde{U}_\tau^t)$  is a multiplicative subgroup of  $S^1$  (generated by  $\sigma_p(U_\tau^t)$ ). Specifically,  $\tilde{U}_\tau^t$  admits the eigendecomposition

$$\tilde{U}_\tau^t 1_{\mathbb{C}} = 1_{\mathbb{C}}, \quad \tilde{U}_\tau^t \zeta_{\vec{j},\tau} = e^{i\omega_{\vec{j},\tau} t} \zeta_{\vec{j},\tau}, \quad (12)$$

where  $\vec{j} = (j_1, \dots, j_N) \in \mathbb{N}_0^N$  is a multi-index of arbitrary length  $N \in \mathbb{N}$ ,  $\omega_{\vec{j},\tau} = \omega_{j_1,\tau} + \dots + \omega_{j_N,\tau}$  are eigenfrequencies, and the corresponding eigenvectors  $\zeta_{\vec{j},\tau} = \zeta_{j_1,\tau} \otimes \dots \otimes \zeta_{j_N,\tau}$  form an orthonormal basis of  $F(\mathcal{H}_\tau)$ .

In other words, the unitary evolution  $\tilde{U}_\tau^t$  captures frequency content from all integer linear combinations  $q_1 \omega_{1,\tau} + \dots + q_m \omega_{m,\tau}$  with  $q_1, \dots, q_m \in \mathbb{Z}$  of the eigenfrequencies of  $W_\tau$ . Intuitively, if  $W_\tau$  well-approximates  $V$  in the sense of the Leibniz rule (5), then  $\omega_{\vec{j},\tau}$  can be viewed as an approximate eigenfrequency of  $V$ , and the pointwise product  $\prod_{i=1}^N \zeta_{j_i,\tau} \in \mathcal{H}_\tau$  associated with eigenvector  $\zeta_{\vec{j},\tau}$  behaves as an approximate corresponding eigenfunction. Importantly, a finite collection of incommensurate eigenfrequencies  $\omega_{i,\tau}$  and their corresponding eigenfunctions  $\zeta_{i,\tau}$  can generate arbitrarily large families of such approximate Koopman eigenfrequencies and eigenfunctions.

*Remark 1.* Throughout this paper, our approach for dilating the vector  $\xi \in \mathcal{H}_\tau$  to the Fock space is based on the roots  $\xi^{1/n}$  in accordance with (10). It should be noted that many other choices are available besides this scheme. In particular, (10) can be replaced by

$$\eta_{\tau,n} = w_n \frac{\xi^{(1)} \otimes \dots \otimes \xi^{(n)}}{\|\xi^{(1)}\|_{\mathcal{H}_\tau} \dots \|\xi^{(n)}\|_{\mathcal{H}_\tau}}$$

for any collection of vectors  $\xi^{(i)} \in \mathcal{H}_\tau$  whose pointwise product  $\prod_{i=1}^n \xi^{(i)}$  is equal to  $\xi$ . We comment on possibilities of using such generalized dilation schemes in Section 8.

### 3.3. Quantum evolution

Let  $\mathfrak{B} = B(H)$  as in Section 2.4, and define the operator algebras  $\mathfrak{B}_\tau := B(\mathcal{H}_\tau)$  and  $\mathfrak{F}_\tau := B(F(\mathcal{H}_\tau))$  for  $\tau > 0$ . The unitary operators  $U_\tau^t$  induce evolution operators on quantum observables and states on the RKHA  $\mathcal{H}_{\tau_2}$ :  $\mathcal{U}_\tau^t: \mathfrak{B}_\tau \rightarrow \mathfrak{B}_\tau$  and  $\mathcal{P}_\tau^t: \mathfrak{B}_{\tau^*} \rightarrow \mathfrak{B}_{\tau^*}$ , respectively, where  $\mathcal{U}_\tau^t A = U_\tau^t A U_\tau^{t*}$  and  $\mathcal{P}_\tau^t \rho = U_\tau^{t*} \rho U_\tau^t$ . Similarly,  $\tilde{U}_\tau^t: F(\mathcal{H}_\tau) \rightarrow F(\mathcal{H}_\tau)$  induce quantum evolution operators on the Fock space,  $\tilde{\mathcal{U}}_\tau^t: \mathfrak{F}_\tau \rightarrow \mathfrak{F}_\tau$  and  $\tilde{\mathcal{P}}_\tau^t: \mathfrak{F}_{\tau^*} \rightarrow \mathfrak{F}_{\tau^*}$ , where

$$\tilde{\mathcal{U}}_\tau^t A = \tilde{U}_\tau^t A \tilde{U}_\tau^{t*}, \quad \tilde{\mathcal{P}}_\tau^t \rho = \tilde{U}_\tau^{t*} \rho \tilde{U}_\tau^t. \quad (13)$$

Note that all of the quantum evolutions  $\mathcal{U}_\tau^t$ ,  $\mathcal{P}_\tau^t$ ,  $\tilde{\mathcal{U}}_\tau^t$ , and  $\tilde{\mathcal{P}}_\tau^t$  are automatically multiplicative. In particular,  $\mathcal{U}_\tau^t$  and  $\mathcal{P}_\tau^t$  are multiplicative even though  $U_\tau^t$  is not.

The unit vector  $\eta_\tau$  from the preceding subsection induces a density operator  $\nu_\tau = \langle \eta_\tau, \cdot \rangle_{F(\mathcal{H}_\tau)} \eta_\tau$  on the Fock space and a corresponding vector state  $\mathbb{E}_{\nu_\tau} \in S_*(\mathfrak{F}_\tau)$ . With  $f \in \mathfrak{A}$  a real-valued classical observable and  $\pi f \in \mathfrak{B}$  the corresponding (self-adjoint) multiplication operator, we define, for each  $n \in \{2, 3, \dots\}$ , a self-adjoint quantum observable  $A_{f,\tau,n} \in \mathfrak{F}_\tau$  acting on the Fock space, where

$$A_{f,\tau,n} = \Delta_{n-1} M_{f,\tau} \Delta_{n-1}^*, \quad M_{f,\tau} = K_\tau M_f K_\tau^* \in \mathfrak{B}_\tau, \quad M = \pi f \in \mathbb{B}. \quad (14)$$

Here,  $\Delta_n: \mathcal{H}_\tau \rightarrow F(\mathcal{H}_\tau)$  is an amplification of the comultiplication  $\Delta$  mapping into the  $(n+1)$ -fold tensor product space  $\mathcal{H}_\tau^{\otimes(n+1)}$ . Moreover,  $K_\tau: H \rightarrow \mathcal{H}_\tau$  is an integral operator induced by the reproducing kernel of  $\mathcal{H}_\tau$ . Precise definitions of these operators will be given in Sections 4 and 5. For now, we note that well-definition of  $\Delta_n$  depends on coassociativity of  $\Delta$ . In addition, by standard RKHS results,  $K_\tau^*$  is equal to the inclusion map from functions in  $\mathcal{H}_\tau$  to their corresponding equivalence classes in  $H$ , and  $\text{ran } K_\tau^*$  is a subspace of  $\mathfrak{A}$ . Viewed as a map from  $\mathcal{H}_\tau$  into  $\mathfrak{A}$ ,  $K_\tau^*$  is multiplicative,  $K_\tau^*(fg) = (K_\tau^*f)(K_\tau^*g)$ . Intuitively, we think of  $M_{f,\tau}$  in (14) as a smoothed multiplication operator.

Let  $\xi_\tau = \xi/\|\xi\|_{\mathcal{H}_\tau}$  be the unit vector in  $\mathcal{H}_\tau$  along  $\xi$  and  $\sigma_\tau = \langle \xi_\tau, \cdot \rangle_{\mathcal{H}_\tau} \xi_\tau$  the corresponding density operator. By the spectral convergence of  $W_\tau$  to  $V$ , the quantum evolution  $f_\tau^{(t)} := \mathbb{E}_{\mathcal{P}_\tau^t(\sigma_\tau)} M_{f,\tau}$  consistently approximates the classical statistical evolution  $f^{(t)}$ , viz.  $\lim_{\tau \rightarrow 0} f_\tau^{(t)} = f^{(t)}$ . Alternatively, for any  $n \in \{2, 3, \dots\}$ ,  $f^{(t)}$  can be approximated by a normalized quantum expectation over the Fock space,

$$f_{\tau,n}^{(t)} = \frac{g_{\tau,n}^{(t)}}{C_{\tau,n}^{(t)}}, \quad g_{\tau,n}^{(t)} = \mathbb{E}_{\tilde{\mathcal{P}}_\tau^t \rho_\tau} A_{f,\tau,n}, \quad C_{\tau,n}^{(t)} = \mathbb{E}_{\tilde{\mathcal{P}}_\tau^t \rho_\tau} A_{\mathbf{1},\tau,n}, \quad (15)$$

where the normalization constant  $C_{\tau,n}^{(t)}$  does not depend on  $f$ .

The behavior of the quantum expectations  $\mathbb{E}_{\tilde{\mathcal{P}}_\tau^t \rho_\tau} A_{f,\tau,n}$  and  $\mathbb{E}_{\tilde{\mathcal{P}}_\tau^t \rho_\tau} A_{\mathbf{1},\tau,n}$  in (15) giving  $f_{\tau,n}^{(t)}$  through  $g_{\tau,n}^{(t)}$  and  $C_{\tau,n}^{(t)}$ , respectively, can be understood as follows.

- As mentioned above, the component of the vector  $\eta_\tau$  in the subspace  $\mathcal{H}_\tau^{\otimes n} \subset F(\mathcal{H}_\tau)$  is a scalar multiple of  $(\xi^{1/n})^{\otimes n}$ . Evolving the density operator  $\rho_\tau$  by  $\tilde{\mathcal{P}}_\tau^t$  evolves this vector to  $(U_\tau^{t*} \xi^{1/n})^{\otimes n}$ . This evolution captures frequency content from all  $n$ -fold integer linear combinations of the eigenfrequencies  $\omega_{i,\tau}$  (i.e., all frequencies  $\omega_{\vec{j},\tau}$  with  $\vec{j} \in \mathbb{N}_0^n$ ).

- With the above time evolution of the state, multiplicativity of  $K_\tau^*$ , and up to a proportionality constant that is eliminated upon division by  $C_{\tau,n}^{(t)}$ , the quantum expectation  $\mathbb{E}_{\tilde{\mathcal{P}}_\tau^t \rho_\tau} A_{f,\tau,n}$  reduces to

$$\langle \Delta_{n-1}^*(U_\tau^{t*} \xi^{1/n})^{\otimes n}, M_{f,\tau} \Delta_{n-1}^*(U_\tau^{t*} \xi^{1/n})^{\otimes n} \rangle_{F(\mathcal{H}_\tau)} \equiv \langle (K_\tau^* U_\tau^{t*} \xi^{1/n})^n, (\pi f)(K_\tau^* U_\tau^{t*} \xi^{1/n})^n \rangle_H. \quad (16)$$

In essence, this corresponds (again up to proportionality) to expectation of the multiplication operator  $\pi f \in \mathfrak{B}$  with respect to a vector state induced by the vector  $(K_\tau^* U_\tau^{t*} \xi^{1/n})^n \in \mathfrak{A} \subset H$ . This latter vector reassembles the dynamically evolved factors  $U_\tau^{t*} \xi^{1/n} \in \mathcal{H}_\tau$  from the tensor product  $(U_\tau^{t*} \xi^{1/n})^{\otimes n} \in \mathcal{H}_\tau$  into a pointwise product, while capturing higher-order frequency content from  $\omega_{\vec{j},\tau}$ .

- As  $\tau \rightarrow 0$ , the restriction of  $K_\tau^* U_\tau^{t*}$  on  $\mathcal{H}_1$  converges strongly to  $U^t \iota$ ; see Lemma 6. As a result, since  $U^{t*} = U^{-t}$  is multiplicative, we have

$$\lim_{\tau \rightarrow 0} \langle (K_\tau^* U_\tau^{t*} \xi^{1/n})^n, (\pi f)(K_\tau^* U_\tau^{t*} \xi^{1/n})^n \rangle_H = \langle (U^{t*} \iota \xi^{1/n})^n, (\pi f)(U^{t*} \iota \xi^{1/n})^n \rangle_H = \langle U^{t*} \iota \xi, (\pi f) U^{t*} \iota \xi \rangle_H = f^{(t)}.$$

A similar calculation shows that  $\lim_{\tau \rightarrow 0^+} C_{\tau,n}^{(t)} = 1$ , so the Fock-space-based approximation  $f_{\tau,n}^{(t)}$  from (15) recovers  $f^{(t)}$  as  $\tau \rightarrow 0$  for any  $n \in \mathbb{N}$ . A precise statement of this result is given in Proposition 9.

### 3.4. Finite-rank compression

For  $d \in \mathbb{N}$ , let  $\mathcal{Z}_{\tau,d}$  be the  $(2d+1)$ -dimensional subspace of  $\mathcal{H}_\tau$  spanned by  $\zeta_{0,\tau}, \dots, \zeta_{2d,\tau}$ , and  $F(\mathcal{Z}_{\tau,d}) \subset F(\mathcal{H}_\tau)$  the Fock space generated by  $\mathcal{Z}_{\tau,d}$ . Note that  $\mathcal{Z}_{\tau,d}$  is spanned by the constant function  $\zeta_{0,\tau} = \mathbf{1}$  (the unit of  $\mathcal{H}_\tau$ ) and, for  $1 \leq j \leq d$ , complex-conjugate pairs of eigenfunctions  $\{\zeta_{2j,\tau}, \zeta_{2j-1,\tau}\}$  with corresponding eigenfrequencies  $\omega_{2j,\tau} = -\omega_{2j-1,\tau}$ . Moreover, the image of  $\mathcal{Z}_{\tau,d}^{\otimes n} \subset F(\mathcal{Z}_{\tau,d})$  is spanned by polynomials in  $\zeta_{0,\tau}, \dots, \zeta_{2d,\tau}$  of degree up to  $n$ .

We approximate the observable evolution  $f_{\tau,n}^{(t)}$  from (15) by projecting the state vector  $\eta_\tau$  onto the finitely generated Fock space  $F(\mathcal{Z}_{\tau,d})$ . Our approach results in approximations of  $g_{\tau,n}^{(t)}$  and  $C_{\tau,n}^{(t)}$  that can be efficiently evaluated using TTNs, as follows.

Let  $Z_{\tau,d}: \mathcal{H}_\tau \rightarrow \mathcal{H}_\tau$  and  $\tilde{Z}_{\tau,d}: F(\mathcal{H}_\tau) \rightarrow F(\mathcal{H}_\tau)$  be the orthogonal projections with  $\text{ran } Z_{\tau,d} = \mathcal{Z}_{\tau,d}$  and  $\text{ran } \tilde{Z}_{\tau,d} = F(\mathcal{Z}_{\tau,d})$ , respectively. Defining the projected state vector  $\eta_{\tau,d} = \tilde{Z}_{\tau,d}\eta_\tau / \|\tilde{Z}_{\tau,d}\eta_\tau\|_{F(\mathcal{H}_\tau)}$ , we obtain a compressed density operator  $\nu_{\tau,d} := \langle \eta_{\tau,d}, \cdot \rangle_{F(\mathcal{H}_\tau)} \eta_{\tau,d}$  that will serve as our approximation of  $\nu_\tau$ . As  $d \rightarrow \infty$ , the density operators  $\nu_{\tau,d}$  converge to  $\nu_\tau$  in the trace norm of  $\mathfrak{F}_{\tau*}$ .

The density operators  $\nu_{\tau,d}$  lead to the following approximation of  $f_\tau^{(t)}$ :

$$f_{\tau,n,d}^{(t)} = \frac{g_{\tau,n,d}^{(t)}}{C_{\tau,n,d}^{(t)}}, \quad g_{\tau,n,d}^{(t)} = \mathbb{E}_{\tilde{\mathcal{P}}_\tau^t \nu_{\tau,d}} A_{f,\tau,n}, \quad C_{\tau,n,d}^{(t)} = \mathbb{E}_{\tilde{\mathcal{P}}_\tau^t \nu_{\tau,d}} A_{\mathbf{1},\tau,n}. \quad (17)$$

A key property of this approximation is that it reduces to computing expectations of finite-rank quantum observables. Indeed, noticing that  $\tilde{U}_\tau^t$  and  $\tilde{Z}_{\tau,d}$  commute, we have that  $g_{\tau,n,d}^{(t)}$  equals, up to an unimportant proportionality constant,

$$\begin{aligned} \langle \Delta_{n-1}^* \tilde{U}_\tau^{t*} \tilde{Z}_{\tau,d} \eta_\tau, M_{f,\tau} \Delta_{n-1}^* \tilde{U}_\tau^{t*} \tilde{Z}_{\tau,d} \eta_\tau \rangle_{F(\mathcal{H}_\tau)} &= \langle \Delta_{n-1}^* \tilde{Z}_{\tau,d} \tilde{U}_\tau^{t*} \eta_\tau, M_{f,\tau} \Delta_{n-1}^* \tilde{Z}_{\tau,d} U_\tau^{t*} \eta_\tau \rangle_{F(\mathcal{H}_\tau)} \\ &= \langle \tilde{U}_\tau^{t*} \eta_\tau, A_{f,\tau,n,d} \tilde{U}_\tau^{t*} \eta_\tau \rangle_{F(\mathcal{H}_\tau)}, \end{aligned}$$

where

$$A_{f,\tau,n,d} := \tilde{Z}_{\tau,d} A_{f,\tau,n} \tilde{Z}_{\tau,d} \in \mathfrak{F}_\tau \quad (18)$$

is a quantum observable on the Fock space that has finite rank. The latter, stems from the fact that the restriction of  $\tilde{Z}_{\tau,d}$  on  $\mathcal{H}_\tau^{\otimes n}$  is equal to  $Z_{\tau,d}^{\otimes n}$ ; in particular,  $\text{ran } \tilde{Z}_{\tau,d}|_{\mathcal{H}_\tau^{\otimes n}} = \mathcal{Z}_{\tau,d}^{\otimes n}$ , and thus  $\tilde{Z}_{\tau,d}|_{\mathcal{H}_\tau^{\otimes n}}$  has rank  $(2d+1)^n$ . Since  $\text{ran } \Delta_{n-1} \subset \mathcal{H}_\tau^{\otimes n}$ , it follows that  $\Delta_{n-1}^* \tilde{Z}_{\tau,d} = (\tilde{Z}_{\tau,d} \Delta_{n-1})^*$  is a finite-rank operator, and thus so is  $A_{f,\tau,n,d}$ .

By multiplicativity of  $\tilde{U}_\tau^t$ , we also have

$$\langle \Delta_{n-1}^* \tilde{U}_\tau^{t*} \tilde{Z}_{\tau,d} \eta_\tau, M_{f,\tau} \Delta_{n-1}^* \tilde{U}_\tau^{t*} \tilde{Z}_{\tau,d} \eta_\tau \rangle_{F(\mathcal{H}_\tau)} \propto \langle \Delta_{n-1}^* (U_\tau^{t*} \xi_{\tau,n,d})^{\otimes n}, M_{f,\tau} \Delta_{n-1}^* (U_\tau^{t*} \xi_{\tau,n,d})^{\otimes n} \rangle_{F(\mathcal{H}_\tau)} \quad (19a)$$

$$= \langle K_\tau^* (U_\tau^{t*} \xi_{\tau,n,d})^n, (\pi f) K_\tau^* (U_\tau^{t*} \xi_{\tau,n,d})^n \rangle_H, \quad (19b)$$

where  $\xi_{\tau,n,d} = Z_{\tau,d} \xi_\tau^{1/n} / \|Z_{\tau,d} \xi_\tau^{1/n}\|_{\mathcal{H}_\tau}$  and the proportionality constant in (19a) is again unimportant. Comparing (16) and (19b), we see that the approximation  $f_{\tau,n,d}^{(t)}$  essentially involves approximating the vector state on  $\mathfrak{B}$  induced by the pointwise product  $K_\tau^* (U_\tau^{t*} \xi_\tau^{1/n})^n$  by the pointwise product  $K_\tau^* (U_\tau^{t*} \xi_{\tau,n,d})^n$  involving the projected  $n$ -th root  $\xi_{\tau,n,d}$ . Note that  $K_\tau^* (U_\tau^{t*} \xi_{\tau,n,d})^n = (K_\tau^* U_\tau^{t*} \xi_{\tau,n,d})^n$  by multiplicativity of  $K_\tau^*$ .

Using the tensor product structure  $(U_\tau^{t*} \xi_{\tau,n,d})^{\otimes n}$  appearing in the right-hand side of (19a) and associativity of  $\Delta_{n-1}^*$ , we can express the computation of  $f_{\tau,n,d}^{(t)}$  through a tree tensor network where the operator  $\Delta^*$  is applied recursively to assemble the pointwise product  $U_\tau^{t*} \xi_{\tau,n,d}$  without requiring explicit formation of the  $(2d+1)^n$ -dimensional tensor product  $(U_\tau^{t*} \xi_{\tau,n,d})^{\otimes n}$ . See Fig. 3 for a diagrammatic illustration. This tensor network architecture forms the centerpiece of our Koopman operator approximation framework.

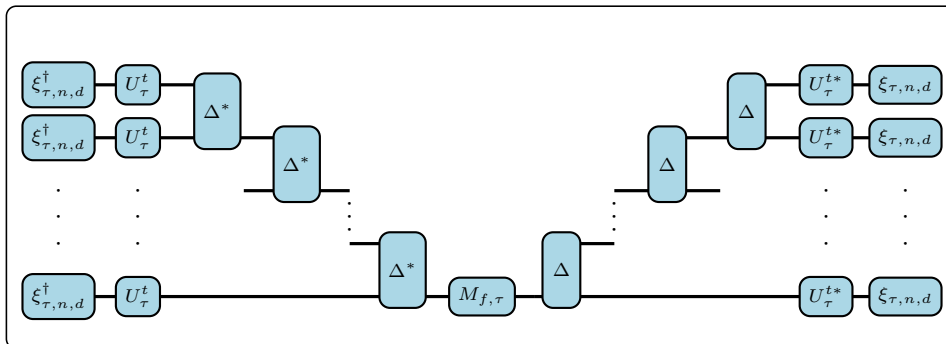


Figure 3: Tree tensor network used to compute the Fock space evolution  $f_{\tau,n,d}^{(t)}$  in (17).

*Two forms of approximation.* As noted above, for any fixed  $n \in \{2, 3, \dots\}$  the Fock space approximation  $f_{\tau,n,d}^{(t)}$  from (17) converges to  $f_\tau^{(t)}$  as  $d \rightarrow \infty$ . This convergence is an elementary consequence of the fact that the eigenfunctions  $\zeta_{j,\tau}$  form an orthonormal basis of  $\mathcal{H}_\tau$ —this means that the subspaces  $\mathcal{Z}_{\tau,d}$  increase to  $\mathcal{H}_\tau$ , and thus that the associated Fock spaces  $F(\mathcal{Z}_{\tau,d})$  increase to  $F(\mathcal{H}_\tau)$ , recovering the formula for  $f_\tau^{(t)}$  in (15) which holds for any  $n \in \{2, 3, \dots\}$ .

Besides approximations of this type, one of our primary interests in this work is on approximations performed at *fixed*  $d$  with *increasing*  $n \rightarrow \infty$ . In this scenario, the approximation space is a fixed, infinite-dimensional but strict subspace  $F(\mathcal{Z}_{\tau,d})$  of the full Fock space  $F(\mathcal{H}_\tau)$ , and within this subspace we compute expectations of the quantum observables  $A_{f,\tau,n,d}$  from (18). As  $n$  increases, these observables have increasingly high rank and access increasingly high gradings  $\mathcal{Z}_{\tau,d}^{\otimes n}$  of  $F(\mathcal{Z}_{\tau,d})$ . To the extent that  $W_\tau$  sufficiently well-approximates  $V$  for  $n$ -fold products of eigenfunctions  $\zeta_{0,\tau}, \dots, \zeta_{2d,\tau}$  to behave approximately as Koopman eigenfunctions (as would have been the case if  $W_\tau$  perfectly recovered  $V$  as a derivation obeying the Leibniz rule), increasing  $n$  at sufficiently large, but fixed,  $d$  can potentially reconstruct the full evolution  $f_\tau^{(t)}$ . As a simple example, if  $V$  is the generator of a circle rotation,  $\Phi^t(\theta) = \theta + \alpha t \pmod{2\pi}$ , the eigenfunctions of  $V$  are Fourier functions,  $\phi_j(\theta) = e^{ij\theta}$  with  $j \in \mathbb{Z}$ , so if  $\zeta_{\tau,0}, \zeta_{\tau,1}$ , and  $\zeta_{\tau,2}$  well-approximate  $\phi_0, \phi_1$ , and  $\phi_{-1}$ , respectively, fixing the Fock space  $F(\mathcal{Z}_{\tau,d})$  with  $d = 1$  and increasing  $n$  could potentially approximate  $f_\tau^{(t)}$  to arbitrarily high precision. In Theorem 12 below, we show that such a result indeed holds for  $d = 2$  in a joint limit of  $n \rightarrow \infty$  and  $\tau \rightarrow 0$ .

We have two major motivations to explore approximations of this latter type:

1. In practical applications, the eigenfrequencies  $\omega_{j,\tau}$  and corresponding eigenfunctions  $\zeta_{j,\tau}$  can seldom be computed exactly. Instead, one has to resort to numerical approximations obtained from some type of discretization of the eigenvalue problem for  $W_\tau$ . Obtaining high-fidelity approximations of large numbers  $d$  of eigenfunctions can be computationally costly, and in certain important cases (e.g., data-driven approximations using a fixed amount of available training data), altogether infeasible. An algebraic approach for building high-dimensional approximation spaces from a modest number,  $2d + 1$ , of basic functions (here, via tensor products) is a promising strategy for amplifying the utility of numerical Koopman spectral decompositions.

2. Working at fixed  $d$  as  $n$  increases allows one to leverage the tensor network construction in Fig. 3, and access approximation spaces  $\mathcal{Z}_{\tau,d}^{\otimes n}$  of exponentially high dimension,  $(2d + 1)^n$ , by composing operations on  $(2d + 1)$ -dimensional vectors.

### 3.5. Numerical implementation

Our numerical implementation begins by discretizing the eigenvalue problem for  $W_\tau$  in (9) in finite-dimensional subspaces  $\mathcal{H}_{\tau,m}$  of the RKHA  $\mathcal{H}_\tau$ ,

$$W_{\tau,m} \zeta_{j,\tau,m} = i\omega_{j,\tau,m} \zeta_{j,\tau,m}. \quad (20)$$

Here,  $W_{\tau,m}: \mathcal{H}_{\tau,m} \rightarrow \mathcal{H}_{\tau,m}$  is a skew-adjoint operator that approximates  $W_\tau$ ,  $\omega_{j,\tau,m} \in \mathbb{R}$  are its eigenfrequencies, and  $\zeta_{j,\tau,m}$  are corresponding eigenfunctions that form an orthonormal basis of  $\mathcal{H}_{\tau,m}$ . The specific choice of approximation spaces  $\mathcal{H}_{\tau,m}$  will depend on the application at hand, but in general we require that  $W_{\tau,m}$  converges spectrally to  $W_\tau$  as  $m \rightarrow \infty$ . Note that since  $\mathcal{H}_\tau$  is a space of functions (as opposed to equivalence classes of functions in  $L^p$  spaces), the approximate eigenfunctions  $\zeta_{j,\tau,m}$  are everywhere-defined functions that can be represented computationally as function objects (as opposed to arrays containing values of functions). Similarly, as we elaborate in Section 5.2 below,  $W_{\tau,m}$  can be implemented natively as an operator on functions using automatic differentiation of the reproducing kernel of  $\mathcal{H}_\tau$ .

With these approximations for  $W_\tau$  and its eigenvalues/eigenfunctions, the approximation scheme from Section 3.4 based on subspaces  $\mathcal{Z}_{\tau,d} \subset \mathcal{H}_\tau$  proceeds in a structurally similar manner, replacing  $\mathcal{Z}_{\tau,d}$  by  $\mathcal{Z}_{\tau,d,m} = \text{span}\{\zeta_{0,\tau,m}, \dots, \zeta_{2d,\tau,m}\} \subseteq \mathcal{H}_{\tau,m}$  and the unitaries  $U_\tau^t$  by  $U_{\tau,m}^t := e^{tW_{\tau,m}}$ . A detailed description of these schemes will be given in Section 5.2.

#### 4. Reproducing kernel Hilbert algebras

We briefly review the definition, properties, and constructions of RKHAs employed in this paper. A detailed analysis of these objects can be found in [80]. For expositions of RKHS theory, see [110, 111].

##### 4.1. Definitions and basic constructions

Let  $\mathcal{H}$  be an RKHS of complex-valued functions on a set  $X$  with reproducing kernel  $k: X \times X \rightarrow \mathbb{C}$  and inner product  $\langle \cdot, \cdot \rangle_{\mathcal{H}}$ . We use  $k_x := k(x, \cdot)$  to denote the kernel section at  $x \in X$  and  $\delta_x: \mathcal{H} \rightarrow \mathbb{C}$  to denote the corresponding pointwise evaluation functional,  $\delta_x f = f(x) = \langle k_x, f \rangle_{\mathcal{H}}$ . We also let  $\varphi: X \rightarrow \mathcal{H}$  denote the canonical feature map,  $\varphi(x) = k_x$ .

**Definition 2 (RKHA).** An RKHS  $\mathcal{H}$  on a set  $X$  is a *reproducing kernel Hilbert algebra (RKHA)* if  $k_x \mapsto k_x \otimes k_x$ ,  $x \in X$ , extends to a bounded linear map  $\Delta: \mathcal{H} \rightarrow \mathcal{H} \otimes \mathcal{H}$ .

Since

$$\langle k_x, \Delta^*(f \otimes g) \rangle_{\mathcal{H}} = \langle \Delta k_x, f \otimes g \rangle_{\mathcal{H}} = \langle k_x \otimes k_x, f \otimes g \rangle_{\mathcal{H} \otimes \mathcal{H}} = \langle k_x, f \rangle_{\mathcal{H}} \langle k_x, g \rangle_{\mathcal{H}} = f(x)g(x),$$

it follows that  $\Delta^*$  is a bounded linear map that implements pointwise multiplication. As a result,  $\mathcal{H}$  is simultaneously a Hilbert function space and commutative algebra with respect to pointwise function multiplication. Letting  $\pi: \mathcal{H} \rightarrow B(\mathcal{H})$  be the multiplier representation that maps  $f \in \mathcal{H}$  to the multiplication operator  $(\pi f): g \mapsto fg$ , one readily verifies that the operator norm,  $\|f\|_{\text{op}} := \|\pi f\|_{B(\mathcal{H})}$ , generates a coarser topology than the Hilbert space norm on  $\mathcal{H}$ , and satisfies

$$\|fg\|_{\text{op}} \leq \|f\|_{\text{op}} \|g\|_{\text{op}}.$$

Thus,  $\mathcal{H}$  has the structure of a Banach algebra with respect to pointwise function multiplication. When  $k$  is a real-valued kernel we may further equip  $\mathcal{H}$  with pointwise complex conjugation  $*$ :  $f \mapsto \bar{f}$  as an isometric involution, making it a Banach  $*$ -algebra. When the constant function  $\mathbf{1}: X \rightarrow \mathbb{C}$  with  $\mathbf{1}(x) = 1$  lies in  $\mathcal{H}$ , then  $\mathcal{H}$  is a unital algebra with unit  $\mathbf{1}$ . Furthermore, the Hilbert space norm and operator norms become equivalent since  $\|f\|_{\mathcal{H}} \leq \|\mathbf{1}\|_{\mathcal{H}} \cdot \|f\|_{\text{op}}$ , i.e.,

$$\frac{1}{\|\mathbf{1}\|_{\mathcal{H}}} \|f\|_{\mathcal{H}} \leq \|f\|_{\text{op}} \leq \|\Delta\|_{B(\mathcal{H})} \|f\|_{\mathcal{H}}.$$

In addition to having Banach algebra structure, an RKHA  $\mathcal{H}$  is a cocommutative, coassociative coalgebra with  $\Delta: \mathcal{H} \rightarrow \mathcal{H} \otimes \mathcal{H}$  as its comultiplication operator. In particular, coassociativity of  $\Delta$ , i.e.,  $(\Delta \otimes \text{Id}) \circ \Delta = (\text{Id} \otimes \Delta) \circ \Delta$ , is an important property that follows from associativity of multiplication (i.e.,  $\Delta^*$ ). This property allows us to amplify  $\Delta$  from  $\mathcal{H}$  to the tensor product spaces  $\mathcal{H}^{\otimes(n+1)}$ ,  $n \in \mathbb{N}$ , by defining  $\Delta_n: \mathcal{H} \rightarrow \mathcal{H}^{\otimes(n+1)}$  as

$$\Delta_1 = \Delta, \quad \Delta_n = (\Delta \otimes \text{Id}^{\otimes(n-1)}) \Delta_{n-1} \quad \text{for } n > 1.$$

Next, let  $\sigma(\mathcal{H})$  be the spectrum of an RKHA  $\mathcal{H}$  as Banach algebra, i.e., the set of (automatically continuous) multiplicative linear functionals  $\chi: \mathcal{H} \rightarrow \mathbb{C}$ ,

$$\chi(fg) = (\chi f)(\chi g), \quad \forall f, g \in \mathcal{H},$$

equipped with the weak-\* topology of  $\mathcal{H}^* \supset \sigma(\mathcal{H})$ . The pointwise evaluation functionals  $\delta_x = \langle \varphi(x), \cdot \rangle_{\mathcal{H}}$  are elements of the spectrum for every  $x \in X$ , inducing a map  $\hat{\varphi}: X \rightarrow \sigma(\mathcal{H})$  by  $\hat{\varphi}(x) = \delta_x$ . If the feature map  $\varphi$  is injective, then so is  $\hat{\varphi}$  and the spectrum  $\sigma(\mathcal{H})$  contains a copy of  $X$  as a subset.

In this work, our focus will be on unital RKHAs whose corresponding map  $\hat{\varphi}$  is a bijection. This property implies (e.g., [78, Corollary 7]) that the spectrum  $\sigma_{\mathcal{H}}(f)$  of each element  $f \in \mathcal{H}$  (i.e., the set of complex numbers  $z$  such that  $f - z$  does not have a multiplicative inverse in  $\mathcal{H}$ ) is equal to its range,  $\sigma_{\mathcal{H}}(f) = f(X)$ . This enables in turn the use of holomorphic functional calculus of functions in  $\mathcal{H}$ ,

$$a(f) = \frac{1}{2\pi i} \int_{\Gamma} \frac{a(z)}{z - f} dz,$$

where  $a: D \rightarrow \mathbb{C}$  is any holomorphic function on a domain  $D \subseteq \mathbb{C}$  that contains  $\sigma_{\mathcal{H}}(f)$  and  $\Gamma$  is an appropriate union of Jordan curves that encircle  $\sigma_{\mathcal{H}}(f)$ . In particular, for every  $\xi \in \mathcal{H}$  satisfying  $\xi(x) \geq \varepsilon > 0$  for all  $x \in X$ , the  $n$ -th root  $\xi^{1/n}$  lies in  $\mathcal{H}$  for every  $n \in \mathbb{N}$  by the holomorphic functional calculus. As alluded to in Section 3.2, the well-definition of such roots as elements of  $\mathcal{H}$  plays a key role in our tensor network approximation scheme.

#### 4.2. Examples of RKHAs

The main class of examples considered here are built on compact abelian groups,  $G$ . Let  $\hat{G}$  be the Pontryagin dual of  $G$ , and  $\mu, \hat{\mu}$  the Haar measures on  $G, \hat{G}$ , respectively. We use  $\mathcal{F}: L^1(G) \rightarrow C_0(\hat{G})$  and  $\hat{\mathcal{F}}: L^1(\hat{G}) \rightarrow C_0(G)$  to denote the Fourier transforms, and  $*$ :  $L^1(\hat{G}) \times L^1(\hat{G}) \rightarrow L^1(\hat{G})$  to denote convolution on the dual group:

$$(\mathcal{F}f)(\gamma) = \int_G f(x)\gamma(-x) d\mu(x), \quad (\hat{\mathcal{F}}\hat{f})(x) = \int_{\hat{G}} \hat{f}(\gamma)\gamma(x) d\hat{\mu}(\gamma), \quad (\hat{f} * \hat{g})(\gamma) = \int_{\hat{G}} \hat{f}(\gamma')g(\gamma - \gamma') d\hat{\mu}(\gamma').$$

Note that, by compactness of  $G$ , the dual group  $\hat{G}$  has a discrete topology and  $\hat{\mu}$  is a counting measure. See, e.g., [112] for further details on Fourier analysis on groups.

By Bochner's theorem, for every positive function  $\lambda \in L^1(\hat{G})$  the translation-invariant function  $k: G \times G \rightarrow \mathbb{C}$  defined as  $k(x, x') = (\hat{\mathcal{F}}\lambda)(x - x')$  is a continuous, positive-definite kernel with an associated RKHS  $\mathcal{H}$  of continuous functions. The space  $\mathcal{H}$  can be characterized in terms of a decay condition on Fourier coefficients,

$$\mathcal{H} = \left\{ f \in C(G) \mid \sum_{\gamma \in \hat{G}} \frac{|\mathcal{F}f(\gamma)|^2}{\lambda(\gamma)} < \infty \right\}.$$

Moreover, by Mercer's theorem, the reproducing kernel  $k$  can be expressed in terms of the uniformly convergent series

$$k(x, x') = \sum_{\gamma \in \hat{G}} \lambda(\gamma) \overline{\gamma(x)} \gamma(x'), \quad \forall x, x' \in G,$$

and  $\{\psi_{\gamma} := \sqrt{\lambda(\gamma)} \gamma\}_{\lambda(\gamma) \neq 0}$  is an orthonormal basis of  $\mathcal{H}$ . If  $\lambda$  is a strictly positive function, then  $\mathcal{H}$  is a dense subspace of  $C(G)$  (equivalently,  $k$  is a so-called universal kernel [113]) and the corresponding feature map  $\varphi: G \rightarrow \mathcal{H}$  is injective.

**Definition 3.** A strictly positive, summable function  $\lambda: \hat{G} \rightarrow \mathbb{R}_{>0}$  is said to be *subconvolutive* if there exists  $C > 0$  such that  $\lambda * \lambda \leq C\lambda$  pointwise on  $\hat{G}$ .

Subconvolutive functions have a rich history of study in the context of Beurling convolution algebras, e.g., [114–116]. In [80], the RKHS  $\mathcal{H}$  induced by a subconvolutive function  $\lambda$  is shown to be an RKHA and  $\Delta$  is easily diagonalizable by

$$\Delta\psi_\gamma = \sum_{\alpha+\beta=\gamma} \sqrt{\frac{\lambda(\alpha)\lambda(\beta)}{\lambda(\gamma)}} \psi_\alpha \otimes \psi_\beta, \quad \gamma \in \hat{G}.$$

Standard examples for  $G = \mathbb{T}^N$ ,  $\hat{G} \cong \mathbb{Z}^N$ , include the families of functions  $\{\lambda_\tau: \mathbb{Z}^N \rightarrow \mathbb{R}_{>0}\}_{\tau>0}$  with subexponential decay, where

$$\lambda_\tau(j) = \prod_{i=1}^N e^{-\tau|j_i|^p} \quad (21)$$

for fixed  $p \in (0, 1)$ . For each such  $p$ , we have a one-parameter family of unital RKHAs  $\mathcal{H}_\tau$  generated by a Markovian family of kernels  $k_\tau$ , i.e.,  $k_\tau \geq 0$  and

$$k_\tau(x, x') \geq 0, \quad \int_G k_\tau(x, \cdot) d\mu = 1, \quad \forall x, x' \in X; \quad (22)$$

see [78]. Moreover, in this setting the elements  $\gamma$  of the dual group  $\hat{G}$  are standard Fourier functions,  $\gamma_j(x) = e^{ij \cdot x}$  for some  $j \in \mathbb{Z}^N$  using the parameterization  $x \in [0, 2\pi)^N$  for the  $N$ -torus.

**Definition 4.** A function  $\lambda: \hat{G} \rightarrow \mathbb{R}_{>0}$  is said to satisfy the *Gelfand–Raikov–Shilov (GRS)* condition if

$$\lim_{n \rightarrow \infty} \lambda(n\gamma)^{1/n} = 1, \quad \forall \gamma \in \hat{G},$$

and the *Beurling–Domar (BD)* condition if

$$\sum_{n=1}^{\infty} \frac{\ln(\lambda^{-1}(n\gamma))}{n^2} < \infty, \quad \forall \gamma \in \hat{G}.$$

Functions in the subexponential family from (21) satisfy both the GRS and BD conditions, which has two implications for  $\mathcal{H}_\tau$ . First, the GRS condition implies that the associated map  $\hat{\varphi}_\tau: G \rightarrow \sigma(\mathcal{H}_\tau)$  is a homeomorphism [79, 80]. Second, as shown in [80], the BD condition implies that  $\mathcal{H}_\tau$  contains functions with arbitrary compact support. These two conditions play a vital role for the construction of RKHAs on generic compact Hausdorff spaces  $X \subseteq \mathbb{T}^N$  (e.g., attractors of dynamical systems). We may restrict to  $\mathcal{H}_\tau(X) := \text{span}\{k_{\tau,x} \mid x \in X\}$  which is also an RKHA with comultiplication  $\Delta|_{\mathcal{H}_\tau(X)}$ . More importantly, the spectrum of  $\mathcal{H}_\tau(X)$  as a Banach algebra is  $X$ , hence,  $\sigma_{\mathcal{H}_\tau(X)}(f) = f(X)$ . This enables the use of the holomorphic functional calculus of functions in  $\mathcal{H}_\tau(X)$  as outlined in Section 4.1.

## 5. Tensor network approximation method

In this section, we give a precise description of the tensor network approximation framework introduced in Section 3.

### 5.1. Dynamical system and function spaces

We consider a dynamical flow  $\Phi^t: G \rightarrow G$ ,  $t \in \mathbb{R}$ , on a compact Lie group  $G$  generated by a continuous vector field  $\vec{V}: G \rightarrow TG$ , and possessing a Borel, invariant, ergodic probability measure  $\mu$  with (compact) support  $X \subseteq G$ . Following the notation of Section 2, we let  $U^t: L^p(\mu) \rightarrow L^p(\mu)$  be the associated Koopman operators,  $U^t f = f \circ \Phi^t$ , defined for  $p \in [1, \infty]$  and  $t \in \mathbb{R}$ . We also let  $V: D(V) \rightarrow H$  be the skew-adjoint generator on  $H = L^2(\mu)$  defined as in (1). Note that  $V$  reduces to a directional derivative along  $\vec{V}$  when acting on continuously differentiable functions. That is, we have

$$Vf = \iota\vec{V} \cdot \nabla f, \quad \forall f \in C^1(G), \quad (23)$$



where  $\iota: C(G) \rightarrow L^p(\mu)$  denotes the restriction map from continuous functions to  $L^p$  spaces.

We assume that  $G$  is equipped with a one-parameter family of kernels  $k_\tau: G \times G \rightarrow \mathbb{R}_+$ ,  $\tau > 0$ , such that the corresponding RKHSs  $\mathcal{H}_\tau$  are unital RKHAs. In addition, we require that the kernels  $k_\tau$  have the following properties:

- (K1)  $k_\tau$  is continuous, and  $\mathcal{H}_\tau$  is a dense subspace of  $C(G)$ .
- (K2) For every invariant vector field  $\partial$  on  $G$ , the derivatives  $(\partial \times \partial)k_\tau$  exist and are continuous.
- (K3)  $k_\tau$  is Markovian with respect to  $\mu$ ; i.e., (22) holds.
- (K4) The integral operators  $\mathcal{K}_\tau: L^p(\mu) \rightarrow L^p(\mu)$ , where  $p \in [1, \infty)$  and  $\mathcal{K}_\tau f = \int_X k_\tau(\cdot, x)f(x) d\mu(x)$ , are bounded and have the semigroup property,  $\mathcal{K}_\tau \mathcal{K}_{\tau'} = \mathcal{K}_{\tau+\tau'}$ . Moreover,  $\mathcal{K}_\tau$  converges strongly to the identity on  $L^p(\mu)$  as  $\tau \rightarrow 0^+$ .

By standard RKHS results (e.g., [111, Chapter 4]),  $\mathcal{K}_\tau: H \rightarrow H$  is a strictly positive, self-adjoint, trace class operator. This operator admits the factorization  $\mathcal{K}_\tau = K_\tau^* K_\tau$ , where  $K_\tau: H \rightarrow \mathcal{H}_\tau$ ,  $K_\tau f = \int_X k_\tau(\cdot, x)f(x) d\mu(x)$ , is Hilbert–Schmidt, and  $K_\tau^*$  implements the restriction map from  $\mathcal{H}_\tau$  to  $H$ ,  $K_\tau^* = \iota|_{\mathcal{H}_\tau}$ . This latter map restricts to a compact embedding  $K_\tau^*: \mathcal{H}_\tau(X) \hookrightarrow H$  with dense image  $H_\tau := K_\tau^*(\mathcal{H}_\tau) \subseteq H$ . The pseudoinverse  $K_\tau^{*+}: H_\tau \rightarrow \mathcal{H}_\tau(X)$  is a (possibly unbounded) operator, known as the Nyström operator, that recovers the representative in  $\mathcal{H}_\tau(X)$  of an element  $f \in H_\tau$ ; i.e.  $K_\tau^* K_\tau^{*+} f = f$ . The Nyström operator induces a Dirichlet energy functional  $\mathcal{E}_\tau: H_\tau \rightarrow \mathbb{R}_+$ ,

$$\mathcal{E}_\tau(f) = \frac{\|K_\tau^{*+} f\|_{\mathcal{H}_\tau}^2}{\|f\|_H^2} - 1.$$

Intuitively,  $\mathcal{E}_\tau(f)$  measures an average notion of spatial variability of elements of  $H_\tau$ ; in particular,  $\mathcal{E}_\tau(f) = 0$  iff  $f$  is  $\mu$ -a.e. constant. We also have that  $\text{ran } K_\tau$  is a dense subspace of  $\mathcal{H}_\tau(X)$  and, by Property (K2),  $\text{ran } K_\tau^*$  lies in the domain  $D(V)$  of the generator.

The following are consequences of the semigroup property in (K4) [35]:

- (K5) The spaces  $\mathcal{H}_\tau$  form a nested family,  $\mathcal{H}_\tau \subseteq \mathcal{H}_{\tau'}$  for  $0 < \tau' < \tau$ .
- (K6)  $K_\tau$  admits the polar decomposition  $K_\tau = T_\tau \mathcal{K}_{\tau/2}$ , where  $T_\tau: H \rightarrow \mathcal{H}_\tau$  is an isometry with  $\text{ran } T_\tau = \mathcal{H}_\tau(X)$  and  $\text{ran } T_\tau^* = H$ .

Define now the space  $\mathcal{H}_\infty = \bigcap_{\tau>0} \mathcal{H}_\tau(X)$ . Another consequence of property (K4) is that the operators  $\mathcal{K}_\tau$  are simultaneously diagonalized in an orthonormal basis  $\{\phi_j\}_{j \in \mathbb{N}_0}$  of  $H$  with representatives  $\varphi_j \in \mathcal{H}_\infty$ , viz.

$$\mathcal{K}_\tau \phi_j = \Lambda_{j,\tau} \phi_j, \quad \phi_j = \iota \varphi_j, \quad \varphi_j = \frac{1}{\Lambda_{j,\tau}} K_\tau \phi_j, \quad (24)$$

where the eigenvalues  $\Lambda_{j,\tau}$  are strictly positive and satisfy  $\Lambda_{j,\tau} \Lambda_{j,\tau'} = \Lambda_{j,\tau+\tau'}$ . The representatives  $\varphi_j \in \mathcal{H}_\infty$  can be employed in a Mercer sum of the restriction of the kernel  $k_\tau$  on  $X \times X$ ,

$$k_\tau(x, x') = \sum_{j=0}^{\infty} \Lambda_{j,\tau} \overline{\varphi_j(x)} \varphi_j(y), \quad \forall x, x' \in X.$$

Moreover, the set  $\{\psi_{j,\tau}\}_{j \in \mathbb{N}_0}$  with

$$\psi_{j,\tau} = \frac{1}{\Lambda_{j,\tau/2}} K_\tau \phi_j = \Lambda_{j,\tau/2} \varphi_j \quad (25)$$

is an orthonormal basis of  $\mathcal{H}_\tau(X)$ .

For later convenience, we note that the Nyström representative  $K_\tau^{*+}$  of  $f = \sum_{j \in \mathbb{N}_0} c_j \phi_j \in H_\tau$  is given by

$$K_\tau^{*+} f = \sum_{j=0}^{\infty} \frac{c_j}{\Lambda_{j,\tau/2}} \psi_{j,\tau}.$$

This leads to the following formula for the Dirichlet energy,

$$\mathcal{E}_\tau(f) = \frac{\sum_{j=1}^{\infty} |c_j|^2 \Lambda_{j,\tau}^{-1}}{\sum_{j=0}^{\infty} |c_j|^2}. \quad (26)$$

Similarly, for  $f = \sum_{j \in \mathbb{N}_0} c_j \varphi_j \in \text{ran } K_\tau$ , the pseudoinverse  $K_\tau^+ f \in H$  can be computed as

$$K_\tau^+ f = \sum_{j=0}^{\infty} \frac{c_j}{\Lambda_{j,\tau}} \phi_j. \quad (27)$$

Defining  $\mathcal{H}_1 = \bigcap_{\tau \in (0,1]} \mathcal{H}_\tau$  as in Section 3.2, we see from (26) that  $\iota(\mathcal{H}_1)$  contains elements of  $H$  with uniformly bounded Dirichlet energies over  $\tau \in (0, 1]$ .

In the numerical experiments of Section 7 we have  $G = X = \mathbb{T}^2$ , and we build  $k_\tau$  from the subexponential families of weights in (21). In this case, the functions  $\varphi_j \in \mathcal{H}_\infty$  can be chosen as characters  $\gamma$  of the group (Fourier functions) as described in Section 4.2. Besides this setting, our scheme can be generalized to cases where the support  $X$  of the invariant measure is a strict subset of  $G$ , and/or cases where  $G$  is a forward-invariant subset of an ambient metric space  $\mathcal{M}$  in which the flow  $\Phi^t: \mathcal{M} \rightarrow \mathcal{M}$  takes place.

## 5.2. Spectral approximation

We will make use of the following notions of convergence of skew-adjoint operators; e.g., [117, 118].

**Definition 5.** Let  $A: D(A) \rightarrow \mathbb{H}$  be a skew-adjoint operator on a Hilbert space  $\mathbb{H}$  and  $A_\tau: D(A_\tau) \rightarrow \mathbb{H}$  a family of skew-adjoint operators indexed by  $\tau$ , with resolvents  $R_z(A) = (zI - A)^{-1}$  and  $R_z(A_\tau) = (zI - A_\tau)^{-1}$  respectively, for a complex number  $z$  in the resolvent sets of  $A$  and  $A_\tau$ .

1. The family  $A_\tau$  is said to converge in *strong resolvent sense* to  $A$  as  $\tau \rightarrow 0^+$  if for some (and thus, every)  $z \in \mathbb{C} \setminus i\mathbb{R}$  the resolvents  $R_z(A_\tau)$  converge strongly to  $R_z(A)$ ; that is,  $\lim_{\tau \rightarrow 0^+} R_z(A_\tau)f = R_z(A)f$  for every  $f \in \mathbb{H}$ .
2. The family  $A_\tau$  is said to converge in *strong dynamical sense* to  $A$  as  $\tau \rightarrow 0^+$  if for every  $t \in \mathbb{R}$ , the unitary operators  $e^{tA_\tau}$  converge strongly to  $e^{tA}$ ; that is,  $\lim_{\tau \rightarrow 0^+} e^{tA_\tau} f = e^{tA} f$  for every  $f \in \mathbb{H}$ .

It can be shown, e.g., [118, Proposition 10.1.8], that strong resolvent convergence and strong dynamical convergence are equivalent notions. For our purposes, this implies that if a family of skew-adjoint operators  $V_\tau$  on  $H$  converges to the Koopman generator  $V$  in strong resolvent sense, the unitary evolution groups  $e^{tV_\tau}$  generated by these operators consistently approximate the Koopman group  $U^t = e^{tV}$  generated by  $V$ . Strong resolvent convergence and strong dynamical convergence also imply a form of strong convergence of spectral measures, e.g., [35, Proposition 13].

With these definitions, the first step in our tensor network approximation scheme is to build a family of approximating operators  $V_\tau: D(V_\tau) \rightarrow H$  with the following properties:

- (V1)  $V_\tau$  is skew-adjoint.
- (V2)  $V_\tau$  is real, i.e.,  $\overline{V_\tau f} = V_\tau \bar{f}$  for all  $f \in D(V_\tau)$ .
- (V3)  $V_\tau$  is diagonalizable.
- (V4)  $V_\tau$  has a simple eigenvalue at 0 with  $\mathbf{1}$  as a corresponding eigenfunction.

(V5)  $D(V_\tau)$  includes  $\text{ran } \mathcal{K}_{\tau/2}$  as a subspace.

(V6) As  $\tau \rightarrow 0^+$ ,  $V_\tau$  converges in strong resolvent sense, and thus in strong dynamical sense, to  $V$ .

For any family of operators  $V_\tau$  satisfying properties (V1)–(V6), we define the skew-adjoint operators  $W_\tau: D(W_\tau) \rightarrow \mathcal{H}_\tau$  on the dense domains  $D(W_\tau) = T_\tau(D(V_\tau)) \oplus \mathcal{H}_\tau(X)^\perp$  as  $W_\tau = T_\tau V_\tau T_\tau^*$ . Note that the well-definition of  $W_\tau$  depends on property (V5). By property (V3), for every  $\tau > 0$ ,  $W_\tau$  is a diagonalizable operator. Moreover, by property (V4), the restriction of  $W_\tau$  on  $\mathcal{H}_\tau(X)$  admits the eigendecomposition given earlier in (9), reproduced here for convenience:

$$W_\tau \zeta_{j,\tau} = i\omega_{j,\tau} \zeta_{j,\tau}, \quad j \in \mathbb{N}_0, \quad \omega_{0,\tau} = 0, \quad \omega_{2j,\tau} = -\omega_{2j-1,\tau}$$

The following lemma establishes how the unitaries  $e^{tV_\tau}$  and  $e^{tW_\tau}$  can be used interchangeably to approximate the Koopman evolution of observables in  $H$ .

**Lemma 6.** *For every  $f \in H$ ,  $t \in \mathbb{R}$ , and  $\tau > 0$ , we have  $K_\tau^* e^{tW_\tau} K_\tau f = \mathcal{K}_{\tau/2} e^{tV_\tau} \mathcal{K}_{\tau/2} f$ . Moreover, the following hold.*

1. For every  $f \in H$ ,  $\lim_{\tau \rightarrow 0^+} K_\tau^* e^{tW_\tau} K_\tau f = U^t f$ .
2. For every  $f \in \mathcal{H}_1$ ,  $\lim_{\tau \rightarrow 0^+} K_\tau^* e^{tW_\tau} f = U^t \iota f$ .

*Proof.* For  $h_0 \in D(W_\tau)$ , define  $h: \mathbb{R} \rightarrow \mathcal{H}_\tau$  by  $h(t) = T_\tau e^{tV_\tau} T_\tau^* h_0$ . Then,  $T_\tau^* h_0$  lies in  $D(V_\tau)$ , and by the generator equation for the one-parameter unitary group  $\{e^{tV_\tau}\}_{t \in \mathbb{R}}$  we have

$$\frac{dh(t)}{dt} = T_\tau V_\tau e^{tV_\tau} T_\tau^* h_0 = W_\tau T_\tau e^{tV_\tau} T_\tau^* h_0 = W_\tau h(t).$$

Thus,  $h(t)$  satisfies the generator equation for  $\{e^{tW_\tau}\}_{t \in \mathbb{R}}$  with initial condition  $h(0) = h_0$ , which implies that  $h(t) = e^{tW_\tau} h_0$ . Letting  $h_0 = K_\tau f$  (which is an element of  $D(W_\tau)$  by property (V5)), it follows that  $T_\tau e^{tV_\tau} T_\tau^* K_\tau f = e^{tW_\tau} K_\tau f$  and thus  $T_\tau e^{tV_\tau} \mathcal{K}_{\tau/2} f = e^{tW_\tau} K_\tau f$  by the polar decomposition from property (K6). Pre-multiplying both sides of the last equation by  $K_\tau^*$  and using again property (K6), we get  $\mathcal{K}_{\tau/2} e^{tV_\tau} \mathcal{K}_{\tau/2} f = K_\tau^* e^{tW_\tau} K_\tau f$  as claimed.

For Claim 1 of the lemma, we use the result just proved in conjunction with strong convergence of  $e^{tV_\tau}$  to  $U^t$  (property (V6)) and strong convergence of  $\mathcal{K}_{\tau/2}$  to  $\text{Id}$  (property (K4)) to deduce

$$\lim_{\tau \rightarrow 0^+} K_\tau^* e^{tW_\tau} K_\tau f = \lim_{\tau \rightarrow 0^+} \mathcal{K}_{\tau/2} e^{tV_\tau} \mathcal{K}_{\tau/2} f = U^t f.$$

For Claim 2, note that for  $\tau \in [0, 1)$ ,  $K_\tau^+|_{\mathcal{H}_1}$  is a right inverse for  $K_\tau$ , i.e.,  $K_\tau K_\tau^+ f = f$  for  $f \in \mathcal{H}_1$ . Moreover, we have  $M = \sup_{\tau \in (0, 1]} \sum_{j=0}^{\infty} |\langle \phi_j, \iota f \rangle_H|^2 \Lambda_{j,\tau}^{-1} < \infty$ , so for every  $\epsilon > 0$  there exists  $J \in \mathbb{N}$  such that  $\sum_{j=J+1}^{\infty} |\langle \phi_j, \iota f \rangle_H|^2 < \epsilon$  and, for every  $\tau > 0$ ,  $\sum_{j=J+1}^{\infty} |\langle \phi_j, \iota f \rangle_H|^2 \Lambda_{j,\tau}^{-1} < \epsilon M$ . Thus, since  $\lim_{\tau \rightarrow 0^+} \Lambda_{j,\tau} = 1$  (by property (K4)), we have

$$\begin{aligned} \limsup_{\tau \rightarrow 0} \|K_\tau^+ f - \iota f\|_H^2 &= \limsup_{\tau \rightarrow 0} \left( \sum_{j=0}^J |\langle \phi_j, \iota f \rangle_H|^2 (\Lambda_{j,\tau/2}^{-1} - 1)^2 + \sum_{j=J+1}^{\infty} |\langle \phi_j, \iota f \rangle_H|^2 (\Lambda_{j,\tau/2}^{-1} - 1)^2 \right) \\ &\leq \epsilon(3M + 1), \end{aligned}$$

and thus  $\lim_{\tau \rightarrow 0^+} K_\tau^+ f = \iota f$  since  $\epsilon$  was arbitrary. Therefore, using Claim 1, we obtain

$$\lim_{\tau \rightarrow 0^+} K_\tau^* e^{tW_\tau} f = \lim_{\tau \rightarrow 0^+} K_\tau^* e^{tW_\tau} K_\tau K_\tau^+ f = U^t \iota f.$$

This proves Claim 2 and completes the proof of the lemma.  $\square$

In line with the notation of Section 3.1, we will let  $U_\tau^t := e^{tW_\tau}$  denote the unitary evolution operators on  $\mathcal{H}_\tau$  generated by  $W_\tau$ .

Next, in Sections 5.2.1 and 5.2.2, we give concrete examples of operators satisfying properties (V1)–(V6) based on the techniques proposed in [30, 31, 35]. Besides these schemes, any approximation technique for Koopman operators satisfying the requisite properties may be employed in the subsequent steps of our tensor network approximation framework.

### 5.2.1. Compact approximations

The scheme of [35] produces a family of skew-adjoint compact operators  $V_\tau: H \rightarrow H$  by smoothing  $V$  by conjugation with the integral operators  $\mathcal{K}_\tau$ . These operators are defined as  $V_\tau = \mathcal{K}_{\tau/2} V \mathcal{K}_{\tau/2}$ , giving  $W_\tau = K_\tau^* V K_\tau$  for the corresponding operators on the RKHA  $\mathcal{H}_\tau$  which are also skew-adjoint and compact. It is shown [35, Proposition 19] that under analogous assumptions to properties (K1)–(K6), as  $\tau \rightarrow 0^+$   $V_\tau$  converges strongly to  $V$  on  $D(V)$ . For skew-adjoint operators this implies strong resolvent convergence (e.g., [118, Propositions 10.1.8, 10.1.8]) and thus strong dynamical convergence, as required. Moreover, skew-adjointness and compactness of  $V_\tau$  means that its eigendecomposition can be computed stably and consistently using finite-rank compressions of the operator.

Fixing  $\tau > 0$  and choosing  $m \in \mathbb{N}$  such that  $\Lambda_{m,\tau} \neq \Lambda_{m-1,\tau}$ , we have that the orthogonal projection  $\Pi_m: H \rightarrow H$  with  $\text{ran } \Pi_m = \text{span}\{\phi_0, \dots, \phi_{m-1}\}$  projects onto a union of eigenspaces of  $\mathcal{K}_\tau$ . Our finite-rank approximations to  $V_\tau$  are given by  $V_{\tau,m} = \Pi_m \mathcal{K}_{\tau/2} V \mathcal{K}_{\tau/2} \Pi_m$ , and are concretely represented by  $m \times m$  skew-symmetric matrices  $\mathbf{V}_{\tau,m} = [V_{ij}]$  with elements  $V_{ij} = \Lambda_{\tau/2,i} \langle \phi_i, V \phi_j \rangle_H \Lambda_{\tau/2,j}$ . Similarly, using the basis vectors  $\psi_{j,\tau}$  from (25), we define the subspaces  $\mathcal{H}_{\tau,m} = \text{span}\{\psi_{0,\tau}, \dots, \psi_{m-1,\tau}\} \subset \mathcal{H}_\tau$ , the orthogonal projections  $\Psi_{\tau,m}: \mathcal{H}_\tau \rightarrow \mathcal{H}_\tau$  with  $\text{ran } \Psi_{\tau,m} = \mathcal{H}_{\tau,m}$ , and the compressed operators  $W_{\tau,m} = \Psi_{\tau,m} W_\tau \Psi_{\tau,m}$ . By construction, the matrix elements  $W_{ij} = \langle \psi_{i,\tau}, W_\tau \psi_{j,\tau} \rangle_{\mathcal{H}_\tau}$  are equal to  $V_{ij}$ .

To compute these matrix elements, we take advantage of (23) in conjunction with the fact that the  $\phi_j$  have smooth representatives  $\varphi_j \in \mathcal{H}_\infty$ , giving

$$V_{ij} = \Lambda_{\tau/2,i} \langle \iota \varphi_i, \iota \vec{V} \cdot \nabla \varphi_j \rangle_H \Lambda_{\tau/2,j}. \quad (28)$$

In [35], the directional derivatives  $\vec{V} \cdot \nabla \varphi_j$  are approximated using finite-difference methods along sampled dynamical trajectories. Another approach [31] takes advantage of the kernel integral representation of  $\varphi_j$  (see (24)) to evaluate these derivatives via automatic differentiation. Specifically, we have

$$\vec{V} \cdot \nabla \varphi_j = \frac{1}{\Lambda_{j,\tau}} \int_X \vec{V} \cdot \nabla k_\tau(\cdot, x) \phi_j(x) d\mu(x),$$

and the function  $\vec{V} \cdot \nabla k_\tau(\cdot, x)$  can be computed via automatic differentiation of the kernel section  $k_\tau(\cdot, x)$  at any point  $x' \in G$  where the tangent vector  $\vec{V}(x') \in T_{x'}G$  is known. In scenarios with known equations of motion, this will include every point  $x' \in G$ .

Finally, computation of  $V_{ij}$  requires a means of evaluating  $\langle \cdot, \cdot \rangle_H$  inner products. A common data-driven approach (adopted, e.g., in [35]) is to approximate the invariant measure  $\mu$  by a time average along a dynamical trajectory. By ergodicity, such an approximation converges for  $\mu$ -a.e. initial point  $x_0 \in G$  of that trajectory. In systems with so-called observable invariant measures (e.g., [119]), convergence holds for initial conditions  $x_0$  in a set of positive ambient (Haar) measure. In the examples of Section 7, the components of  $\vec{V}$  in a frame of  $G$ -invariant vector fields are polynomials in the characters  $\gamma$  of the group. This allows evaluation of the matrix elements  $V_{ij}$  analytically.

Next, we compute the eigenvalues and corresponding eigenvectors of  $V_{\tau,m}$  and  $W_{\tau,m}$  by solving the matrix eigenvalue problem

$$\mathbf{V}_{\tau,m} \mathbf{c}_j = i\omega_{j,\tau,m} \mathbf{c}_j,$$

where the eigenvectors  $\mathbf{c}_j = (c_{0j}, \dots, c_{m-1,j})^\top \in \mathbb{C}^m$  are orthonormal with respect to the standard inner product on  $\mathbb{C}^m$ . The elements of these eigenvectors are expansion coefficients of eigenvectors  $u_{j,\tau,m} = \sum_{i=0}^{m-1} c_{ij} \phi_j \in H_\tau$  of  $V_{\tau,m}$  and eigenvectors  $\zeta_{j,\tau,m} = \sum_{i=0}^{m-1} c_{ij} \psi_{i,\tau} \in \mathcal{H}_\tau(X)$  of  $W_{\tau,m}$ , both with corresponding eigenfrequencies  $\omega_{j,\tau,m}$  (cf. (20)). As noted in Section 3.1, the eigenvectors  $\zeta_{j,\tau,m}$  are everywhere-defined functions (vs. equivalence classes of  $\mu$ -a.e. defined functions in the case of  $u_{j,\tau,m}$ ) and can be manipulated as function objects in computational implementations (allowing, e.g., for automatic differentiation and lazy evaluation).

Following [35], we order eigenvectors and eigenfrequencies in order of increasing Dirichlet energy  $\mathcal{E}_\tau(u_{j,\tau,m})$ . The latter, can be computed directly from the  $\mathbf{c}_j$  through the formula

$$\mathcal{E}_\tau(u_{j,\tau,m}) = \frac{\sum_{i=1}^{m-1} |c_{ij}|^2 \Lambda_{i,\tau}^{-1}}{\sum_{i=0}^{m-1} |c_{ij}|^2}. \quad (29)$$

With this choice, we build the approximation spaces in subsequent steps of our approach so as to contain functions of high regularity with respect to  $\mathcal{E}_\tau$ .

### 5.2.2. Approximations with compact resolvent

Rather than approximating the generator  $V$  by compact operators, the schemes of [30, 31] approximate it by a two-parameter family of skew-adjoint operators  $V_{z,\tau}: D(V_{z,\tau}) \rightarrow H$ ,  $z, \tau > 0$ , with *compact resolvent*. An advantageous aspect of this form of approximation is that infinite-rank operators with compact resolvents have genuinely discrete spectra. This is in contrast to infinite-rank compact operators such as  $V_\tau$  from Section 5.2.1, which exhibit accumulation of the eigenvalues at 0 causing potentially high sensitivity of the spectrum to approximation parameters such as  $\tau$ . Infinite-rank operators with compact resolvents are also unbounded, and thus structurally closer in some sense to the unperturbed generator. In this subsection, we give an overview of the resolvent compactification scheme proposed in [31].

For  $z > 0$ , define the resolvent function  $r_z: i\mathbb{R} \rightarrow \mathbb{C}$  on the imaginary line as

$$r_z(i\omega) = \frac{1}{z - i\omega}.$$

This function gives the resolvent  $R_z: H \rightarrow H$  of the generator via the Borel functional calculus,

$$R_z = r_z(V) = \frac{1}{z - V}.$$

The scheme of [31] considers the skew-adjoint, bounded operator  $Q_z: H \rightarrow H$ ,

$$Q_z = q_z(V) = R_z^* V R_z,$$

obtained from the function  $q_z: i\mathbb{R} \rightarrow \mathbb{C}$ , where

$$q_z(i\omega) = \frac{i\omega}{z^2 + \omega^2}, \quad \text{ran } q_z = i \left[ -\frac{1}{2z}, \frac{1}{2z} \right].$$

While  $q_z$  is not an invertible function, its restriction  $\tilde{q}_z$  on the subset  $\Omega_z := i(-\infty, -z] \cup i[z, \infty)$  of the imaginary line is invertible, with inverse  $\tilde{q}_z^{-1}: i[-(2z)^{-1}, (2z)^{-1}] \rightarrow i\mathbb{R}$ ,

$$\tilde{q}_z^{-1}(i\omega) = i \frac{1 + \sqrt{1 - 4z^2\omega^2}}{2\omega}. \quad (30)$$

As a result,  $\tilde{V}_z := \tilde{q}_z^{-1}(Q_z)$  is a skew-adjoint operator that reconstructs the generator  $V$  on the spectral domain  $\Omega_z$ . It is shown [31] that as  $z \rightarrow 0^+$ ,  $\tilde{V}_z$  converges to  $V$  in strong resolvent sense. In what follows, we let  $\tilde{q}_z^{-1}: i\mathbb{R} \rightarrow i\mathbb{R}$  be any continuous extension of  $\tilde{q}_z^{-1}$  on the entire imaginary line.

Next, for a choice of kernels  $k_\tau$  satisfying properties (K1)–(K6), we approximate  $Q_z$  by the compact operators  $Q_{z,\tau}: H \rightarrow H$ , where

$$Q_{z,\tau} = R_z^* \mathcal{K}_{\tau/2} V \mathcal{K}_{\tau/2} R_z \equiv R_z^* V_\tau R_z.$$

It can be shown that as  $\tau \rightarrow 0^+$ ,  $Q_{z,\tau}$  converges strongly to  $Q_z$ . Thus,  $\tilde{V}_{z,\tau} := \tilde{q}_z^{-1}(Q_{z,\tau})$  is a family of skew-adjoint operators with compact resolvents that converge in strong resolvent sense to  $V$  in the iterated limits  $z \rightarrow 0^+$  after  $\tau \rightarrow 0^+$ . In particular, the two-parameter family  $\{\tilde{V}_{z,\tau}\}_{z,\tau>0}$  satisfies properties (V1)–(V6), with the  $\tau \rightarrow 0^+$  limit in property (V6) replaced by the iterated limit just mentioned.

Let

$$Q_{z,\tau} \tilde{u}_{j,z,\tau} = \beta_{j,z,\tau} \tilde{u}_{j,z,\tau}, \quad \beta_{j,z,\tau} \in i\mathbb{R}, \quad (31)$$

be an eigendecomposition of  $Q_{z,\tau}$ , where the eigenvalues/eigenvectors are indexed by  $j \in \mathbb{N}_0$ , and  $\{\tilde{u}_{j,z,\tau}\}_{j \in \mathbb{N}_0}$  is an orthonormal basis of  $H$  (such a basis exists by skew-adjointness and compactness of  $Q_{z,\tau}$ ). One readily verifies that  $\mathbf{1}$  is an eigenvector corresponding to eigenvalue 0, and that the eigenvalues/eigenvectors

corresponding to nonzero eigenvalues come in complex-conjugate pairs. We can therefore order the solutions of (31) similarly to those of (9), i.e.,  $\beta_{0,z,\tau} = 0$ ,  $\zeta_{0,z,\tau} = \mathbf{1}$ , and  $\beta_{2j,\tau,z} = \overline{\beta_{2j-1,z,\tau}}$ ,  $\tilde{u}_{2j,z,\tau}^* = \tilde{u}_{2j-1,z,\tau}$  for  $j \in \mathbb{N}$ . Applying  $\overline{\tilde{q}_z^{-1}}$  to the eigenvalues of  $Q_{z,\tau}$  leads to an eigendecomposition of  $\tilde{V}_{z,\tau}$ ,

$$\tilde{V}_{z,\tau} \tilde{u}_{j,z,\tau} = i \tilde{\omega}_{j,z,\tau} \tilde{u}_{j,z,\tau}, \quad i \tilde{\omega}_{j,z,\tau} = \overline{\tilde{q}_z^{-1}}(\beta_{j,z,\tau}). \quad (32)$$

Note that unlike the compact operator  $V_\tau$  from Section 5.2.1, whose eigenvalues cluster at 0, the spectrum of  $\tilde{V}_{z,\tau}$  consists entirely of isolated eigenvalues of finite multiplicity. In particular,  $\tilde{V}_{z,\tau}$  has eigenvalues of minimal modulus  $|\tilde{\omega}_{j,z,\tau}|$ , corresponding to eigenvalues of  $Q_{z,\tau}$  of maximal modulus  $|\beta_{j,z,\tau}|$ . This allows the use of iterative numerical algorithms to obtain low-frequency eigenvalues/eigenvectors of  $\tilde{V}_{z,\tau}$  by computing large-modulus eigenvalues/eigenvectors of  $Q_{z,\tau}$ .

*Remark 7.* In general, the spectrum of  $Q_{z,\tau}$  need not be a subset of the interval  $i[-(2z)^{-1}, (2z)^{-1}]$  that contains the spectrum of  $Q_z$ . Still, in the applications presented in this paper we have not observed any cases where the inclusion  $\sigma(Q_{z,\tau}) \subset i[-(2z)^{-1}, -(2z)^{-1}]$  is violated. With such an inclusion, we have  $\overline{\tilde{q}_z^{-1}}(\beta_{j,z,\tau}) = \tilde{q}_z^{-1}(\beta_{j,z,\tau})$  and an explicit choice of extension  $\overline{\tilde{q}_z^{-1}}$  is not needed.

The approach proposed in [31] solves (31) by solving an equivalent generalized eigenvalue problem,

$$V_\tau u_{j,z,\tau} = \beta_{j,z,\tau}(z^2 - V^2)u_{j,z,\tau}, \quad u_{j,z,\tau} \in D(V^2). \quad (33)$$

Since  $\text{ran } V_\tau \subset H_\tau$ , from the above it follows that the range of  $Q_{z,\tau}$  is contained in  $H_\tau$ . We may therefore order the solutions of (31) and (33) in increasing order of Dirichlet energy  $\mathcal{E}_\tau(\tilde{u}_{j,z,\tau})$  of the eigenvectors. Analogously to  $W_\tau$  from Section 5.2.1, we define the skew-adjoint operator  $\tilde{W}_{z,\tau} = T_\tau \tilde{V}_{z,\tau} T_\tau^*$  with domain  $D(\tilde{W}_{z,\tau}) = T_\tau(D(\tilde{V}_{z,\tau})) \oplus \mathcal{H}_\tau(X)^\perp$  and eigendecomposition

$$\tilde{W}_{z,\tau} \tilde{\zeta}_{j,z,\tau} = i \tilde{\omega}_{j,z,\tau} \tilde{\zeta}_{j,z,\tau}, \quad \tilde{\zeta}_{j,z,\tau} = T_\tau \tilde{u}_{j,z,\tau},$$

where the eigenfunctions  $\tilde{\zeta}_{j,z,\tau}$  form an orthonormal basis of  $\mathcal{H}_\tau(X)$ .

The generalized eigenvalue problem for  $Q_{z,\tau}$  in (33) can be solved using similar techniques to those described in Section 5.2.1 for  $V_\tau$ . These methods result in a matrix generalized eigenvalue problem

$$\mathbf{V}_{\tau,m} \tilde{\mathbf{c}}_j = i \beta_{j,z,\tau,m} \mathbf{B}_m \tilde{\mathbf{c}}_j, \quad (34)$$

where  $\mathbf{V}_{\tau,m}$  is an  $m \times m$  regularized generator matrix defined as in Section 5.2.1,  $\mathbf{B}_m = [B_{ij}]$  is a positive-definite  $m \times m$  matrix with elements

$$B_{ij} = z^2 \langle \phi_i, \phi_j \rangle_H - \langle V \phi_i, V \phi_j \rangle_H = z^2 \delta_{ij} - \langle V \phi_i, V \phi_j \rangle_H,$$

and the generalized eigenvectors  $\tilde{\mathbf{c}}_j$  give the expansion coefficients of  $\tilde{u}_{j,z,\tau,m}$  (resp.  $\tilde{\zeta}_{j,z,\tau,m}$ ) with respect to the  $\phi_i$  (resp.  $\psi_{i,\tau}$ ) basis vectors of  $H$  (resp.  $\mathcal{H}_\tau(X)$ ). The matrix elements  $B_{ij}$  can be computed by means of analogous automatic differentiation and/or ergodic averaging methods as in the computation of  $V_{ij}$ . Dirichlet energies  $\mathcal{E}_\tau(\tilde{u}_{j,z,\tau,m})$  can similarly be computed by applying (29) to the generalized eigenvectors  $\tilde{\mathbf{c}}_j$ .

### 5.3. Amplification to Fock space and quantum evolution

Let  $k_\tau: G \times G \rightarrow \mathbb{R}_+$ ,  $\tau > 0$ , be a family of kernels satisfying properties (K1)–(K6). Assume, in addition:

(K7) The RKHSs  $\mathcal{H}_\tau(X)$  associated with  $k_\tau$  are (unital) RKHAs with homeomorphic spectra  $\sigma(\mathcal{H}_\tau)$  to  $X$ .

Since  $\mathcal{H}_\tau$  is a subspace of  $C(G)$ , we have  $\text{ran } K_\tau^* \subset \mathfrak{A} \equiv L^\infty(\mu)$ . Thus, as noted in Section 3.3,  $K_\tau^*$  is a multiplicative map when  $\mathcal{H}_\tau$  is an RKHA,

$$K_\tau^*(fg) = (K_\tau^*f)(K_\tau^*g), \quad \forall f, g \in \mathcal{H}_\tau.$$

Using standard constructions from many-body quantum theory [81], we define the Fock space  $F(\mathcal{H}_\tau)$  as the Hilbert space closure of the tensor algebra  $T(\mathcal{H}_\tau) := \mathbb{C} \oplus \mathcal{H}_\tau \oplus \mathcal{H}_\tau^{\otimes 2} \oplus \dots$  with respect to the inner product defined by linear extension of

$$\langle f_1 \otimes \dots \otimes f_n, g_1 \otimes \dots \otimes g_n \rangle_{T(\mathcal{H}_\tau)} = \langle f_1, g_1 \rangle_{\mathcal{H}_\tau} \cdots \langle f_n, g_n \rangle_{\mathcal{H}_\tau},$$

where  $f_1, \dots, f_n, g_1, \dots, g_n \in \mathcal{H}_\tau$ . The  $n$ -fold comultiplication and multiplication operators  $\Delta_{n-1}$  and  $\Delta_{n-1}^*$ , respectively, associated with the tensor product space  $\mathcal{H}_\tau^{\otimes n}$  (referred to in this context as the  $n$ -th grading of the Fock space) canonically extend to operators on  $F(\mathcal{H}_\tau)$ . Reusing notation, we will denote these operators as  $\Delta_n: \mathcal{H}_\tau \rightarrow F(\mathcal{H}_\tau)$  and  $\Delta_n^*: F(\mathcal{H}_\tau) \rightarrow \mathcal{H}_\tau$ , where  $\text{ran } \Delta_n \subset \mathcal{H}_\tau^{\otimes n}$  and  $\ker \Delta_n^* = (\mathcal{H}_\tau^{\otimes n})^\perp$ .

With these definitions, we lift the unitary evolution operators  $U_\tau^t: \mathcal{H}_\tau \rightarrow \mathcal{H}_\tau$  on the RKHA to unitary operators  $\tilde{U}_\tau^t: F(\mathcal{H}_\tau) \rightarrow F(\mathcal{H}_\tau)$  as described in Section 3.2. As noted there, a key property of these operators is that they act multiplicatively with respect to the tensor product of  $T(\mathcal{H}_\tau)$ ; see (11). For  $n \in \mathbb{N}$ , we lift classical observables  $f \in \mathfrak{A} \equiv L^\infty(\mu)$  to bounded quantum observables  $A_{f,\tau,n} \in \mathfrak{F}_\tau \equiv B(F(\mathcal{H}_\tau))$  according to the formula (14). These quantum observables evolve under conjugation operators  $\tilde{U}_\tau^t: \mathfrak{F}_\tau \rightarrow \mathfrak{F}_\tau$  induced from  $\tilde{U}_\tau^t$ ; see (13).

The following lemma proves the assertion made in Section 3.2 that the evolution  $\mathbb{E}_q(U^t f)$  of an observable  $f \in \mathfrak{A}$  with respect to a probability density  $q \in S_*(\mathfrak{A})$  can be approximated at arbitrary accuracy by the evolution  $\mathbb{E}_p(U^t f)$  with respect to a density  $p \in S_*(\mathfrak{A})$  with a strictly positive representative  $\varrho \in \mathcal{H}_1$ .

**Lemma 8.** *For every  $q \in S_*(\mathfrak{A})$  and  $\epsilon > 0$ , there exists a probability density  $p = \iota\varrho \in \mathfrak{A}_*$  with a representative  $\varrho \in \mathcal{H}_1$  such that (i)  $\varrho(x) > 0$  for all  $x \in G$ ; and (ii) for every  $f \in \mathfrak{A}$  and  $t \in \mathbb{R}$ ,  $|\mathbb{E}_p(U^t f) - E_q(U^t f)| < \epsilon$ .*

*Proof.* Since  $U^t$  acts as an isometry of  $\mathfrak{A}$ , it suffices to prove the lemma for  $t = 0$ . To that end, for  $\epsilon > 0$  choose  $g \in C(G)$ ,  $g \geq 0$ , such that  $\|q - \iota g\|_{L^1(\mu)} < \epsilon$ . For  $\delta \geq 0$ , define  $g_\delta \in C(G)$  such that  $g_\delta(x) = g(x) + \delta$ . By density of  $\mathcal{H}_1$  in  $C(G)$ , there exists  $h_\delta \in \mathcal{H}_1$  such that  $\|h_\delta - g_\delta\|_{C(G)} \leq \delta/2$ . In particular,  $h_\delta$  is a strictly positive function with  $h_\delta(x) \geq \delta/2$ . We also have  $\|\iota g_\delta\|_{L^1(\mu)} = 1 + \delta$ , and since

$$\left| \|\iota h_\delta\|_{L^1(G)} - \|\iota g_\delta\|_{L^1(G)} \right| \leq \|\iota(h_\delta - g_\delta)\|_{L^1(\mu)} \leq \|h_\delta - g_\delta\|_{C(G)} \leq \delta/2,$$

it follows that  $c_\delta := \|\iota h_\delta\|_{L^1(\mu)} \geq 1$ . We let  $M$  be an upper bound for  $\|h_\delta\|_{C(G)}/c_\delta$  over  $\delta \geq 0$ .

Next, define  $\varrho_\delta = h_\delta/c_\delta$ . Then,  $p_\delta := \iota\varrho_\delta$  is a probability density in  $L^1(\mu)$  with a strictly positive representative  $\varrho_\delta \in \mathcal{H}_1$ . In addition, we have

$$\begin{aligned} \|q - p_\delta\|_{L^1(\mu)} &= \|q - \iota\varrho_\delta + \iota g - \iota g\|_{L^1(\mu)} \leq \|q - \iota g\|_{L^1(\mu)} + \|\varrho_\delta - g\|_{C(G)} < \epsilon + \|\varrho_\delta - g\|_{C(G)}, \\ \|\varrho_\delta - g\|_{C(G)} &\leq \|\varrho_\delta - g_\delta\|_{C(G)} + \|g_\delta - g\|_{C(G)} \leq \|\varrho_\delta - g_\delta\|_{C(G)} + \delta, \\ \|\varrho_\delta - g_\delta\|_{C(G)} &\leq \|\varrho_\delta - h_\delta\|_{C(G)} + \delta/2, \\ \|\varrho_\delta - h_\delta\|_{C(G)} &= \|h_\delta\|_{C(G)} \frac{|1 - c_\delta|}{c_\delta} \leq M|1 - c_\delta|. \end{aligned}$$

Moreover, since  $c_\delta \geq 1$ ,

$$\begin{aligned} \|1 - c_\delta\| &= c_\delta - 1 \\ &\leq \|\iota h_\delta - \iota g_\delta\|_{L^1(\mu)} + \|g_\delta\|_{L^1(\mu)} - 1 \leq \|h_\delta - g_\delta\|_{C(G)} + \|g_\delta\|_{L^1(\mu)} - 1 \\ &\leq \frac{\delta}{2} + 1 + \delta - 1 = \frac{3\delta}{2}. \end{aligned}$$

Combining the above estimates, we obtain

$$\|q - p_\delta\|_{L^1(\mu)} \leq \epsilon + \delta + \frac{\delta}{2} + \frac{3M\delta}{2} = \epsilon + \frac{3(M+1)\delta}{2},$$

and thus  $\|q - p\|_{L^1(\mu)} < \epsilon$  for  $p = p_\delta$  and sufficiently small  $\epsilon, \delta$ . The claim of the lemma follows from  $|\mathbb{E}_p f - E_q f| \leq \|p - q\|_{L^1(\mu)} \|f\|_{L^\infty(\mu)}$ .  $\square$

In light of Lemma 8, we henceforth consider approximating the evolution of expectations with respect to a probability density  $p \in \mathfrak{A}_*$  with a strictly positive representative  $\varrho \in \mathcal{H}_1$ . For such a density the square root  $\xi := \varrho^{1/2}$  and the  $n$ -th roots  $\xi^{1/n}$ ,  $n \in \mathbb{N}$ , are all well-defined elements of  $\mathcal{H}_1$  obtained from the holomorphic functional calculus (see Section 4.1). We lift the density  $p$  to a rank-1 density operator  $\nu_\tau \in \mathfrak{F}_{\tau*}$  with associated state vector  $\eta_\tau \in F(\mathcal{H}_\tau)$ , i.e.,  $\nu_\tau = \langle \eta_\tau, \cdot \rangle_{F(\mathcal{H}_\tau)} \eta_\tau$ . We define this vector as

$$\eta_\tau = w_1 \frac{\xi}{\|\xi\|_{\mathcal{H}_\tau}} + w_2 \frac{\xi^{1/2} \otimes \xi^{1/2}}{\|\xi^{1/2}\|_{\mathcal{H}_\tau}^2} + w_3 \frac{\xi^{1/3} \otimes \xi^{1/3} \otimes \xi^{1/3}}{\|\xi^{1/3}\|_{\mathcal{H}_\tau}^3} + \dots, \quad (35)$$

where  $w = (w_1, w_2, \dots) \in \ell^1(\mathbb{N})$  is any probability vector with strictly positive elements (i.e.,  $w_n > 0$  and  $\sum_{n=1}^\infty w_n = 1$ ). Note that the state vector  $\eta_\tau$  has nonzero projections onto all gradings  $\mathcal{H}_\tau^{\otimes n} \subset F(\mathcal{H}_\tau)$  of the Fock space. As a result, the associated quantum state  $\mathbb{E}_{\nu_\tau} \in S_*(\mathfrak{F}_\tau)$  is faithful on the quantum observables  $A_{f,\tau,n}$  from (14), meaning that  $\mathbb{E}_{\nu_\tau} A_{f,\tau,n}$  vanishes for  $f \geq 0$  iff  $f = 0$ .

The density operator  $\nu_\tau$  evolves under the conjugation operators  $\tilde{\mathcal{P}}_\tau^t: \mathfrak{F}_{\tau*} \rightarrow \mathfrak{F}_{\tau*}$  from (13). Using the latter equation together with (14) and (35), we get

$$g_{\tau,n}^{(t)} := \mathbb{E}_{\tilde{\mathcal{P}}_\tau^t \nu_\tau} A_{f,\tau,n} = \frac{w_n}{\|\xi^{1/n}\|_{\mathcal{H}_\tau}^n} \langle \Delta_{n-1}^*(U_\tau^{t*} \xi^{1/n})^{\otimes n}, M_{f,\tau} \Delta_{n-1}^*(U_\tau^{t*} \xi^{1/n})^{\otimes n} \rangle_{F(\mathcal{H}_\tau)},$$

giving (16) up to an  $f$ -independent proportionality constant. Similarly, we have

$$C_{\tau,n}^{(t)} := \mathbb{E}_{\tilde{\mathcal{P}}_\tau^t \nu_\tau} A_{1,\tau,n} = \frac{w_n}{\|\xi^{1/n}\|_{\mathcal{H}_\tau}^n} \|K_\tau^*(U_\tau^{t*} \xi^{1/n})^n\|_H^2,$$

and the fraction  $f_{\tau,n}^{(t)} := g_{\tau,n}^{(t)}/C_{\tau,n}^{(t)}$  gives (15) in a  $w$ -independent manner,

$$f_{\tau,n}^{(t)} = \frac{\langle \Delta_{n-1}^*(U_\tau^{t*} \xi^{1/n})^{\otimes n}, M_{f,\tau} \Delta_{n-1}^*(U_\tau^{t*} \xi^{1/n})^{\otimes n} \rangle_{F(\mathcal{H}_\tau)}}{\|K_\tau^*(U_\tau^{t*} \xi^{1/n})^n\|_H^2} = \frac{\langle K_\tau^*(U_\tau^{t*} \xi^{1/n})^n, (\pi f) K_\tau^*(U_\tau^{t*} \xi^{1/n})^n \rangle_H}{\|K_\tau^*(U_\tau^{t*} \xi^{1/n})^n\|_H^2}.$$

An observation worthwhile making about these approximations is that  $f_{\tau,n}^{(0)}$  is independent of  $n$  at fixed  $\tau$ . Thus, the trajectories  $t \mapsto f_{\tau,n}^{(t)}$  start from the same initial value at  $t = 0$  but follow different subsequent evolutions for different  $n$  (at fixed  $\tau$ ).

The following proposition establishes the  $\tau \rightarrow 0^+$  convergence result claimed in Section 3.2.

**Proposition 9.** *Assume that the kernels  $k_\tau$  and regularized generators  $V_\tau$  have properties (K1)–(K7) and properties (V1)–(V6), respectively. Suppose also that  $p \in \mathfrak{A}_*$  is a probability density with a strictly positive representative  $\varrho \in \mathcal{H}_1$ . Then, for every classical observable  $f \in \mathfrak{A}$ , evolution time  $t \in \mathbb{R}$ , and  $n \in \mathbb{N}$ , the Fock space evolution  $f_{\tau,n}^{(t)}$  converges to the classical statistical evolution  $f^{(t)} = \mathbb{E}_{\mathcal{P}^t p} f$ , i.e.,  $\lim_{\tau \rightarrow 0^+} f_{\tau,n}^{(t)} = f^{(t)}$ .*

*Proof.* Since  $K_\tau^*$  is multiplicative, we have  $K_\tau^*(U_\tau^{t*} \xi^{1/n})^n = (K_\tau^* U_\tau^{t*} \xi^{1/n})^n$  in  $\mathfrak{A}$ . Meanwhile, since  $\xi^{1/n} \in \mathcal{H}_1$ , Lemma 6 implies that  $\lim_{\tau \rightarrow 0^+} K_\tau^* U_\tau^{t*} \xi^{1/n} = U^{t*} \xi^{1/n}$ . Using these facts and multiplicativity of  $U^{t*} \equiv U^{-t}$  on  $\mathfrak{A}$  it follows that  $\lim_{\tau \rightarrow 0^+} K_\tau^*(U_\tau^{t*} \xi^{1/n})^n = (U^{t*} \xi^{1/n})^n = U^{t*} \xi$ . Thus, using the classical–quantum correspondence (8), we deduce

$$\lim_{\tau \rightarrow 0^+} f_{\tau,n}^{(t)} = \lim_{\tau \rightarrow 0^+} \frac{\langle K_\tau^*(U_\tau^{t*} \xi^{1/n})^n, (\pi f) K_\tau^*(U_\tau^{t*} \xi^{1/n})^n \rangle_H}{\|K_\tau^*(U_\tau^{t*} \xi^{1/n})^n\|_H^2} = \frac{\langle U^{t*} \xi, (\pi f) U^{t*} \xi \rangle_H}{\|U^{t*} \xi\|_H^2} = \frac{\mathbb{E}_{\mathcal{P}^t(\Gamma(p))}(\pi f)}{\|p\|_{\mathfrak{A}_*}} = f^{(t)}. \quad \square$$

With the convergence result from Proposition 9 in place, the approximation  $f_{\tau,n,d}^{(t)}$  based on the  $(2d+1)$ -dimensional approximation spaces  $\mathcal{Z}_{\tau,d} = \text{span}\{\zeta_{0,\tau}, \dots, \zeta_{2d,\tau}\} \subseteq \mathcal{H}_\tau$  and the associated Fock spaces  $F(\mathcal{Z}_{\tau,d}) \subseteq F(\mathcal{H}_\tau)$  proceed as described in Section 3.4. As noted there, convergence of these approximations as  $d \rightarrow \infty$  is an immediate consequence of the fact that the eigenfunctions  $\zeta_{j,\tau}$  form an orthonormal basis of  $\mathcal{H}_\tau(X)$ . However, our main interest here is on approximations obtained by increasing  $n$  at fixed  $d$ . An analysis of such approximations in particular cases will be taken up in Section 6.



#### 5.4. Numerical implementation

We now consider the numerical implementation of the scheme described above. We let  $W_{\tau,m}: \mathcal{H}_\tau \rightarrow \mathcal{H}_\tau$  represent finite-rank approximations of either  $W_\tau$  or  $\tilde{W}_{z,\tau}$  from Sections 5.2.1 and 5.2.2, and we will continue to use  $\omega_{j,\tau,m} \in \mathbb{R}$  and  $\zeta_{j,\tau,m} \in \mathcal{H}_\tau$  to denote corresponding eigenfrequencies and eigenfunctions, respectively. We also let  $U_{\tau,m}^t = e^{tW_{\tau,m}}$ ,  $t \in \mathbb{R}$ , denote the unitary evolution operators generated by  $W_{\tau,m}$ . Using this data, we build approximations of the finite-rank Fock space approximation scheme from Section 3.4.

For  $d \in \mathbb{N}$  chosen such that  $2d+1 \leq \dim \mathcal{H}_{\tau,m}$ , consider the subspace  $\mathcal{Z}_{\tau,d,m} = \text{span}\{\zeta_{0,\tau,m}, \dots, \zeta_{2d,\tau,m}\} \subseteq \mathcal{H}_{\tau,m}$ , and let  $Z_{\tau,d,m}: \mathcal{H}_\tau \rightarrow \mathcal{H}_\tau$  be the orthogonal projection with  $\text{ran } Z_{\tau,d,m} = \mathcal{Z}_{\tau,d,m}$ ; that is,  $Z_{\tau,d,m} = \sum_{j=0}^{2d} \langle \zeta_{j,\tau,m}, f \rangle_{\mathcal{H}_\tau} \zeta_{j,\tau,m}$ . Defining the projected state vector  $\xi_{\tau,n,d,m} = \frac{1}{\|Z_{\tau,d,m}\xi^{1/n}\|_{\mathcal{H}_\tau}} Z_{\tau,d,m}\xi^{1/n}$ , we approximate the functions  $U_\tau^{t*} \xi_{\tau,n,d} \in \mathcal{H}_\tau$  appearing in (19b) by  $U_{\tau,m}^{t*} \xi_{\tau,n,d,m} \in \mathcal{H}_{\tau,m}$ . We similarly approximate  $(U_\tau^{t*} \xi_{\tau,n,d})^n$  by the  $n$ -fold pointwise function product  $(U_{\tau,m}^{t*} \xi_{\tau,n,d,m})^n$ , but note that since, in general, the subspace  $\mathcal{H}_{\tau,m}$  is not an algebra,  $(U_{\tau,m}^{t*} \xi_{\tau,n,d,m})^n$  must be viewed as an element of the RKHA  $\mathcal{H}_\tau \supseteq \mathcal{H}_{\tau,m}$ . Similarly to the approximations of  $W_{\tau,m}$  in Section 5.2, these approximations are again implemented using function objects, and converge as  $m \rightarrow \infty$  to  $(U_\tau^{t*} \xi_{\tau,n,d})^n$  in the norm of  $\mathcal{H}_\tau$ .

The remaining ingredients needed to approximate the right-hand side of (19b) are approximations of (i) the multiplication operator  $\pi f \in \mathfrak{B} \equiv B(H)$ ; and (ii)  $L^2$  inner products  $\langle \cdot, \cdot \rangle_H$  with respect to the invariant measure  $\mu$ . To that end, for each  $l \in \mathbb{N}$  we introduce a sequence of points  $x_0^{(l)}, \dots, x_{N_l-1}^{(l)} \in G$  whose associated sampling measures

$$\mu_l := \frac{1}{N_l} \sum_{i=0}^{N_l-1} \delta_{x_i} \quad (36)$$

converge as  $l \rightarrow \infty$  to the invariant measure  $\mu$  in weak-\* sense. This means  $\lim_{l \rightarrow \infty} \int_G \tilde{f} d\mu_l = \int_G \tilde{f} d\mu$  for every continuous function  $\tilde{f}: G \rightarrow \mathbb{C}$ . Possible choices for the  $x_i^{(l)}$  are grid nodes on  $G$  of increasingly small spacing as  $l$  increases, or trajectories of points under discrete-time dynamics having  $\mu$  as an ergodic invariant measure (obtained, e.g., by sampling the continuous-time dynamical flow  $\Phi^t$  at an interval  $\Delta t > 0$ ). Assuming that  $f$  has a representative  $\tilde{f} \in C(G)$  (we will relax this assumption below), we further require that the values  $y_i^{(l)} = \tilde{f}(x_i^{(l)}) \in \mathbb{R}$  are known on the  $x_i^{(l)}$ .

For each  $l \in \mathbb{N}$  the samples  $y_i^{(l)}$  induce an element  $f_l$  in the finite-dimensional von Neumann algebra  $\mathfrak{A}_l = L^\infty(\mu_l)$ . Letting  $H_l = L^2(\mu_l)$  and  $\mathfrak{B}_l = B(H_l)$ ,  $f_l$  induces in turn a multiplication operator  $(\pi_l f_l) \in \mathfrak{B}_l$ , where  $(\pi_l g)h = gh$  for every  $g \in \mathfrak{A}_l$  and  $h \in H_l$ . Moreover, analogously to  $K_\tau: H \rightarrow \mathcal{H}_\tau$ , for every  $l \in \mathbb{N}$  there is a finite-rank integral operator  $K_{\tau,l}: H_l \rightarrow \mathcal{H}_\tau$ , where

$$K_{\tau,l} f = \int_G k_\tau(\cdot, x) f(x) d\mu_l(x) = \frac{1}{l} \sum_{i=0}^{N_l-1} k_\tau(\cdot, x_i^{(l)}) f(x_i^{(l)}). \quad (37)$$

The adjoint  $K_{\tau,l}^*$  is a multiplicative map that implements restriction (sampling) of functions in  $\mathcal{H}_\tau$  to equivalence classes of functions in  $H_l$ . With these definitions, we approximate

$$\langle (U_\tau^{t*} \xi_{\tau,n,d})^n, M_{f,\tau} (U_\tau^{t*} \xi_{\tau,n,d})^n \rangle_H \equiv \langle K_\tau^* (U_\tau^{t*} \xi_{\tau,n,d})^n, (\pi f) K_\tau^* (U_\tau^{t*} \xi_{\tau,n,d})^n \rangle_H$$

in the right-hand side of (19b) by

$$\langle (U_{\tau,m}^{t*} \xi_{\tau,n,d,m})^n, M_{f,\tau,l} (U_{\tau,m}^{t*} \xi_{\tau,n,d,m})^n \rangle_{H_l} \equiv \langle K_{\tau,l}^* (U_{\tau,m}^{t*} \xi_{\tau,n,d,m})^n, (\pi_l f_l) K_{\tau,l}^* (U_{\tau,m}^{t*} \xi_{\tau,n,d,m})^n \rangle_{H_l},$$

where

$$M_{f,\tau,l} = K_{\tau,l} \pi_l f_l K_{\tau,l}^*. \quad (38)$$

This approximation converges as  $l, m \rightarrow \infty$ , where the limits can be taken in either order. Using this approximation of (19b), we define  $g_{\tau,n,d,m}^{(t)}: X \rightarrow \mathbb{R}$  and  $C_{\tau,n,d,m,l}^{(t)} > 0$  analogously to  $g_{\tau,n,d}^{(t)}$  and  $C_{\tau,n,d}^{(t)}$  from (17), respectively, using the evolution operators  $\tilde{U}_{\tau,m}^t: \mathfrak{F}_\tau \rightarrow \mathfrak{F}_\tau$  and  $\tilde{\mathcal{P}}_{\tau,m}^t: \mathfrak{F}_{\tau^*} \rightarrow \mathfrak{F}_{\tau^*}$  defined as  $\tilde{U}_{\tau,m}^t = U_{\tau,m}^t A U_{\tau,m}^{t*}$  and  $\tilde{\mathcal{P}}_{\tau,m}^t = U_{\tau,m}^{t*} \rho U_{\tau,m}^t$ , together with the quantum observable

$$A_{f,\tau,n,l} = \Delta_n M_{f,\tau,l} \Delta_n^* \in \mathfrak{F}_\tau \quad (39)$$

acting on the Fock space (cf. (14)). Our numerical approximation of the statistical evolution  $f^{(t)}$  is given by

$$f_{\tau,n,d,m,l}^{(t)} = \frac{g_{\tau,n,d,m,l}^{(t)}}{C_{\tau,n,d,m,l}^{(t)}}, \quad g_{\tau,n,d,m,l}^{(t)} = \mathbb{E}_{\tilde{\mathcal{P}}_{\tau,m}^t \nu_{\tau,d,m}} A_{f,\tau,n,l}, \quad C_{\tau,n,d,m,l}^{(t)} = \mathbb{E}_{\tilde{\mathcal{P}}_{\tau,m}^t \nu_{\tau,d,m}} A_{\mathbf{1},\tau,n,l}, \quad (40)$$

where  $\nu_{\tau,d,m} = \langle \eta_{\tau,d,m}, \cdot \rangle_{\mathcal{H}_\tau} \eta_{\tau,d,m} \in \mathfrak{F}_{\tau^*}$  is the density operator associated with the state vector  $\eta_{\tau,d,m} = \sum_{n=1}^{\infty} w_n \xi_{\tau,n,d,m}^{\otimes n} \in F(\mathcal{Z}_{\tau,d,m})$ . This approximation converges to  $f_{\tau,n,d}^{(t)}$  as  $l, m \rightarrow \infty$ .

Finally, if  $f$  does not have a continuous representative, for a tolerance  $\epsilon > 0$ , pick  $\tilde{f} \in C(G)$  such that  $\|f - \iota\tilde{f}\|_{L^1(\mu)} < \epsilon$ . Since  $H_\tau$  is a subspace of  $L^\infty(\mu)$ , for every  $g \in \mathcal{H}_\tau$  we have

$$\begin{aligned} |\langle K_\tau^* g, (f - \iota\tilde{f}) K_\tau^* g \rangle_H| &\leq \|f - \iota\tilde{f}\|_{L^1(\mu)} \|K_\tau^* g\|_{L^\infty(\mu)}^2 \\ &\leq \|f - \iota\tilde{f}\|_{L^1(\mu)} \|k_\tau\|_{C(G \times G)}^2 \|g\|_{\mathcal{H}_\tau}^2 \\ &< \epsilon \|k_\tau\|_{C(G \times G)}^2 \|g\|_{\mathcal{H}_\tau}^2. \end{aligned}$$

This means that for sufficiently small  $\epsilon$  and large  $l$ ,  $\langle K_\tau^*(U_\tau^{t*} \xi_{\tau,n,d})^n, (\pi f) K_\tau^*(U_\tau^{t*} \xi_{\tau,n,d})^n \rangle_H$  can be approximated to any desired accuracy by  $\langle K_{\tau,l}^*(U_{\tau,m}^{t*} \xi_{\tau,n,d,m})^n, (\pi_l f_l) K_{\tau,l}^*(U_{\tau,m}^{t*} \xi_{\tau,n,d,m})^n \rangle_{H_l}$ , where  $f_l$  is the element of  $\mathfrak{A}_l$  represented by  $\tilde{f}$ . Correspondingly,  $f_{\tau,n,d}^{(t)}$  can also be represented to any accuracy by  $f_{\tau,n,d,m,l}^{(t)}$  from (40) computed using samples of  $\tilde{f}$ .

### 5.5. Approximation of pointwise evaluation

Thus far, we have considered approximation of the evolution of expectation values of observables with respect to general probability densities  $p \in \mathfrak{A}_*$  using quantum states on the Fock space  $F(\mathcal{H}_\tau)$ . In this subsection, we specialize these constructions to quantum states that approximate pointwise evaluation of continuous functions on the  $N$ -torus,  $G = \mathbb{T}^N$ . Following [56], we build these states via a ‘‘quantum feature map’’, i.e., a map  $\Xi_{\kappa,\tau}: G \rightarrow S_*(\mathfrak{F}_\tau)$ , which we parameterize here by a sharpness parameter  $\kappa > 0$ . For  $\tilde{f} \in C(G)$ , our goal is to show that the observable  $\tilde{f}_{\kappa,\tau,n}^{(t)} \in C(G)$ , where  $\tilde{f}_{\kappa,\tau,n}^{(t)}(x)$  is obtained by applying (15) to the observable  $f = \iota\tilde{f} \in \mathfrak{A}$  and the quantum state  $\Xi_{\kappa,\tau}(x)$ , well-approximates  $(U^t \tilde{f})(x) = \tilde{f}(\Phi^t(x))$ , where  $U^t: C(G) \rightarrow C(G)$  denotes the time- $t$  Koopman operator on continuous functions.

Our construction employs isotropic von Mises density functions on  $\mathbb{T}^N$ , which we build starting from the circle,  $N = 1$ . The von Mises probability density function  $\sigma_{\mu,\kappa} \in C^\infty(\mathbb{T})$  is parameterized by a sharpness parameter  $\kappa > 0$ , a parameter  $\mu \in [0, 2\pi)$  controlling the mode (location of maximum value) of the distribution, and is defined as

$$\sigma_{\mu,\kappa}(\theta) = \frac{e^{\kappa \cos(\theta - \mu)}}{I_0(\kappa)}. \quad (41)$$

Here,  $I_\nu \in C^\infty(\mathbb{R})$ ,  $\nu \geq 0$ , is the modified Bessel function of the first kind of order  $\nu$ . In higher dimensions, we consider the product density  $\sigma_{\boldsymbol{\mu},\boldsymbol{\kappa}} \in C^\infty(\mathbb{T}^N)$  with  $\boldsymbol{\kappa} = (\kappa_1, \dots, \kappa_N) \in \mathbb{R}_+^N$  and  $\boldsymbol{\mu} = (\mu_1, \dots, \mu_N) \in [0, 2\pi)^N$ , given by

$$\sigma_{\boldsymbol{\mu},\boldsymbol{\kappa}} = \prod_{i=1}^N \sigma_{\mu_i, \kappa_i}. \quad (42)$$

By properties of Bessel functions,  $\sigma_{\boldsymbol{\mu},\boldsymbol{\kappa}}$  integrates to 1 with respect to the Haar probability measure on  $\mathbb{T}^N$ .

The following are useful properties of von Mises density functions in the context of the approximation schemes studied in this paper.

- $\sigma_{\mu,\kappa}$  has known expansion coefficients in the character (Fourier) basis of  $\mathbb{T}$ . Specifically, for  $j \in \mathbb{Z} \cong \widehat{\mathbb{T}}$ , we have

$$\hat{\sigma}_{\mu,\kappa}(j) := \langle \iota\gamma_j, \iota\sigma_{\mu,\kappa} \rangle_{L^2(\mathbb{T})} = \frac{I_{|j|}(\kappa) e^{ij\mu}}{I_0(\kappa)}. \quad (43)$$

Similarly, the Fourier coefficients of  $\sigma_{\mu, \kappa}$  on  $\mathbb{T}^N$  are given by

$$\hat{\sigma}_{\mu, \kappa}(j) := \langle \iota\gamma_j, \iota\sigma_{\kappa, \mu} \rangle_{L^2(\mathbb{T}^N)} = \prod_{i=1}^N \hat{\sigma}_{\kappa_i, \mu_i}(j_i), \quad j = (j_1, \dots, j_N). \quad (44)$$

• The  $n$ -th root of a von Mises density function is a von Mises density function up to a proportionality constant,

$$\sigma_{\mu, \kappa}^{1/n} = \prod_{i=1}^N \frac{I_0(\kappa_i/n)}{I_0^{1/n}(\kappa_i)} \sigma_{\mu_i, \kappa_i/n}. \quad (45)$$

• Recall the series representation [120, Chapter 9]

$$I_j(\kappa) = (\kappa/2)^j \sum_{r=0}^{\infty} \frac{(\kappa/2)^{2r}}{r!(r+j)!}, \quad j \in \mathbb{N}_0. \quad (46)$$

The above implies the upper bound

$$I_j(\kappa/n) = \left(\frac{\kappa}{2n}\right)^j \sum_{r=0}^{\infty} \frac{(\frac{\kappa}{2n})^{2r}}{r!(r+j)!} \leq \frac{\kappa^j}{(2n)^j j!} e^{\kappa^2/4n^2}. \quad (47)$$

For the family of weights (21) on  $\mathbb{T}^N$ , the rapid decay of  $I_j(\kappa)$  as  $|j|$  grows ensures that  $\sigma_{\mu, \kappa}$  lies in the RKHA  $\mathcal{H}_\tau$  for every  $\tau > 0$ .

Since  $\sigma_{\mu, \kappa} \in \mathcal{H}_\tau$ , it follows that  $F_{\kappa, \tau}: \mathbb{T}^N \rightarrow \mathcal{H}_\tau$  with  $\kappa > 0$ ,

$$F_{\kappa, \tau}(x) = \sigma_{x, \kappa} / \|\sigma_{x, \kappa}\|_{\mathcal{H}_\tau}, \quad \kappa = (\kappa_1, \dots, \kappa_N) \in \mathbb{R}_+^N, \quad (48)$$

is a well-defined feature map for every  $\tau > 0$ . We lift  $F_{\kappa, \tau}$  to a quantum feature map  $\Xi_{\kappa, \tau}: \mathbb{T}^N \rightarrow S_*(\mathfrak{B}_\tau)$ , where  $\mathfrak{B}_\tau = B(\mathcal{H}_\tau)$  and  $\Xi_{\kappa, \tau}(x)$  is the rank-1 density operator that projects along  $F_{\kappa, \tau}(x)$ ,

$$\Xi_{\kappa, \tau}(x) = \langle F_{\kappa, \tau}(x), \cdot \rangle_{\mathcal{H}_\tau} F_{\kappa, \tau}(x). \quad (49)$$

Given a probability vector  $w \in \ell^1(\mathbb{N})$  with strictly positive entries (as in Section 5.3), we also define variants  $\tilde{F}_{\kappa, \tau}: \mathbb{T}^N \rightarrow F(\mathcal{H}_\tau)$  and  $\tilde{\Xi}_{\kappa, \tau}: \mathbb{T}^N \rightarrow S_*(\mathfrak{F}_\tau)$  of  $F_{\kappa, \tau}$  and  $\Xi_{\kappa, \tau}$ , respectively, mapping into the Fock space,

$$\tilde{F}_{\kappa, \tau}(x) = \eta_\tau, \quad \tilde{\Xi}_{\kappa, \tau}(x) = \langle \eta_\tau, \cdot \rangle_{F(\mathcal{H}_\tau)} \eta_\tau,$$

where  $\eta_\tau$  is obtained by applying (35) to the vector  $\xi = F_{\kappa, \tau}(x) \in \mathcal{H}_\tau$ .

The following lemma establishes that these feature maps can be used to approximate pointwise evaluation for continuous functions.

**Lemma 10.** *Assume the choice of weights  $\lambda_\tau$  in (21). Then for every  $n \in \mathbb{N}$ ,  $\tilde{f} \in C(\mathbb{T}^N)$ , and  $x \in X \equiv \text{supp}(\mu)$ , we have*

$$\lim_{\kappa \rightarrow \infty} \frac{\mathbb{E}_{\Xi_{\kappa, \tau}(x)} M_{f, \tau}}{\mathbb{E}_{\Xi_{\kappa, \tau}(x)} M_{\mathbf{1}, \tau}} = \lim_{\kappa \rightarrow \infty} \frac{\mathbb{E}_{\tilde{\Xi}_{\kappa, \tau}(x)} A_{f, \tau, n}}{\mathbb{E}_{\tilde{\Xi}_{\kappa, \tau}(x)} A_{\mathbf{1}, \tau, n}} = \tilde{f}(x),$$

where the quantum observables  $M_{f, \tau}, M_{\mathbf{1}, \tau} \in \mathfrak{B}_\tau$  and  $A_{f, \tau, n}, A_{\mathbf{1}, \tau, n} \in \mathfrak{F}_\tau$  are determined from (14) for  $f = \iota\tilde{f} \in \mathfrak{A}$ .

*Proof.* By translation invariance of the kernel we may assume, without loss of generality, that the origin lies in  $X$  and the evaluation point is  $x = 0$ .

Let  $h_\kappa(\theta) = e^{\kappa \cos \theta}$  and observe that the feature vector  $F_{\kappa, \tau}(0)$  is equal to  $h_\kappa / \|h_\kappa\|_{\mathcal{H}_\tau}$ . Moreover, we have  $h_\kappa = \sqrt{h_{2\kappa}}$ , so

$$F_{\kappa, \tau}(0) = \frac{\sqrt{\|\iota h_{2\kappa}\|_{L^1(\mu)}}}{\|h_\kappa\|_{\mathcal{H}_\tau}} \sqrt{\frac{h_{2\kappa}}{\|\iota h_{2\kappa}\|_{L^1(\mu)}}} = \frac{\|\iota h_\kappa\|_{L^2(\mu)}}{\|h_\kappa\|_{\mathcal{H}_\tau}} \varrho_\kappa^{1/2},$$

where  $\varrho_\kappa = h_{2\kappa}/\|\iota h_{2\kappa}\|_{L^1(\mu)} \in \mathcal{H}_\tau$  is the representative of a probability density  $p_\kappa = \iota\varrho_\kappa \in L^1(\mu)$ . Thus, using (7), we get

$$\begin{aligned}\mathbb{E}_{\Xi_{\kappa,\tau}(0)} M_{f,\tau} &= \langle F_{\kappa,\tau}(0), K_\tau(\pi f) K_\tau^* F_{\kappa,\tau}(0) \rangle_{\mathcal{H}_\tau} = \langle K_\tau^* F_{\kappa,\tau}(0), (\pi f) K_\tau^* F_{\kappa,\tau}(0) \rangle_{L^2(\mu)} \\ &= \frac{\|\iota h_\kappa\|_{L^2(\mu)}^2}{\|h_\kappa\|_{\mathcal{H}_\tau}^2} \mathbb{E}_{\Gamma(p_\kappa)}(\pi f) = \frac{\|\iota h_\kappa\|_{L^2(\mu)}^2}{\|h_\kappa\|_{\mathcal{H}_\tau}^2} \mathbb{E}_{p_\kappa} f,\end{aligned}$$

and thus

$$\frac{\mathbb{E}_{\Xi_{\kappa,\tau}(0)} M_{f,\tau}}{\mathbb{E}_{\Xi_{\kappa,\tau}(0)} M_{\mathbf{1},\tau}} = \mathbb{E}_{p_\kappa} f.$$

Next, since 0 lies in the support of  $\mu$ , for every neighborhood  $O$  of 0 and  $\epsilon > 0$  there exists  $\kappa_* > 0$  such that for all  $\kappa \geq \kappa_*$ ,  $\int_O \varrho_\kappa d\mu \geq 1 - \epsilon$ . As a result, for every  $g \in C(\mathbb{T}^N)$ , we have  $|\int_{\mathbb{T}^N} g \varrho_\kappa d\mu - g(0)| \leq \epsilon \|g\|_{C(G)} + (\int_O \varrho_\kappa d\mu) \sup_{x \in O} |g(0) - g(x)|$ . Since  $O$  and  $\epsilon$  are arbitrary, it follows that  $\varrho_\kappa \rightarrow \delta_0$  as  $\kappa \rightarrow \infty$  in a distributional sense, so

$$\lim_{\kappa \rightarrow \infty} \frac{\mathbb{E}_{\Xi_{\kappa,\tau}(0)} M_{f,\tau}}{\mathbb{E}_{\Xi_{\kappa,\tau}(0)} M_{\mathbf{1},\tau}} = \lim_{\kappa \rightarrow \infty} \mathbb{E}_{p_\kappa} f = \tilde{f}(0),$$

as claimed. We deduce the second claim of the lemma from the fact that

$$\frac{\mathbb{E}_{\Xi_{\kappa,\tau}(x)} M_{f,\tau}}{\mathbb{E}_{\Xi_{\kappa,\tau}(x)} M_{\mathbf{1},\tau}} = \frac{\mathbb{E}_{\tilde{\Xi}_{\kappa,\tau}(x)} A_{f,\tau,n}}{\mathbb{E}_{\tilde{\Xi}_{\kappa,\tau}(x)} A_{\mathbf{1},\tau,n}}, \quad \forall n \in \{2, 3, \dots\}. \quad \square$$

Combining Lemma 10 with Proposition 9, the same feature maps can also be used to approximate pointwise evaluation of time-evolved continuous observables by taking an additional  $\tau \rightarrow 0^+$  limit.

**Corollary 11.** *With the assumptions and notation of Proposition 9 and Lemma 10, define  $\tilde{f}_{\kappa,\tau,n}^{(t)} \in C(\mathbb{T}^N)$  where  $\tilde{f}_{\kappa,\tau,n}^{(t)}(x)$  is equal to  $f_{\tau,n}^{(t)}$  obtained from the quantum state  $\tilde{\Xi}_{\kappa,\tau}(x)$ , i.e.,*

$$\tilde{f}_{\kappa,\tau,n}^{(t)} = \frac{\mathbb{E}_{\tilde{\mathcal{P}}_\tau^t(\tilde{\Xi}_{\kappa,\tau}(x))} A_{f,\tau,n}}{\mathbb{E}_{\tilde{\mathcal{P}}_\tau^t(\tilde{\Xi}_{\kappa,\tau}(x))} A_{\mathbf{1},\tau,n}}.$$

Then, for every  $x \in X$ ,  $\lim_{\kappa \rightarrow \infty} \lim_{\tau \rightarrow 0^+} \tilde{f}_{\kappa,\tau,n}^{(t)}(x) = U^t \tilde{f}(x)$ .

In the context of the numerical approximations from Section 5.4, we modify the constructions in Corollary 11 by replacing (i)  $M_{f,\tau}$  and  $A_{f,\tau,n}$  by the finite-rank quantum observables  $M_{f,\tau,l}$  and  $A_{f,\tau,n,l}$  obtained via (38) and (39), respectively; and (ii)  $F_{\kappa,\tau}$  by the projected feature map  $F_{\kappa,\tau,d,m}: \mathbb{T}^N \rightarrow \mathcal{H}_{\tau,m}$ , where  $F_{\kappa,\tau,d,m}(x) = Z_{\tau,d,m} F_{\kappa,\tau}(x) / \|Z_{\tau,d,m} F_{\kappa,\tau}(x)\|_{\mathcal{H}_\tau}$ . As above,  $F_{\kappa,\tau,d,m}$  lifts to a Fock-space-valued feature map  $\tilde{F}_{\kappa,\tau,d,m}: \mathbb{T}^N \rightarrow F(\mathcal{H}_\tau)$ , where

$$\tilde{F}_{\kappa,\tau,d,m}(x) = \sum_{n=1}^{\infty} w_n \xi_{\tau,n,d,m}^{\otimes n}. \quad (50)$$

Moreover,  $F_{\kappa,\tau,d,m}$  and  $\tilde{F}_{\kappa,\tau,d,m}$  induce quantum feature maps  $\Xi_{\kappa,\tau,d,m}: \mathbb{T}^N \rightarrow S_*(\mathfrak{B}_\tau)$  and  $\tilde{\Xi}_{\kappa,\tau,d,m}: \mathbb{T}^N \rightarrow S_*(\mathfrak{F}_\tau)$  analogously to  $\Xi_{\kappa,\tau}$  and  $\tilde{\Xi}_{\kappa,\tau}$ , leading to approximations  $\tilde{f}_{\kappa,\tau,d,m}^{(t)}$  and  $\tilde{f}_{\kappa,\tau,n,d,m}^{(t)}$  of  $f_{\kappa,\tau}^{(t)}$  and  $f_{\kappa,\tau,n}^{(t)}$ , respectively, given by

$$\tilde{f}_{\kappa,\tau,d,m}^{(t)}(x) = \frac{\mathbb{E}_{\mathcal{P}_{\tau,m}^t(\Xi_{\kappa,\tau,d,m}(x))} M_{f,\tau}}{\mathbb{E}_{\mathcal{P}_{\tau,m}^t(\Xi_{\kappa,\tau,d,m}(x))} M_{\mathbf{1},\tau}}, \quad \tilde{f}_{\kappa,\tau,n,d,m}^{(t)}(x) = \frac{\mathbb{E}_{\tilde{\mathcal{P}}_{\tau,m}^t(\tilde{\Xi}_{\kappa,\tau,d,m}(x))} A_{f,\tau,n}}{\mathbb{E}_{\tilde{\mathcal{P}}_{\tau,m}^t(\tilde{\Xi}_{\kappa,\tau,d,m}(x))} A_{\mathbf{1},\tau,n}}. \quad (51)$$

We further approximate  $\tilde{f}_{\kappa,\tau,d,m}^{(t)}$  and  $\tilde{f}_{\kappa,\tau,n,d,m}^{(t)}$  by  $\tilde{f}_{\kappa,\tau,d,m,l}^{(t)}$  and  $\tilde{f}_{\kappa,\tau,n,d,m,l}^{(t)}$ , computed from the quantum expectations of  $M_{f,\tau,l}$  and  $A_{f,\tau,n,l}$ , respectively, viz.

$$\tilde{f}_{\kappa,\tau,d,m,l}^{(t)}(x) = \frac{\mathbb{E}_{\mathcal{P}_{\tau,m}^t(\Xi_{\kappa,\tau,d,m}(x))} M_{f,\tau,l}}{\mathbb{E}_{\mathcal{P}_{\tau,m}^t(\Xi_{\kappa,\tau,d,m}(x))} M_{\mathbf{1},\tau,l}}, \quad \tilde{f}_{\kappa,\tau,n,d,m,l}^{(t)}(x) = \frac{\mathbb{E}_{\tilde{\mathcal{P}}_{\tau,m}^t(\tilde{\Xi}_{\kappa,\tau,d,m}(x))} A_{f,\tau,n,l}}{\mathbb{E}_{\tilde{\mathcal{P}}_{\tau,m}^t(\tilde{\Xi}_{\kappa,\tau,d,m}(x))} A_{\mathbf{1},\tau,n,l}}. \quad (52)$$

Note, in particular, that  $\tilde{f}_{\kappa,\tau,n,d,m,l}^{(t)}(x)$  is obtained via (40) for the quantum state  $\tilde{\Xi}_{\kappa,\tau,d,m}(x)$ . These approximations converge pointwise for  $x \in X$  to  $\tilde{f}_{\kappa,\tau,n}^{(t)}$  in the iterated limits of  $d \rightarrow \infty$  after  $m, l \rightarrow \infty$  (see Section 5.4).

## 6. Convergence analysis at fixed $d$

As discussed in Section 3.4, an interesting possibility of the tensor network framework is convergence as  $n$  increases (and possibly other parameters vary), with the dimension parameter  $d$  held fixed. In this section, we study this possibility in the context of the scheme described in Section 5.5 for pointwise approximation of bounded functions on  $\mathbb{T}^N$  using classical and quantum feature maps built from von Mises distributions. Specifically, the conjecture we wish to analyze is the pointwise convergence of  $\tilde{f}_{\kappa,\tau,n,d,m}^{(t)}$  from (51) as  $n, \frac{1}{\tau} \rightarrow \infty$  jointly in an appropriately chosen manner and  $\kappa, t, m$ , and (importantly)  $d$  held constant.

We focus on the simplest possible case of a circle rotation. In Section 6.1, we prove the following theorem.

**Theorem 12.** *Set  $N = 1$  and  $\Phi^t(\theta) = t + \alpha\theta \pmod{2\pi}$ . Then, with the notation given above, for every  $f \in L^\infty(\mathbb{T})$  there are constants  $c_1, c_2 \in \mathbb{R}_{>0}$  such that for every  $\theta \in \mathbb{T}$ ,  $\tilde{f}_{\kappa,\tau,n,d,m}^{(t)}(\theta)$  from (51) converges as  $\varepsilon \rightarrow 0^+$  to  $\mathbb{E}_{p_{\theta,2\kappa}}(U^t f)$  for  $p_{\theta,2\kappa} = \nu_{\sigma_{\theta,2\kappa}}$ , and  $(n, \tau) = (\lceil \frac{c_1}{\varepsilon} \rceil, c_2 \varepsilon^2)$ , and with  $d = 2, t, \kappa$ , and  $m \geq 2d + 1$  held constant.*

A similar argument to the  $N = 1$  case implies convergence for torus rotation dynamical systems of arbitrary dimension  $N$  with  $d$  at least  $\lceil 1 + \frac{4}{N} \rceil^N$  and  $n \sim \frac{1}{\varepsilon}, \tau \sim \varepsilon^2$ . We omit further discussion of this result in the interest of brevity. In Section 6.2, we will consider the challenges for analytically proving convergence for a generic smooth dynamical system.

### 6.1. Circle rotation

Multiplicativity of the Koopman operator on  $L^\infty(\mu)$  and the following lemma are the main components for proving convergence analytically for the circle rotation. These two facts also require the estimate to be done with the infinity norm instead of the weaker two-norm which would otherwise be sufficient.

**Lemma 13.** *Let  $y, \tilde{y} \in \mathbb{C}$ . If  $|y - \tilde{y}| \leq \frac{1}{n}$  then  $|y^n - \tilde{y}^n| \leq en \cdot \min\{|y|^n, |\tilde{y}|^n\} |y - \tilde{y}|$ .*

*Proof.* Without loss of generality  $|y|^n \leq |\tilde{y}|^n$ , and so

$$\begin{aligned} |y^n - \tilde{y}^n| &= \left| \sum_{m=1}^n \binom{n}{m} y^{n-m} (\tilde{y} - y)^m \right| \leq n |\tilde{y} - y| \sum_{m=1}^n \frac{(n-1) \cdots (n-m+1)}{m!} |y|^{n-m} \frac{1}{n^{(m-1)}} \\ &\leq en \cdot \min\{|y|^n, |\tilde{y}|^n\} |y - \tilde{y}|. \end{aligned} \quad \square$$

By translation invariance of the kernel  $k_\tau$ , the associated integral operator  $\mathcal{K}_\tau: L^2(\mu) \rightarrow L^2(\mu)$  commutes with the Koopman operator  $U^t$  of the circle rotation. As result, for any of the approximation schemes in Sections 5.2.1 and 5.2.2, the regularized generator  $V_\tau$  commutes with  $\mathcal{K}_\tau$ , and we may choose the Fourier functions  $\{\phi_j\}_{j \in \mathbb{Z}}$  and the scaled Fourier functions  $\{\psi_j = \sqrt{\lambda_\tau(j)} \varphi_j\}_{j \in \mathbb{Z}}$  as eigenfunctions of  $V_{\tau,m}$  and  $W_{\tau,m}$ , respectively, for any  $\tau > 0$  and  $m \in \mathbb{N}$ . The Dirichlet energies of the Fourier functions are  $\mathcal{E}_\tau(\phi_j) = 1/\lambda_\tau(j)$ , giving the eigenfunctions  $\zeta_{\tau,m,0}, \zeta_{\tau,m,1,j}, \zeta_{\tau,m,2}, \zeta_{\tau,m,3}, \zeta_{\tau,m,4}, \dots$  of  $W_{\tau,m}$  as  $\psi_{0,\tau}, \psi_{1,\tau}, \psi_{-1,\tau}, \psi_{2,\tau}, \psi_{-2,\tau}, \dots$ , respectively, in accordance with our energy-based ordering from Section 5.2. For simplicity of exposition, we will assume that  $V_\tau$  is obtained via the generator compactification scheme from Section 5.2.1, so that the corresponding eigenfrequencies  $\omega_{0,\tau,m}, \dots, \omega_{4,\tau,m}$  are  $0, \alpha\lambda_\tau(1), -\alpha\lambda_\tau(-1), 2\alpha\lambda_\tau(2), -2\alpha\lambda_\tau(-2), \dots$ . The analysis in the case of the resolvent compactification scheme from Section 5.2.2 proceeds in a similar manner after modification of the eigenfrequencies. For any value of the dimension parameter  $d \leq (m-1)/2$ , the projection of  $f = \sum_{j \in \mathbb{Z}} f_j \psi_j$  onto  $\mathcal{Z}_{\tau,d,m} \subset \mathcal{H}_\tau$  is given by  $Z_{\tau,d,m} f = \sum_{j=-d}^d f_j \psi_j$ . Moreover, for any  $j_1, \dots, j_n \in \mathbb{Z}$  with  $|j_i| \leq d$ , the lifted Koopman operator  $\tilde{U}_\tau^t: F(\mathcal{H}_\tau) \rightarrow F(\mathcal{H}_\tau)$  on the Fock space satisfies

$$\tilde{U}_{\tau,m}^t(\psi_{j_1} \otimes \cdots \otimes \psi_{j_n}) = e^{i\alpha t \sum_{r=-d}^d j_r \lambda_\tau(j_r)} \psi_{j_1} \otimes \cdots \otimes \psi_{j_n}. \quad (53)$$

Next, set the evaluation point  $x = 0$  without loss of generality, define  $p_\kappa := p_{0,\kappa}$ , and note, using (8), that

$$\mathbb{E}_{p_{2\kappa}}(U^t f) = \mathbb{E}_{\Gamma(p_{2\kappa})}(\mathcal{U}^t f) = \langle U^{-t} p_{2\kappa}^{1/2}, M_f U^{-t} p_{2\kappa}^{1/2} \rangle_{L^2(\mathbb{T})} = \langle \iota U^{-t} \tilde{\sigma}_\kappa, M_f \iota U^{-t} \tilde{\sigma}_\kappa \rangle_{L^2(\mathbb{T})},$$

where

$$\tilde{\sigma}_\kappa = \frac{h_\kappa}{c_\kappa}, \quad h_\kappa(\theta) = e^{\kappa \cos \theta}, \quad c_\kappa = \|\iota h_\kappa\|_{L^2(\mathbb{T})}.$$

Moreover, we have  $F_{\kappa,\tau}(0) = h_\kappa / \|h_\kappa\|_{\mathcal{H}_\tau}$  so that

$$\tilde{F}_{\kappa,\tau,d,m}(0) = \sum_{n=1}^{\infty} w_n \tilde{\sigma}_{\kappa,\tau,n,d}, \quad \tilde{\sigma}_{\kappa,\tau,n,d} = \frac{1}{\|Z_{\tau,d,m} h_\kappa^{1/n}\|_{\mathcal{H}_\tau}^n} (Z_{\tau,d,m}(h_\kappa^{1/n}))^{\otimes n},$$

giving

$$\begin{aligned} \tilde{f}_{\kappa,\tau,n,d,m}^{(t)}(0) &= \frac{\mathbb{E}_{\tilde{\sigma}_{\kappa,\tau,d,m}(0)} A_{f,\tau,n}}{\mathbb{E}_{\tilde{\sigma}_{\kappa,\tau,d,m}(0)} A_{\mathbf{1},\tau,n}} = \frac{\langle K_\tau^* \Delta_n^* \tilde{U}_\tau^{-t} \tilde{F}_{\kappa,\tau,d,m}(0), M_f K_\tau^* \Delta_n^* \tilde{U}_\tau^{-t} \tilde{F}_{\kappa,\tau,d,m}(0) \rangle_{L^2(\mathbb{T})}}{\langle K_\tau^* \Delta_n^* \tilde{U}_\tau^{-t} \tilde{F}_{\kappa,\tau,d,m}(0), K_\tau^* \Delta_n^* \tilde{U}_\tau^{-t} \tilde{F}_{\kappa,\tau,d,m}(0) \rangle_{L^2(\mathbb{T})}} \\ &= \frac{\langle K_\tau^* \Delta_n^* \tilde{U}_\tau^{-t} \tilde{\sigma}_{\kappa,\tau,n,d}, M_f K_\tau^* \Delta_n^* \tilde{U}_\tau^{-t} \tilde{\sigma}_{\kappa,\tau,n,d} \rangle_{L^2(\mathbb{T})}}{\langle K_\tau^* \Delta_n^* \tilde{U}_\tau^{-t} \tilde{\sigma}_{\kappa,\tau,n,d}, K_\tau^* \Delta_n^* \tilde{U}_\tau^{-t} \tilde{\sigma}_{\kappa,\tau,n,d} \rangle_{L^2(\mathbb{T})}}. \end{aligned}$$

Our first goal is to estimate the difference between the  $n^{\text{th}}$  root of  $c_\kappa U^{-t} \tilde{\sigma}_\kappa$  and  $c_\kappa^{1/n} U_\tau^{-t} Z_{\tau,d,m}(\tilde{\sigma}_\kappa^{1/n})$ . Due to multiplicativity of  $U^{-t}$  on continuous functions,  $(U^{-t} \tilde{\sigma}_\kappa)^{1/n} = U^{-t}(\tilde{\sigma}_\kappa^{1/n})$ , and using the series representation of  $I_j$  from (46), we get

$$c_\kappa^{1/n} (U^{-t} \tilde{\sigma}_\kappa)^{1/n}(\theta) = e^{\kappa \cos(\theta - \alpha t)/n} = \sum_{j=-\infty}^{\infty} I_{|j|}(\kappa/n) e^{ij(\theta - \alpha t)}.$$

Similarly, using the eigenvalue relation  $U_\tau^t \psi_j = e^{-i\alpha t j \lambda_\tau(j)} \psi_j$ , we obtain

$$c_\kappa^{1/n} U_\tau^{-t} Z_{\tau,d,m}(\tilde{\sigma}_\kappa^{1/n})(\theta) = \sum_{j=-d}^d I_{|j|}(\kappa/n) e^{ij(\theta - \alpha t)}.$$

The series representation of  $I_j$  also leads to the following useful inequality:

$$\left| \sum_{j=d}^{\infty} I_j(\kappa) \right| = \left| \sum_{j=d}^{\infty} \sum_{r=0}^{\infty} \frac{(\kappa/2)^j (\kappa/2)^{2r}}{(r+j)! r!} \right| \leq \left| (\kappa/2)^d \sum_{j=d}^{\infty} \sum_{r=0}^{\infty} \frac{(\kappa/2)^{j-d} (\kappa/2)^{2r}}{(j-d)! (r+d)! r!} \right| \leq e^{\kappa/2} I_d(\kappa). \quad (54)$$

We may now estimate the difference of  $n^{\text{th}}$  roots mentioned above. For simplicity, we can assume that  $n \geq \kappa$ , however the following estimates do not rely on this being the case. Using (47), (54) and Lemma 13,

we obtain

$$\begin{aligned}
& \left| c_\kappa^{1/n} (U^{-t} \tilde{\sigma}_\kappa)^{1/n}(\theta) - c_\kappa^{1/n} U_\tau^{-t} Z_{\tau,d,m}(\tilde{\sigma}_\kappa^{1/n})(\theta) \right| \\
&= \left| \sum_{j=-\infty}^{\infty} I_{|j|}(\kappa/n) e^{-i\alpha j t} e^{ij\theta} - \sum_{j=-d}^d I_{|j|}(\kappa/n) e^{i\alpha j \lambda_\tau(j)t} e^{ij\theta} \right| \\
&\leq \left| \sum_{j=-d}^d I_{|j|}(\kappa/n) e^{ij\theta} \left( e^{-i\alpha j t} - e^{-i\alpha j \lambda_\tau(j)t} \right) \right| + 4 \left| \sum_{j=d}^{\infty} I_{|j|}(\kappa/n) \right| \\
&\leq 4e^{\kappa/2n} I_d(\kappa/n) + \sum_{j=-d}^d I_{|j|}(\kappa/n) \left| 1 - e^{-i\alpha j t(1-\lambda_\tau(j))} \right| \\
&\leq 4e^{\kappa/2n} I_d(\kappa/n) + 2 \max_{1 \leq j \leq d} |\sin(\alpha j t(1-\lambda_\tau(j))/2)| e^{\kappa/2n} I_0(\kappa/n) \\
&\leq 4e^{\kappa/n} \left( I_d(\kappa/n) + \max_{1 \leq j \leq d} |\sin(\alpha j t(1-\lambda_\tau(j))/2)| \right).
\end{aligned}$$

Fix  $\varepsilon > 0$ . For  $d \geq 2$  there exists an  $n$  such that

$$I_d(\kappa/n) \leq \frac{\kappa^d}{(2n)^d d!} e^{\kappa^2/4n^2} \leq \frac{\varepsilon}{ne^{\kappa+1}} \frac{c_\kappa}{8e^{\kappa/n}}.$$

Thus, for fixed  $\varepsilon > 0$ ,  $\alpha$ , and  $t$  there is a  $\tau > 0$  such that

$$\max_{1 \leq l \leq d} |\sin(\alpha l t(1-\lambda_\tau(l))/2)| < \frac{\varepsilon}{ne^{\kappa+1}} \frac{c_\kappa}{8e^{\kappa/n}}.$$

Then for such an  $n$  and  $\tau$ ,

$$\left| c_\kappa^{1/n} (U^{-t} \tilde{\sigma}_\kappa)^{1/n}(\theta) - c_\kappa^{1/n} U_\tau^{-t} Z_{\tau,d,m}(\tilde{\sigma}_\kappa^{1/n})(\theta) \right| \leq \frac{\varepsilon c_\kappa}{ne^{\kappa+1}} \quad (55)$$

Observe now that (53) implies

$$\begin{aligned}
\Delta_n^* \tilde{U}_{\tau,n}^{-t} \tilde{\sigma}_{\kappa,\tau,n,d}(\theta) &= \left( \frac{1}{\|Z_{\tau,d,m}(h_\kappa^{1/n})\|_{\mathcal{H}_\tau}} \sum_{j=-d}^d I_{|j|}(\kappa/n) e^{-i\alpha j \lambda_\tau(j)t} e^{ij\theta} \right)^n \\
&= \frac{1}{\|Z_{\tau,d,m}(h_\kappa^{1/n})\|_{\mathcal{H}_\tau}} U_\tau^{-t} Z_{\tau,d,m}(\tilde{\sigma}_\kappa^{1/n})
\end{aligned}$$

Using (55), it follows that

$$\left\| c_\kappa^{1/n} U^{-t} (\tilde{\sigma}_\kappa^{1/n}) - \|Z_{\tau,d,m}(h_\kappa^{1/n})\|_{\mathcal{H}_\tau} \left( \Delta_n^* \tilde{U}_{\tau,n}^{-t} (\tilde{\sigma}_{\kappa,\tau,n,d}) \right)^{1/n} \right\|_{C(\mathbb{T})} \leq \frac{\varepsilon c_\kappa}{ne^{\kappa+1}},$$

and thus, by Lemma 13,

$$\left\| U^{-t} \tilde{\sigma}_\kappa - \frac{\|Z_{\tau,d,m}(h_\kappa^{1/n})\|_{\mathcal{H}_\tau}^n}{c_\kappa} \Delta_n^* \tilde{U}_{\tau,n}^{-t} \tilde{\sigma}_{\kappa,\tau,n,d} \right\|_{C(\mathbb{T})} \leq \varepsilon.$$

Taking  $\eta = \iota U^{-t} \tilde{\sigma}_\kappa$  and  $\tilde{\eta} = \frac{\|Z_{\tau,d,m}(h_\kappa^{1/n})\|_{\mathcal{H}_\tau}^n}{c_\kappa} K_\tau^* \Delta_n^* \tilde{U}_{\tau,n}^{-t} (\tilde{\sigma}_{\kappa,\tau,n,d})$ , we have  $\|\eta - \tilde{\eta}\|_{L^\infty(\mathbb{T})} \leq \varepsilon$  and

$$|\langle \eta, f \eta \rangle_{L^2(\mathbb{T})} - \langle \tilde{\eta}, f \tilde{\eta} \rangle_{L^2(\mathbb{T})}| \leq 2\|f\|_{L^\infty(\mathbb{T})} \varepsilon,$$

and so

$$\begin{aligned} \left| \mathbb{E}_{p_{2\kappa}}(U^t f) - \tilde{f}_{\kappa,\tau,n,d,m}^{(t)}(0) \right| &= \left| \langle \iota U^{-t} \tilde{\sigma}_\kappa, f \iota U^{-t} \tilde{\sigma}_\kappa \rangle_{L^2(\mathbb{T})} - \frac{\langle K_\tau^* \Delta_n^* \tilde{U}_\tau^{-t} \tilde{\sigma}_{\kappa,\tau,n,d}, f K_\tau^* \Delta_n^* \tilde{U}_\tau^{-t} \tilde{\sigma}_{\kappa,\tau,n,d} \rangle_{L^2(\mathbb{T})}}{\langle K_\tau^* \Delta_n^* \tilde{U}_\tau^{-t} \tilde{\sigma}_{\kappa,\tau,n,d}, K_\tau^* \Delta_n^* \tilde{U}_\tau^{-t} \tilde{\sigma}_{\kappa,\tau,n,d} \rangle_{L^2(\mathbb{T})}} \right| \\ &= \left| \langle \iota U^{-t} \tilde{\sigma}_\kappa, f \iota U^{-t} \tilde{\sigma}_\kappa \rangle_{L^2(\mathbb{T})} - \frac{\langle \tilde{\eta}, f \tilde{\eta} \rangle_{L^2(\mathbb{T})}}{\langle \tilde{\eta}, \tilde{\eta} \rangle_{L^2(\mathbb{T})}} \right| \\ &\leq 4 \|f\|_{L^\infty(\mathbb{T})} \varepsilon \end{aligned}$$

since  $|1 - \|\tilde{\eta}\|_{L^2(\mathbb{T})}| \leq 2\varepsilon$ .

Finally, we analyze  $c_\kappa$  to determine the rate of convergence in terms of  $n$  and  $\tau$ . Since  $\|\iota \tilde{\sigma}_\kappa^2\|_{L^1(\mathbb{T})} = 1$ , we have  $I_0(2\kappa) = c_\kappa^2$ . Observe that

$$\sqrt{I_0(2\kappa)} = \left\| \left( \frac{\kappa^m}{m!} \right)_m \right\|_2 \geq \frac{\left\| \left( \frac{\kappa^m}{(m+1)!} \right)_m \right\|_1}{\left\| \left( \frac{1}{m+1} \right)_m \right\|_2} \geq \frac{\sqrt{6}(e^\kappa - 1)}{\pi\kappa}.$$

Hence, the two requirements for  $n$  and  $\tau$  above become

$$n^{d-1} \geq \frac{8\kappa^d e^{\kappa/n+\kappa^2/4n^2}}{d!\varepsilon} \frac{e^{\kappa+1}}{\sqrt{I_0(2\kappa)}}, \quad |1 - \lambda_\tau(d)| \leq \frac{\sqrt{6}\varepsilon(1 - e^{-\kappa})}{8e|\alpha t| d n e^{\kappa/n}},$$

and it suffices for

$$n^{d-1} \geq \frac{8e\pi\kappa^{d+1} e^{\kappa/n+\kappa^2/4n^2}}{\sqrt{6}d!\varepsilon(1 - e^{-\kappa})}, \quad \tau \leq \frac{\sqrt{6}\varepsilon(1 - e^{-\kappa})}{8\pi e|\alpha t|\kappa d^{1+p} n e^{\kappa/n}}.$$

With these inequalities we conclude how the joint  $(n, \tau)$  limit must be taken. Asymptotically, for large  $n$ , small  $\tau$ , and  $d = 2$  we see that

$$n \sim \left( \frac{\kappa^{d+1}}{d!\varepsilon} \right)^{1/(d-1)}, \quad \tau \sim \frac{\varepsilon}{|\alpha t|\kappa d^{1+p} n},$$

and Theorem 12 follows with a joint limit  $n \sim \frac{1}{\varepsilon}$  and  $\tau \sim \varepsilon^2$ .

## 6.2. Towards a general convergence analysis

Let  $(X, \mu, \Phi^t)$  be a measure-preserving, ergodic dynamical system as in Section 5.1. Using the  $L^\infty(\mu)$  norm for the main estimate in Section 6.1 is likely much stronger and more restrictive than is necessary for a general such system. This choice is due to the ability to convert an estimate for  $\|y^{1/n} - \tilde{y}^{1/n}\|_{L^\infty(\mu)}$  into an estimate for  $\|y - \tilde{y}\|_{L^\infty(\mu)}$ . One encouraging feature is the convergence of  $\sigma^{1/n} \rightarrow 1$  for a positive element  $\sigma \in L^\infty(\mu)$  and the fact that  $U^t \mathbf{1} = \mathbf{1} = K_\tau^* U_\tau^t \mathbf{1}$ . As  $n$  grows,  $\mathbf{1}$  becomes the main component of  $\sigma^{1/n}$  in  $L^2$ -norm and is preserved by the approximate Koopman operator.

In analogy with Sobolev-type estimates of  $L^\infty$  norms, we may be able to obtain  $L^\infty(\mu)$  estimates from  $L^2(\mu)$  estimates such as

$$\left\| U^t(\sigma^{1/n}) - K_\tau^* \tilde{U}_{\tau,1}^{-t} Z_{\tau,d,m}(\sigma^{1/n}) \right\|_{L^2(\mu)} \leq \left\| (U^t K_\tau^* - K_\tau^* U_{\tau,1}^{-t}) \sigma_\perp^{1/n} \right\|_{L^2(\mu)} + \left\| \sigma_\perp^{1/n} - Z_{\tau,d,m}(\sigma_\perp^{1/n}) \right\|_{L^2(\mu)}$$

and of its derivatives, where  $\sigma_\perp^{1/n} = \sigma^{1/n} - \langle \mathbf{1}, \sigma^{1/n} \rangle_{L^2(\mu)} \mathbf{1}$ . This separates the estimate into two components, convergence of the smoothed Koopman operator, and the efficiency of approximating  $\sigma_\perp^{1/n}$  with  $2d + 1$  eigenfunctions of  $U_\tau^t$ . In general, we expect a joint limit in  $n$ ,  $d$ , and  $\tau$  to be necessary. Further analytical results from this approach are unlikely without specializing to specific families of dynamical systems. We now turn to numerical experiments to verify the torus rotation case and explore more nontrivial dynamics.



## 7. Numerical experiments

We present applications of the tensor network approximation framework described in the preceding sections to two dynamical systems on the 2-torus: an ergodic rotation (Section 7.3.5) and a Stepanoff flow [82] (Section 7.3.6). These examples were chosen on the basis of exhibiting qualitatively different types of spectral characteristics, the former being a prototypical example of a pure-point-spectrum system while the latter is characterized by absence of non-constant continuous Koopman eigenfunctions. Yet, despite their different spectral characteristics, both systems have the Haar probability measure on  $\mathbb{T}^2$  as an ergodic invariant measure  $\mu$ , meaning that in both cases  $G = X = \mathbb{T}^2$  and our method can be implemented using the characters (Fourier functions) of the group as basis functions. This in turn allows assessing the behavior of our approach independently of errors due to data-driven computation of basis functions.

As in Section 4.2, for  $j = (j_1, j_2) \in \mathbb{Z}^2$ , we let  $\gamma_j \in \widehat{G}$  be the Fourier function with wavenumbers  $j_1$  and  $j_2$  along the two torus dimensions,  $\gamma_j(x) = e^{ij \cdot x}$  where  $x = (\theta_1, \theta_2) \in [0, 2\pi)^2$ . We will sometimes use overarrows to distinguish multi-indices from integer-valued indices, i.e.,  $\vec{j} \equiv j = (j_1, j_2)$ . In what follows,  $\mathbf{A}^\dagger$  will denote the complex-conjugate transpose of a matrix  $\mathbf{A}$ . Technical details on numerical implementation and pseudocode are included in Appendix A.

### 7.1. Dynamical systems

*Torus rotation.* Our first example is an ergodic torus rotation generated by the smooth vector field  $\vec{V}: G \rightarrow TG$ , where

$$\vec{V} = \frac{\partial}{\partial \theta_1} + \alpha \frac{\partial}{\partial \theta_2}. \quad (56)$$

Here,  $\alpha$  is an irrational parameter which we set to  $\sqrt{30} \approx 5.477$ . A quiver plot of the vector field for our choice of  $\alpha$  is displayed in Fig. 4(left).

The resulting flow is given by

$$\Phi(x) = x + \alpha t \pmod{2\pi}, \quad (57)$$

and has the Haar measure  $\mu$  as its unique Borel ergodic invariant probability measure. Moreover, the generator  $V$  on  $H$  has pure point spectrum with eigenfrequencies  $\omega_{\vec{j}} = j_1 + j_2\alpha$  and corresponding eigenfunctions  $u_{\vec{j}} = \nu \gamma_{\vec{j}} \in \mathfrak{A} \subset H$  with continuous representatives given by the characters  $\gamma_{\vec{j}} \in \widehat{G}$ . In this system, any pair of eigenfunctions  $\{u_{\vec{j}_1}, u_{\vec{j}_2}\}$  with rationally independent eigenfrequencies  $\omega_{\vec{j}_1}$  and  $\omega_{\vec{j}_2}$  provides a conjugacy with a rotation system in the form of (2). The pair  $\{\omega_{\vec{j}_1}, \omega_{\vec{j}_2}\}$  generates the point spectrum of  $V$  as an additive group,  $\sigma_p(V) = \{i(r_1\omega_{\vec{j}_1} + r_2\omega_{\vec{j}_2})\}_{r_1, r_2 \in \mathbb{Z}}$ , and pointwise products of the corresponding eigenfunctions generate an orthonormal basis of  $H$  as a multiplicative group,  $\{u_{\vec{j}_1}^{r_1} u_{\vec{j}_2}^{r_2}\}_{r_1, r_2 \in \mathbb{Z}}$ .

It should be noted that despite the highly structured nature of this system, numerically approximating its point spectrum and associated eigenfunctions is non-trivial, for  $\sigma_p(V)$  is a dense subset of the imaginary line and thus there are no isolated points in the spectrum.

*Stepanoff flow.* Our second example comes from a class of Stepanoff flows on the 2-torus studied in a paper of Oxtoby [82]. The dynamical vector field  $\vec{V}: G \rightarrow TG$  is defined in terms of smooth functions  $V_1, V_2 \in C^\infty(\mathbb{T}^2)$  as

$$\begin{aligned} \vec{V} &= V_1 \frac{\partial}{\partial \theta_1} + V_2 \frac{\partial}{\partial \theta_2}, \\ V_1(x) &= V_2(x) + (1 - \alpha)(1 - \cos \theta_2), \quad V_2(x) = \alpha(1 - \cos(\theta_1 - \theta_2)), \end{aligned} \quad (58)$$

where  $\alpha$  is a real parameter. One readily verifies that  $\vec{V}$  has zero divergence with respect to the Haar measure  $\mu$ ,

$$\operatorname{div}_\mu \vec{V} = \frac{\partial V_1}{\partial \theta_1} + \frac{\partial V_2}{\partial \theta_2} = 0,$$

which implies that  $\mu$  is an invariant measure under the associated flow  $\Phi^t$ . Moreover, the system exhibits a fixed point at  $x = 0$ . In [82] it is shown that the Haar measure is the unique invariant Borel probability

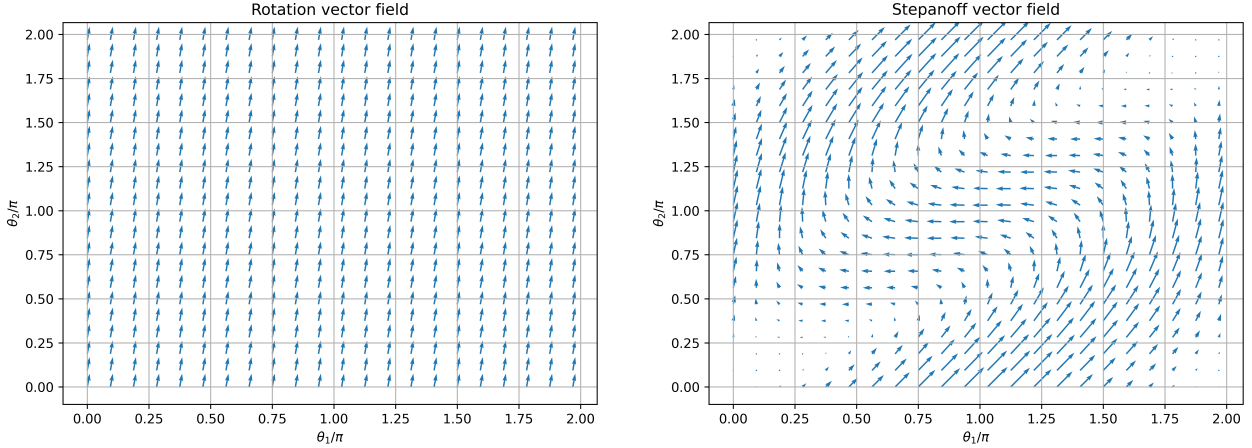


Figure 4: Quiver plots of the dynamical vector fields  $\vec{V}$  for the ergodic torus rotation (left) and Stepanoff flow (right) examples.

measure of this flow that assigns measure 0 to the singleton set  $\{0\} \subset G$  containing the fixed point. In our experiments, we set  $\alpha = \sqrt{20}$  leading to the vector field depicted in Fig. 4(right). Notice the characteristic “S”-shape formed by the arrows as well as the presence of the fixed point at  $x = 0$ .

Since any continuous, non-constant Koopman eigenfunction induces a semi-conjugacy with circle rotation (i.e., a version of (2) with  $N = 1$ ), the existence of the fixed point at  $x = 0$  implies that the system has no continuous Koopman eigenfunctions; i.e., it is topologically weak-mixing. To our knowledge, there are no results in the literature on the measure-theoretic mixing properties of Stepanoff flows. While topological mixing is, in general, independent of measure-theoretic mixing, the absence of continuous Koopman eigenfunctions implies at the very least that data-driven spectral computations are non-trivial for this class of systems (even if eigenfunctions exist in  $L^2(\mu)$ ).

## 7.2. Spectral decomposition

In each example, we work with the RKHA  $\mathcal{H}_\tau$  on  $G$  induced from the family of weights  $\lambda_\tau$  in (21). Fixing a maximal wavenumber parameter  $J \in \mathbb{N}$  and setting  $m = (2J + 1)^2$ , we order the characters  $\gamma_{\vec{j}_0}, \dots, \gamma_{\vec{j}_{m-1}}$  in the set  $\hat{\Gamma}_J = \{\gamma_{\vec{j}} \in \hat{G} : \gamma_{\vec{j}}(x) = e^{i\vec{j} \cdot x} : \vec{j} = (j_1, j_2) : |j_i| \leq J\} \subset \hat{G}$  in order of increasing  $|j_1| + |j_2|$ . This leads to the  $m$ -dimensional subspace  $\mathcal{H}_{\tau,m} = \text{span} \hat{\Gamma}_J \subset \mathcal{H}_\tau$  on which we define the approximate generator  $W_{\tau,m}$  for each system. For consistency with the notation for kernel eigenfunctions in (24), we denote the ordered characters in  $\hat{\Gamma}_J$  as  $\varphi_i \equiv \gamma_{\vec{j}_i}$  and their  $L^2$  equivalence classes as  $\phi_i \equiv \iota \varphi_i$ . We also let  $\Lambda_{i,\tau} \equiv \lambda_\tau(\vec{j}_i)$  be the corresponding eigenvalues.

In the experiments reported here, we set the RKHA parameters  $p = 0.75$ ,  $\tau = 0.001$ , and the maximal wavenumber parameter  $J = 128$  corresponding to approximation space dimension  $m = 16,641$ . We build  $W_{\tau,m}$  using the resolvent compactification procedure described in Section 5.2.2 with resolvent parameter  $z = 0.1$ . This leads to the matrix generalized eigenvalue problem (34) for approximating the eigendecomposition of the operator  $Q_{z,\tau}$ , yielding eigenvalues  $\beta_{j,z,\tau,m} \in i\mathbb{R}$  and generalized eigenvectors  $\tilde{c}_j \in \mathbb{C}^m$ .

In our examples, the components of the dynamical vector field  $\vec{V}$  are polynomials in the characters  $\gamma_j$ , which allows us to compute the elements of the  $\mathbf{V}_m$  and  $\mathbf{B}_m$  matrices appearing in (34) analytically. In the case of the rotation vector field (56), the characters are eigenfunctions of the generator and we immediately obtain

$$\langle \varphi_r, \iota \vec{V} \cdot \nabla \varphi_s \rangle_H = i(j_1 + j_2 \alpha) \delta_{rs}, \quad (59)$$

where  $(j_1, j_2) = \vec{j}_s$ . In the case of the Stepanoff vector field (58), we make use of the relations

$$\cos \theta_2 = \frac{\gamma_{0,1}(x) + \gamma_{0,-1}(x)}{2}, \quad \cos(\theta_1 - \theta_2) = \frac{\gamma_{(1,-1)}(x) + \gamma_{(-1,1)}(x)}{2}, \quad x = (\theta_1, \theta_2),$$

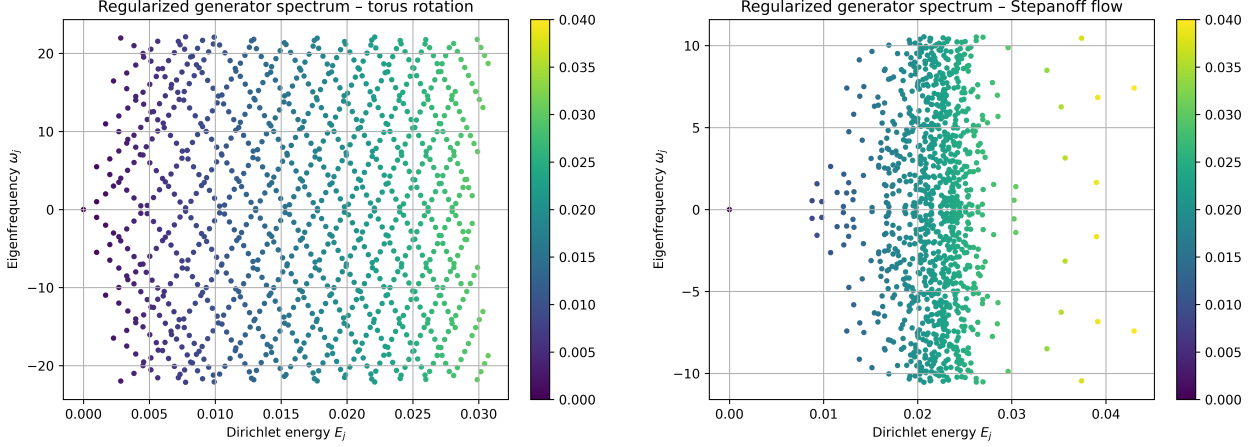


Figure 5: Spectrum of the regularized generator  $W_{\tau,m}$  for the torus rotation (left) and Stepanoff flow (right). The eigenfrequencies  $\omega_j$  are plotted versus the corresponding Dirichlet energies  $E_j$  from the RKHA  $\mathcal{H}_\tau$ . The plotted points are colored by Dirichlet energy to facilitate comparison between the two cases.

together with the group structure of  $\widehat{G}$ ,  $\gamma_{\vec{j}_r + \vec{j}_s} = \gamma_{\vec{j}_r} \gamma_{\vec{j}_s}$ , to compute

$$\begin{aligned}
& \langle \varphi_r, \ell \vec{V} \cdot \nabla \varphi_s \rangle_H \\
&= ij_1 \delta_{rs} - \frac{ij_1 \alpha}{2} (\delta_{i_1, 1+j_1} \delta_{i_2, j_2-1} + \delta_{i_1, j_1-1} \delta_{i_2, j_2+1}) - \frac{ij_1(1-\alpha)}{2} (\delta_{i_1, j_1} \delta_{i_2, j_2+1} + \delta_{i_1, j_1} \delta_{i_2, j_2-1}) \\
&+ ij_2 \delta_{rs} - \frac{ij_2 \alpha}{2} (\delta_{i_1, j_1+1} \delta_{i_2, j_2-1} + \delta_{i_1, j_1-1} \delta_{i_2, j_2+1}),
\end{aligned} \tag{60}$$

where  $(i_1, i_2) = \vec{j}_r$  and  $(j_1, j_2) = \vec{j}_s$ . The above formulas are sufficient to compute the  $\mathbf{V}_m$  and  $\mathbf{B}_m$  matrices for the torus rotation and Stepanoff flow.

We solve (33) using iterative methods, computing  $n_{\text{eig}} = 1024$  eigenvalues  $\beta_{j,z,\tau,m}$  of largest magnitude and the corresponding generalized eigenvectors  $\tilde{\mathbf{c}}_{j,z,\tau,m} = (\tilde{c}_{0j}, \dots, \tilde{c}_{m-1,j})^\top$  for each system. We then compute the eigenfrequencies  $\tilde{\omega}_{j,z,\tau,m} = \overline{q_z}^{-1}(\beta_{j,z,\tau,m})$  (cf. (32)) and corresponding eigenfunctions  $\tilde{\zeta}_{j,z,\tau,m} = \sum_{i=0}^{m-1} \tilde{c}_{ij} \varphi_i \in \mathcal{H}_{\tau,m}$ . Note that our choice of computing largest-magnitude eigenvalues  $\beta_{j,z,\tau,m}$  is equivalent to computing lowest-magnitude nonzero eigenfrequencies  $\tilde{\omega}_{j,z,\tau,m}$ . Moreover, as noted in Section 3.5, our computational representation of  $\tilde{\zeta}_{j,z,\tau,m}$  is through function objects (here, in Python). We order the computed eigenvalue/eigenfunction pairs for the two systems in order of increasing Dirichlet energy, computed by applying (29) to the generalized eigenvectors  $\tilde{\mathbf{c}}_{j,z,\tau,m}$ . The entire procedure is summarized in Algorithm 1. For the remainder of this section we will sometimes use the abbreviated notation  $\omega_j \equiv \tilde{\omega}_{j,z,\tau,m}$  and  $\zeta_j \equiv \tilde{\zeta}_{j,z,\tau,m}$ .

Figure 5 shows scatterplots of the  $n_{\text{eig}}$  computed eigenfrequencies for the torus rotation (left) and Stepanoff flow (right) plotted against their corresponding Dirichlet energies. Perhaps unsurprisingly, the generator spectrum for the torus rotation exhibits regular structure, with the eigenfrequencies visually forming spectral “lines” consistent with well-defined functional relationships between frequency and Dirichlet energy. On the other hand, the Stepanoff spectrum appears markedly less structured, which could be the outcome of discretization of a continuum.

In Fig. 6, we plot the real parts of representative eigenfunctions  $\zeta_j$  from the spectra in Fig. 5 on a regular  $512 \times 512$  grid on  $\mathbb{T}^2$ . In the case of the torus rotation (left-hand column), the plots well-approximate the planar wave patterns expected for real parts of Fourier functions. In particular, eigenfunctions  $\zeta_2$  (top left) and  $\zeta_4$  (center left) exhibit wavenumber-1 oscillations along the  $\theta_1$  and  $\theta_2$  directions, which is consistent with the corresponding eigenfrequencies  $\omega_2 \approx 1.00$  and  $\omega_4 \approx 5.48$ , respectively. Meanwhile,  $\zeta_{12}$  (bottom left) exhibits wavenumber-1 oscillations along both the  $\theta_1$  and  $\theta_2$  directions and a corresponding eigenfrequency  $\omega_{12} \approx \omega_4 - \omega_2$ , consistent with a product structure  $\zeta_{12} \approx \zeta_2^* \zeta_4$ .

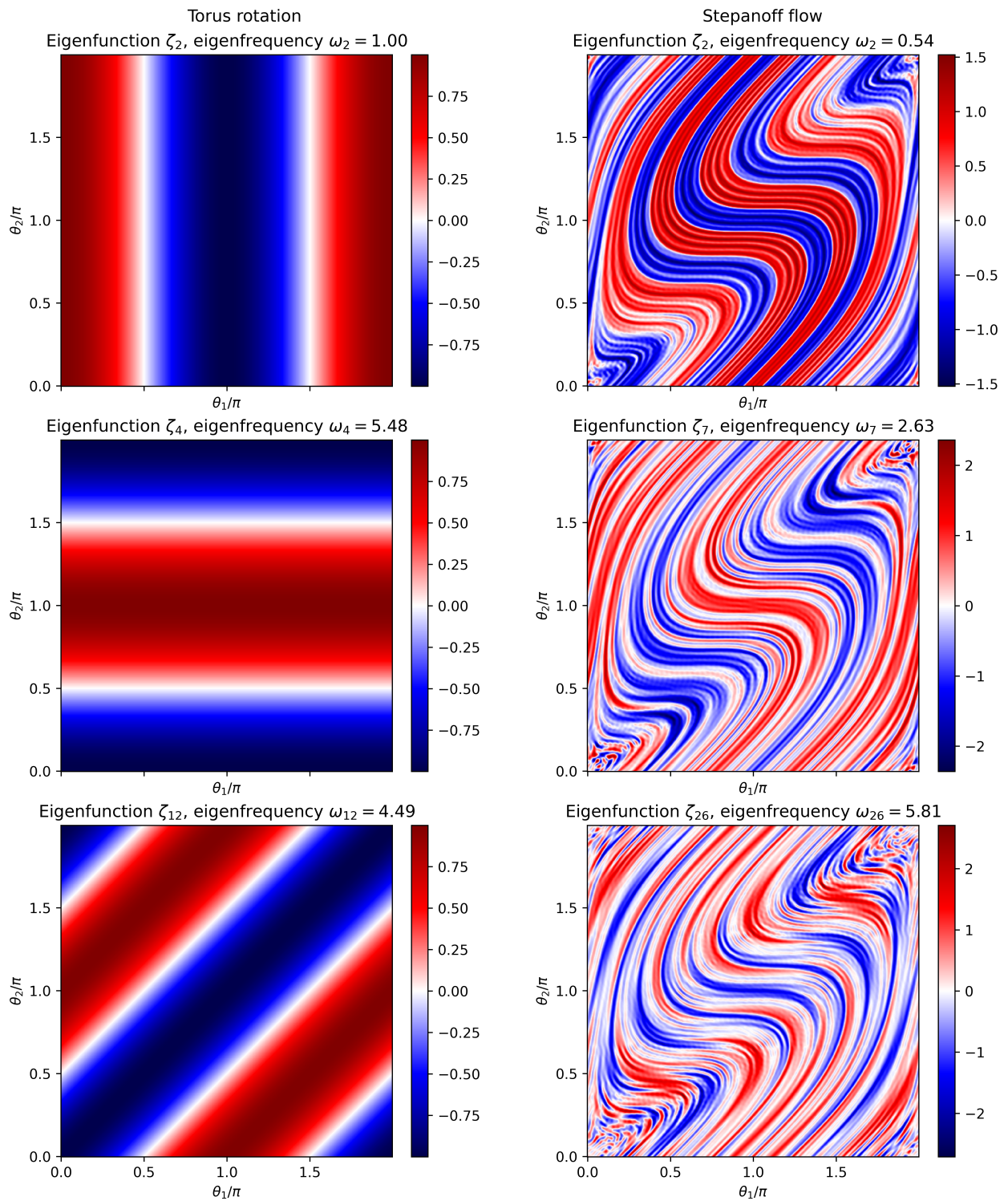


Figure 6: Real parts of representative eigenfunctions  $\zeta_j$  of the regularized generator for the torus rotation (left) and Stepanoff flow (right).

Turning to the Stepanoff flow, the eigenfunctions in this case (right-hand column in Fig. 6) exhibit considerably more intricate spatial structure than their rotation counterparts, in line with the fact that the unperturbed generator  $V$  does not have non-constant continuous eigenfunctions. The plotted eigenfunctions are the second, seventh, and 26th with respect to the Dirichlet energy ordering; i.e., are among the least oscillatory examples among the 1024 computed eigenfunctions. In regions away from the fixed point at  $x = 0$ , the level sets of the plotted eigenfunctions appear to be broadly aligned with the dynamical flow; compare, e.g.,  $\zeta_2$  in the top-right panel of Fig. 6 with the quiver plot of the Stepanoff vector field in Fig. 4. In regions closer to the fixed point, the eigenfunctions develop small-scale oscillations, whose presence is qualitatively consistent with the slowing down of the dynamical flow near the fixed point. Note, in particular, that an orbit passing from a point  $x$  near the fixed point has to cross more eigenfunction wavefronts in a given time interval to produce consistent phase evolution  $\zeta_j(\Phi^t(x)) \approx e^{i\omega_j t} \zeta_j(x)$  with more rapidly evolving orbits away from the fixed point.

In directions transverse to orbits, all computed eigenfunctions exhibit significant oscillatory behavior. For instance, even eigenfunction  $\zeta_2$ , which has the smallest nonzero Dirichlet energy among eigenfunctions in our computed set, exhibits an apparent wavenumber-4 oscillation along the circle  $\theta_1 = \theta_2$  (bottom-left to top-right corner in the  $[0, 2\pi)^2$  periodic box), as opposed to the wavenumber-1 eigenfunctions from the rotation system. As we will see in Section 7.3 below, the strongly oscillatory nature of the eigenfunctions computed from the Stepanoff system will have repercussions on their ability to represent smooth, isotropic observables in EDMD-type approximations.

### 7.3. Dynamical evolution experiments

We use the dynamical systems and spectral decomposition results from Sections 7.1 and 7.2 to benchmark the efficacy of our tensor network scheme based on the Fock space  $F(\mathcal{H}_\tau)$  in approximating the Koopman evolution of observables relative to (i) the “true” model, using the Koopman operator implemented as a composition map by an analytically known flow (the torus rotation), or a numerical flow obtained by an ordinary differential equation (ODE) solver (applied to the Stepanoff system); (ii) a “classical”, EDMD-type approximation using the eigenfunctions from Section 7.2 as basis functions; and (iii) a “quantum mechanical” approximation that approximates pointwise evaluation of the forecast observable as expectation of a smoothed multiplication operator with respect to a quantum state. The latter is effectively a tensor network model utilizing only the  $n = 1$  grading of the Fock space. Pseudocode for the classical, quantum mechanical, and Fock space approximations is listed in Algorithms 2 and 3, and 4, respectively.

In all experiments, we consider the evolution of an observable  $\sigma_{\mu, \kappa} \in C^\infty(\mathbb{T}^2)$  from the von Mises family of probability density functions on the 2-torus, (42) with  $N = 2$ . The following two reasons motivate our use of observables in this family as our forecast observables:

- For any admissible value of the parameters  $\mu$  and  $\kappa$ ,  $\sigma_{\mu, \kappa}$  is a strictly positive function, and is thus suitable for testing the ability of approximation schemes to preserve positivity.
- For any admissible  $\mu$  and  $\kappa = (\kappa, \kappa)$ ,  $\kappa > 0$ ,  $\sigma_{\mu, \kappa}$  is an isotropic function, i.e.,  $\sigma_{\mu, \kappa}(x) = \sigma_{\mu, \kappa}(x')$  whenever  $x - x' = (y, y) \pmod{2\pi}$ . Given their highly anisotropic nature, it is expected that the approximate Koopman eigenfunctions for the Stepanoff flow do not provide an efficient basis for representing  $\sigma_{\mu, \kappa}$  for such parameter values. As a result, approximating the evolution of  $\sigma_{\mu, \kappa}$  constitutes a challenging test of prediction techniques utilizing approximate Koopman eigenfunctions.

In the sequel, we let  $\hat{\sigma}_{\mu, \kappa} = (\langle \phi_0, \sigma_{\mu, \kappa} \rangle_H, \dots, \langle \phi_{m-1}, \sigma_{\mu, \kappa} \rangle_H)^\top$  be the vector in  $\mathbb{C}^m$  containing the leading  $m$  Fourier coefficients of  $\sigma_{\mu, \kappa}$ , determined via (44). Moreover, using the generalized eigenvectors  $\tilde{\mathbf{c}}_j = (\tilde{c}_{0,j}, \dots, \tilde{c}_{m-1,j})^\top \in \mathbb{C}^m$  and the corresponding eigenfrequencies  $\tilde{\omega}_{j,z,\tau,m}$  we define, for an integer  $d \leq (n_{\text{eig}} - 1)/2$ , the  $m \times (2d+1)$  matrix  $\mathbf{C}_d = (\tilde{\mathbf{c}}_0, \dots, \tilde{\mathbf{c}}_{2d})$ , and the  $(2d+1) \times (2d+1)$  diagonal unitary matrix  $\mathbf{U}_d^t = [U_{ij}^t]$  with diagonal entries  $U_{jj}^t = e^{i\tilde{\omega}_{j,z,\tau,m} t}$ . As in Section 5.4,  $\mathcal{Z}_{\tau,d,m} = \text{span}\{\tilde{\zeta}_{0,z,\tau,m}, \dots, \tilde{\zeta}_{2d,z,\tau,m}\}$  will be the subspace of  $\mathcal{H}_{\tau,m}$  spanned by the leading  $2d+1$  eigenfunctions of  $W_{\tau,m}$  and  $Z_{\tau,d,m}$  the orthogonal projection onto  $\mathcal{Z}_{\tau,d,m}$ . With these definitions, the four types of predictive models for  $\sigma_{\mu, \kappa}$  that we examine below are as follows.

### 7.3.1. True model

The true model employs the Koopman evolution  $f_{\text{true}}^{(t)} := \sigma_{\mu, \kappa} \circ \Phi^t$  associated with the dynamical flow  $\Phi^t: G \rightarrow G$ . As mentioned above, in the case of the torus rotation  $\Phi^t$  is known analytically,  $\Phi^t(x) = x + (1, \alpha)t \pmod{2\pi}$ . In the case of the Stepannof flow,  $\Phi^t$  is approximated numerically by means of an ODE solver (see Appendix A for further information).

### 7.3.2. Classical approximation

For a dimension parameter  $d_{\text{cl}} \leq (n_{\text{eig}} - 1)/2$ , the classical approximation utilizes the unitary evolution operators  $U_{\tau, m}^t$  to approximate  $f_{\text{true}}^{(t)}$  by

$$f_{\text{cl}}^{(t)} := U_{\tau, m}^t Z_{\tau, d_{\text{cl}}, m} \sigma_{\mu, \kappa} = \sum_{j=0}^{2d_{\text{cl}}} e^{i\tilde{\omega}_{j, z, \tau, m} t} \langle \tilde{\zeta}_{j, z, \tau, m}, \sigma_{\mu, \kappa} \rangle_{\mathcal{H}_\tau} \tilde{\zeta}_{j, z, \tau, m}.$$

We may expand

$$\tilde{\zeta}_{j, z, \tau, m} = \sum_{i=0}^{m-1} \tilde{c}_{ij} \psi_{i, \tau} = \sum_{i=0}^{m-1} \frac{\tilde{c}_{ij}}{\Lambda_{i, \tau/2}} K_\tau \phi_i,$$

giving

$$\langle \tilde{\zeta}_{j, z, \tau, m}, \sigma_{\mu, \kappa} \rangle_{\mathcal{H}_\tau} = \sum_{i=0}^{m-1} \frac{\overline{\tilde{c}_{ij}}}{\Lambda_{i, \tau/2}} \langle K_\tau \phi_j, \sigma_{\mu, \kappa} \rangle_{\mathcal{H}_\tau} = \sum_{i=0}^{m-1} \frac{\overline{\tilde{c}_{ij}}}{\Lambda_{i, \tau/2}} \langle \phi_j, K_\tau^* \sigma_{\mu, \kappa} \rangle_H = \tilde{\mathbf{c}}_j^\dagger \mathbf{\Lambda}_{\tau/2}^{-1} \hat{\mathbf{f}},$$

where  $\hat{\mathbf{f}} = \hat{\sigma}_{\mu, \kappa}$  and  $\mathbf{\Lambda}_{\tau/2}$  is the  $m \times m$  diagonal matrix with diagonal entries  $\Lambda_{0, \tau/2}, \dots, \Lambda_{m-1, \tau/2}$ . Thus, defining the vector-valued function  $\zeta_d: G \rightarrow \mathbb{C}^{2d+1}$  as  $\zeta_d(x) = (\tilde{\zeta}_{0, z, \tau, m}(x), \dots, \tilde{\zeta}_{2d, z, \tau, m}(x))^\top$ , we can succinctly express  $f_{\text{cl}}^{(t)}$  as

$$f_{\text{cl}}^{(t)} = (\mathbf{C}_{d_{\text{cl}}}^\dagger \hat{\mathbf{f}})^\top U_{d_{\text{cl}}}^t \zeta_{d_{\text{cl}}}. \quad (61)$$

### 7.3.3. Quantum mechanical approximation

Following the approach described in Sections 2.4 and 5.5, the quantum mechanical approximation represents  $\sigma_{\mu, \kappa}$  by the quantum mechanical observable  $M_{f, \tau, l} \in \mathfrak{B}_\tau$  from (38) for  $f = \iota \sigma_{\mu, \kappa}$ , and employs the quantum feature maps from Section 5.5 to approximate pointwise evaluation at  $x \in \mathbb{T}^2$  by the vector state  $\Xi_{\kappa_{\text{eval}}, \tau, d, m}(x) \in S_*(\mathfrak{B}_\tau)$  for a concentration parameter  $\kappa_{\text{eval}} > 0$ . Quantum states  $\rho \in S_*(\mathfrak{B}_\tau)$  (including  $\Xi_{\kappa_{\text{eval}}, \tau, d, m}(x)$ ) evolve under the induced action  $\mathcal{P}_{\tau, m}^t$  of the unitary  $U_{\tau, m}^t$ , i.e.,  $\mathcal{P}_{\tau, m}^t \rho = U_{\tau, m}^{t*} \rho U_{\tau, m}^t$ .

As discussed in Section 5.4, the quantum observable  $M_{f, \tau, l}$  is built by numerical quadrature associated with a finite-dimensional discretization  $H_l$  of the Hilbert space  $H$ . Let  $x_0^{(l)}, \dots, x_{l^2-1}^{(l)}$  be the nodes of a uniform  $l \times l$  grid on  $\mathbb{T}^2$  (with grid spacing  $2\pi/l$ ). Let  $\mu_l$  be the corresponding sampling measure from (36), and  $H_l = L^2(\mu_l)$  and  $\mathfrak{A}_l = L^\infty(\mu_l)$  the associated Hilbert space and algebra of discretely sampled classical observables, respectively. Let also  $K_{\tau, l}: H_l \rightarrow \mathcal{H}_\tau$  be the integral operator from (37). We use the values  $\sigma_{\mu, \kappa}(x_0^{(l)}), \dots, \sigma_{\mu, \kappa}(x_{l^2-1}^{(l)}) \in \mathbb{R}$  and  $K_{\tau, l}$  to build the quantum observable  $M_{f, \tau, l} \in \mathfrak{B}_\tau$  from (38).

Below, we will be making use of the  $l \times l$  diagonal matrix  $\mathbf{M}$  with diagonal entries  $\tilde{f}(x_0^{(l)}), \dots, \tilde{f}(x_{l^2-1}^{(l)})$  and the  $m^2 \times d$  matrix  $\mathbf{Z} = [Z_{ij}]$ , whose entries contain the values of the leading  $2d + 1$  eigenfunctions on the points  $x_i^{(l)}$ ; i.e.,  $Z_{ij} = \tilde{\zeta}_{j, \tau, m}(x_i^{(l)})$ . We also introduce a vector-valued function  $\hat{\mathbf{F}}_\kappa: \mathbb{T}^2 \rightarrow \mathbb{C}^m$ ,  $\hat{\mathbf{F}}_\kappa(x) = \hat{\sigma}_{x, (\kappa, \kappa)}$ , that returns, up to proportionality, the leading  $m$  Fourier coefficients of the feature vectors  $F_{\kappa, \tau}(x)$ .

With these definitions, and for an integer parameter  $d_{\text{qm}} \leq (n_{\text{eig}} - 1)/2$ , the quantum mechanical model

approximates the evolution  $f_{\text{true}}^{(t)}$  by  $f_{\text{qm}}^{(t)} \in C(\mathbb{T}^2)$  using the first formula in (52), i.e.,

$$\begin{aligned} f_{\text{qm}}^{(t)}(x) &= \frac{\mathbb{E}_{\mathcal{P}_{\tau,m}^t}(\Xi_{\kappa_{\text{eval}},\tau,d_{\text{qm}},m}(x)) M_{f,\tau,l}}{\mathbb{E}_{\mathcal{P}_{\tau,m}^t}(\Xi_{\kappa_{\text{eval}},\tau,d_{\text{qm}},m}(x)) M_{\mathbf{1},\tau,l}} \\ &\equiv \frac{\langle K_{\tau,l}^* U_{\tau,m}^{t*} F_{\kappa_{\text{eval}},\tau,d_{\text{qm}},m}(x), (\pi_l f_l) K_{\tau,l}^* U_{\tau,m}^{t*} F_{\kappa_{\text{eval}},\tau,d_{\text{qm}},m}(x) \rangle_{H_l}}{\|K_{\tau,l}^* U_{\tau,m}^{t*} F_{\kappa_{\text{eval}},\tau,d_{\text{qm}},m}(x)\|_{H_l}^2}. \end{aligned} \quad (62)$$

In matrix notation, (62) can be equivalently expressed as

$$f_{\text{qm}}^{(t)}(x) = \frac{\boldsymbol{\xi}_{t,x}^\dagger \mathbf{M} \boldsymbol{\xi}_{t,x}}{\|\boldsymbol{\xi}_{t,x}\|^2}, \quad \boldsymbol{\xi}_{t,x} = \mathbf{Z}_{d_{\text{qm}}} \mathbf{U}_{d_{\text{qm}}}^{t\dagger} \mathbf{C}_{d_{\text{qm}}}^\dagger \hat{\mathbf{F}}_{\kappa_{\text{eval}}}(x). \quad (63)$$

### 7.3.4. Fock space approximation

The Fock space approximation implements the scheme described in Sections 3 and 5 using the quantum observable  $A_{f,\tau,n,l}$  from (39) and the feature map  $\tilde{\Xi}_{\kappa_{\text{eval}},\tau,d_{\text{Fock}}}$  derived from the projections of the roots of the feature vectors  $F_{\kappa_{\text{eval}},\tau}(x)$  onto  $\mathcal{Z}_{\tau,d,m}$ .

Setting an integer parameter  $d_{\text{Fock}} \leq (n_{\text{eig}} - 1)/2$  and using the above feature maps, the Fock space approximation  $f_{\text{Fock}}^{(t)} \in C(\mathbb{T}^2)$ , obtained via the second formula in (52), becomes

$$\begin{aligned} f_{\text{Fock}}^{(t)}(x) &= \frac{\mathbb{E}_{\tilde{\mathcal{P}}_{\tau,m}^t}(\tilde{\Xi}_{\kappa_{\text{eval}},\tau,n,d_{\text{Fock}},m}(x)) A_{f,\tau,n,l}}{\mathbb{E}_{\tilde{\mathcal{P}}_{\tau,m}^t}(\tilde{\Xi}_{\kappa_{\text{eval}},\tau,n,d_{\text{Fock}},m}(x)) A_{\mathbf{1},n,\tau,l}} \\ &\equiv \frac{\langle K_{\tau}^* (U_{\tau,m}^{t*} F_{\tau,n,d,m}(x))^n, (\pi_l f_l) K_{\tau}^* (U_{\tau,m}^{t*} \tilde{F}_{\tau,d,m}(x))^n \rangle_{H_l}}{\|K_{\tau}^* (U_{\tau,m}^{t*} \tilde{F}_{\tau,d,m}(x))^n\|_{H_l}^2}. \end{aligned} \quad (64)$$

Defining  $\hat{\mathbf{F}}_{\kappa,n} : G \rightarrow \mathbb{C}^m$  as  $\hat{\mathbf{F}}_{\kappa,n}(x) = \hat{\boldsymbol{\sigma}}_{x,(\kappa,\kappa)/n}$ , and using  $\mathbf{v}^n$  to denote the elementwise  $n$ -th power of a vector  $\mathbf{v} \in \mathbb{C}^l$ , we can express (64) in matrix form as

$$f_{\text{Fock}}^{(t)}(x) = \frac{\boldsymbol{\xi}_{n,t,x}^\dagger \mathbf{M} \boldsymbol{\xi}_{n,t,x}}{\|\boldsymbol{\xi}_{n,t,x}\|^2}, \quad \boldsymbol{\xi}_{n,t,x} = (\mathbf{Z}_{d_{\text{Fock}}} \mathbf{U}_{d_{\text{Fock}}}^{t\dagger} \mathbf{Z}_{d_{\text{Fock}}}^\dagger \hat{\mathbf{F}}_{\kappa_{\text{eval}},n}(x))^n. \quad (65)$$

Note that, up to proportionality constants that cancel upon taking the ratio, the numerator and denominator in (64) are evaluations of the tensor network in Fig. 3.

### 7.3.5. Torus rotation

In our torus rotation experiments, the forecast observable is an anisotropic von Mises density  $\sigma_{\boldsymbol{\mu},\boldsymbol{\kappa}}$  with  $\boldsymbol{\mu} = (0,0)$  and  $\boldsymbol{\kappa} = (\kappa_1, \kappa_2) \equiv (1,6)$ . Since  $\kappa_2 > \kappa_1$ ,  $\sigma_{\boldsymbol{\mu},\boldsymbol{\kappa}}$  has higher sharpness (faster rate of decay) in the  $\theta_2$  dimension than along  $\theta_1$ , resulting in an oblate appearance of its level sets when visualized in the  $(\theta_1, \theta_2)$  periodic domain. Correspondingly, well-approximating  $\sigma_{\boldsymbol{\mu},\boldsymbol{\kappa}}$  by truncated Fourier series requires more coefficients (higher bandwidth) along the  $\theta_2$  dimension than  $\theta_1$ .

Figure 7 shows scatterplots of the evolution of  $\sigma_{\boldsymbol{\mu},\boldsymbol{\kappa}}$  under the true model, and the classical, quantum mechanical, and Fock space approximations for representative evolution times  $t \in \{0, 1, 2, 4\}$ , plotted on a  $256 \times 256$  uniform grid on  $\mathbb{T}^2$ . The approximate models use the parameters  $d_{\text{cl}} = d_{\text{qm}} = d_{\text{Fock}} = 128$ ,  $l = 512$ ,  $\kappa_{\text{eval}} = 500$ , and  $n = 10$ . Note that working with the same values of  $d_{\text{cl}}$ ,  $d_{\text{qm}}$ , and  $d_{\text{Fock}}$  allows us to compare approximations originating from the same set of eigenfunctions and eigenfrequencies. Moreover, since  $\kappa_{\text{eval}} \gg \max\{\kappa_1, \kappa_2\}$  (and as we discuss momentarily, the initial condition  $\sigma_{\boldsymbol{\mu},\boldsymbol{\kappa}}$  does not experience deformation of its level sets under rotation dynamics), the quantum states utilized by the quantum mechanical and Fock space models are expected to well-approximate pointwise evaluation of the forecast observables.

As expected from the analytically known flow map (57), under the true model  $f_{\text{true}}^{(t)}$  the initial condition  $f_{\text{true}}^{(0)} = \sigma_{\boldsymbol{\mu},\boldsymbol{\kappa}}$  is advected as a rigid body along lines of (irrational) slope  $\alpha_2/\alpha_1$ . This behavior is qualitatively captured by all three models, but there are notable differences in the details of the three approximations:

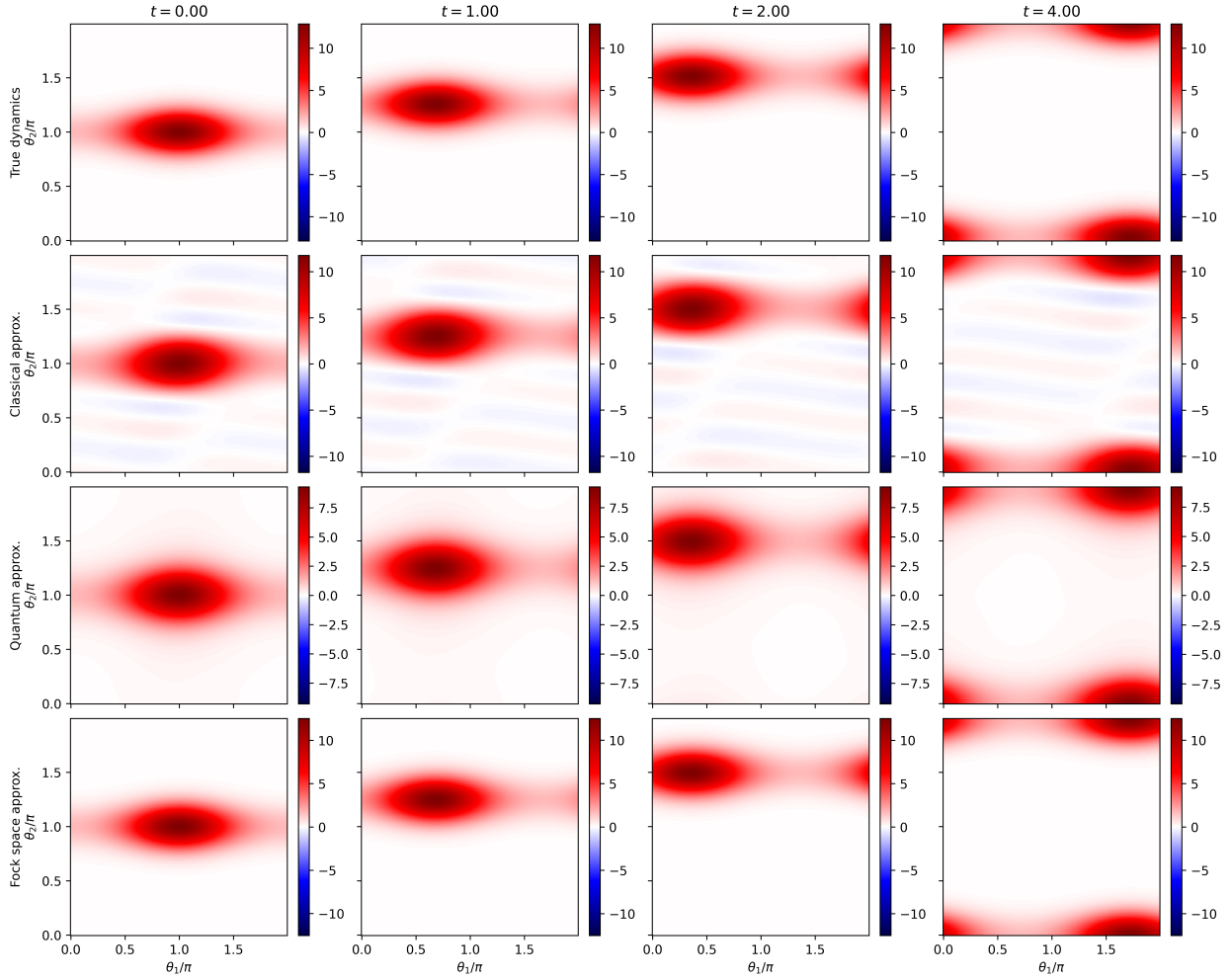


Figure 7: Time evolution of the anisotropic von Mises density  $\sigma_{\mu, \kappa}$  with  $\mu = (0, 0)$  and  $\kappa = (1, 6)$  under the ergodic torus rotation ( $f_{\text{true}}^{(t)}$ ; top row), the classical approximation ( $f_{\text{cl}}^{(t)}$ ; second row from top), the quantum mechanical approximation ( $f_{\text{qm}}^{(t)}$ ; third row from top), and the Fock space approximation ( $f_{\text{Fock}}^{(t)}$ ; bottom row). Columns from left-to-right show snapshots of the evolution times  $t = 0, 1, 2, 4$ .



- Being an orthogonal projection method, the classical approximation  $f_{\text{cl}}^{(t)}$  is not positivity preserving (see Section 2.1). Indeed, oscillations of  $f_{\text{cl}}^{(t)}$  to negative values are evident in the results shown in the second row of Fig. 7. Notice that these oscillations take place primarily along the  $\theta_2$  direction. This is consistent with the fact that  $\sigma_{\mu,\kappa}$  is more susceptible to Fourier truncation errors along  $\theta_2$  than  $\theta_1$  (since  $\kappa_2 > \kappa_1$ ).

- The quantum mechanical approximation  $f_{\text{qm}}^{(t)}$  is positivity preserving (see Section 2.4), which eliminates the oscillations to negative values seen in  $f_{\text{cl}}^{(t)}$ . In some applications, e.g., modeling sign-definite physical quantities, positivity preservation is a highly desirable, or even essential, feature. However, as can be seen in the third row of Fig. 7,  $f_{\text{qm}}^{(t)}$  does not recover as accurately the pointwise value of  $f_{\text{true}}^{(t)}$  near its peak, and generally appears to be more diffusive than  $f_{\text{cl}}^{(t)}$ .

- The Fock space approximation  $f_{\text{Fock}}^{(t)}$  is positivity-preserving similarly to  $f_{\text{qm}}^{(t)}$ , but also overcomes the shortcomings of the latter method in reproducing the extremal values of  $f_{\text{true}}^{(t)}$ . As we discussed in Section 3.4, the Fock space scheme has access to approximation spaces lying in the tensor product space  $\mathcal{H}_\tau^{\otimes n}$ . The higher dimensionality of these spaces may thus avoid the apparent positivity preservation and extremal value reproduction tradeoffs seen in the classical and quantum mechanical approximation schemes.

Next, to study the accuracy of the three approximation schemes in more detail, in Fig. 8 we show plots of their errors,  $f_{\text{cl}}^{(t)} - f_{\text{true}}^{(t)}$ ,  $f_{\text{qm}}^{(t)} - f_{\text{true}}^{(t)}$ , and  $f_{\text{Fock}}^{(t)} - f_{\text{true}}^{(t)}$ , relative to the true evolution. At least for  $t \leq 2$ , the results verify the qualitative observations made above; namely,  $f_{\text{cl}}^{(t)}$  performs better than  $f_{\text{qm}}^{(t)}$  in terms of reconstruction of the extremal values of  $f^{(t)}$  but fails to preserve positivity, and  $f_{\text{Fock}}^{(t)}$  provides “the best of both worlds” in the sense of being positivity-preserving and yielding the best reconstruction accuracy of extremal values. At the same time, the  $t = 4$  results in Fig. 8 indicate that  $f_{\text{Fock}}^{(t)}$  has faster error growth than the other methods. This can be understood from the fact that the amplification to  $\mathcal{H}_\tau^{\otimes n}$  generates frequencies as high as  $n = 10$  times the maximal eigenfrequency corresponding to the approximation space  $\mathcal{Z}_{\tau, d_{\text{Fock}}, m}$ . Any errors in the eigenfrequencies may thus be amplified, causing a build-up of phase errors over time.

A possible remedy to such issues would be to set  $d_{\text{Fock}}$  and/or  $n$  in a  $t$ -dependent manner, with values determined in an offline training procedure. Here, we have opted not to explore such additional tuning steps in order to more directly highlight the benefits and shortcomings of each method.

### 7.3.6. Stepanoff flow

For our Stepanoff flow experiments, we consider the isotropic von Mises density function  $\sigma_{\mu,\kappa}$  with  $\mu = (0, 0)$  and  $\kappa = (1, 1)$  as the forecast observable. We use the approximation parameters  $d_{\text{cl}} = d_{\text{qm}} = d_{\text{Fock}} = 256$ ,  $l = 1024$ ,  $\kappa_{\text{eval}} = 500$ , and  $n = 10$ . Figures 9 and 10 show representative dynamical evolution and error results for time  $t \in \{0, 1, 2, 4\}$  similarly to Figs. 7 and 9, respectively.

First, before delving into the behavior of the dynamics and approximations at  $t > 0$ , it is worthwhile examining the  $t = 0$  results to highlight that even reconstruction of the initial condition  $f_{\text{true}}^{(0)}$  is non-trivial using the basis of approximate Koopman eigenfunctions computed for this system (as alluded to in Section 7.2). This is especially evident in the case of the classical approximation, where the initial reconstruction  $f_{\text{cl}}^{(0)}$  in Fig. 9 has clear imprints of the characteristic sigmoid structure of the eigenfunction level sets (see right-hand column of Fig. 6) and exhibits significant excursions to negative values in regions near the fixed point  $x = (0, 0)$ . This is despite the fact that the true initial condition  $f^{(0)}$  is a smooth, isotropic function (and thus might be considered a “nice” observable) and the number eigenfunctions used,  $2d_{\text{cl}} + 1 = 513$ , is arguably not insignificant. The quantum mechanical reconstruction,  $f_{\text{qm}}^{(0)}$ , improves reconstruction quality by smoothing and eliminating negative values, but the sigmoid pattern inherited from the eigenfunctions is still clearly visible, and as in the case of the torus rotation the amplitude of extremal values is not well-reproduced. The Fock space reconstruction  $f_{\text{Fock}}^{(0)}$ , on the other hand, offers a solid improvement over both its classical and quantum mechanical counterparts. Even though some undulations attributable to the form of the eigenfunctions are still present in  $f_{\text{Fock}}^{(0)}$ , they are considerably

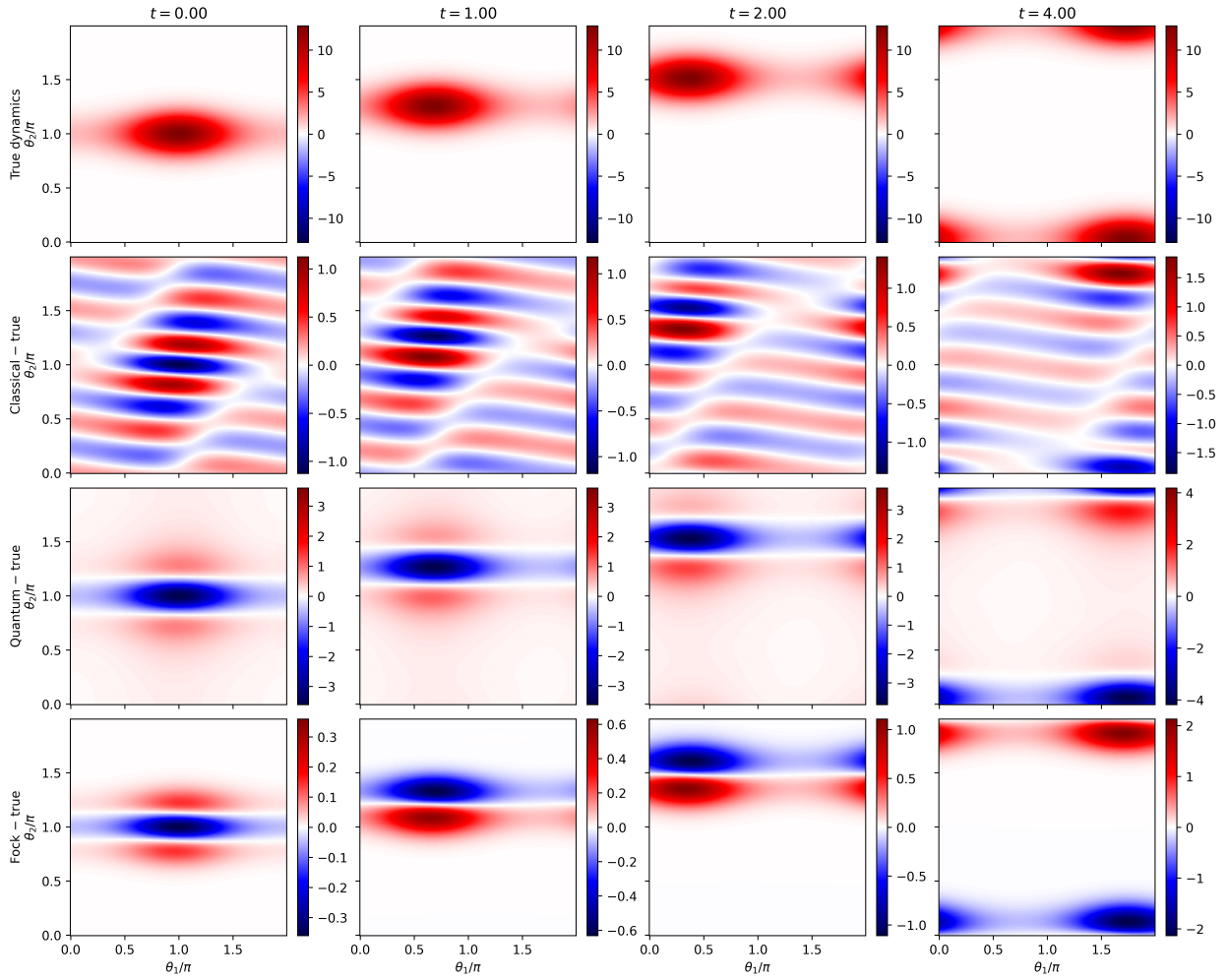


Figure 8: Errors in the classical, quantum mechanical, and Fock space approximations from Fig. 7 (second from top to bottom rows, respectively) relative to the true evolution. The true evolution is plotted in the first row for reference.

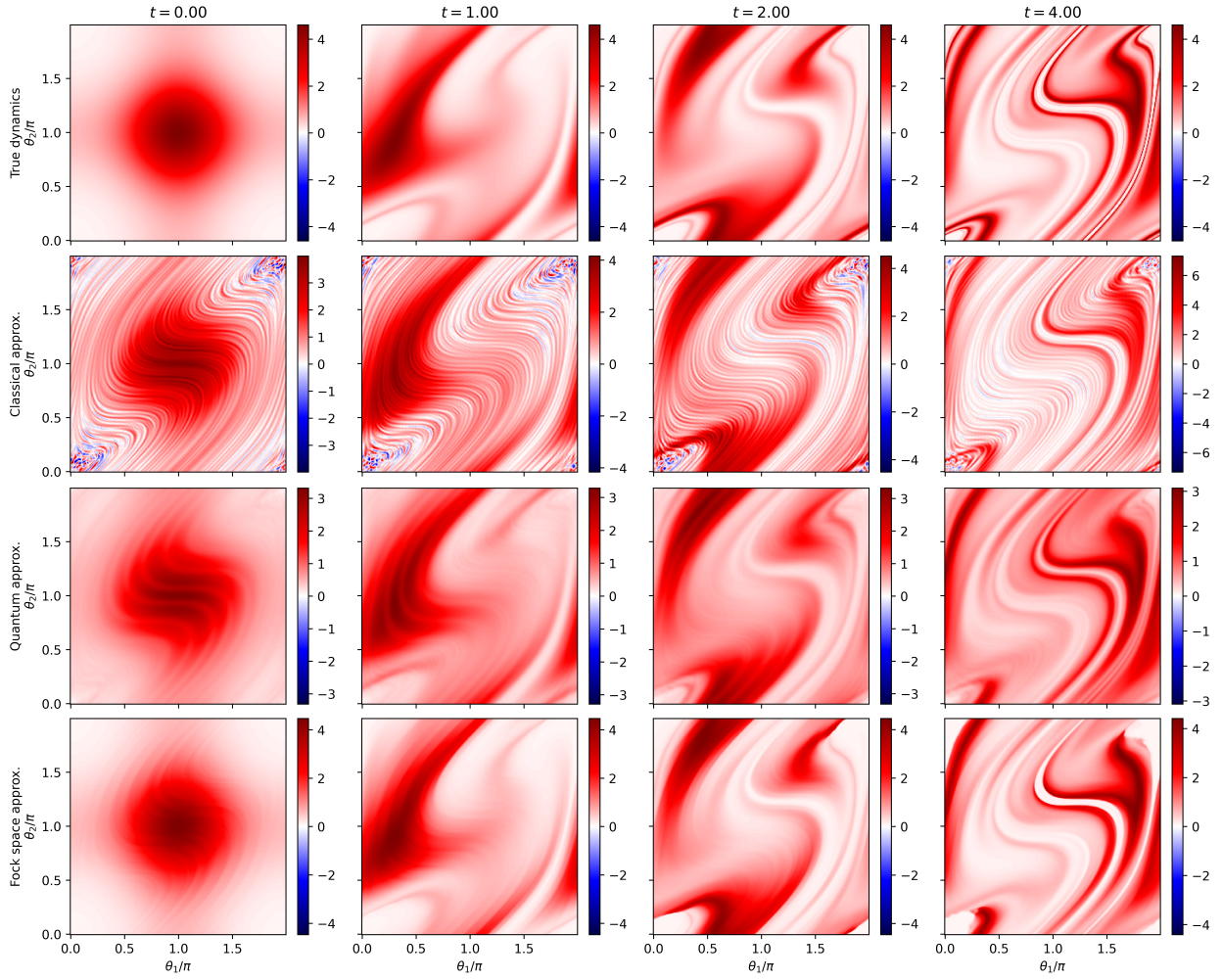


Figure 9: Time evolution of the isotropic von Mises density  $\sigma_{\mu,\kappa}$  with  $\mu = (0, 0)$  and  $\kappa = (1, 1)$  under the Stepanoff flow (top row), and the classical quantum mechanical, and Fock space approximations (second to last rows). The plots are organized similarly to Fig. 7

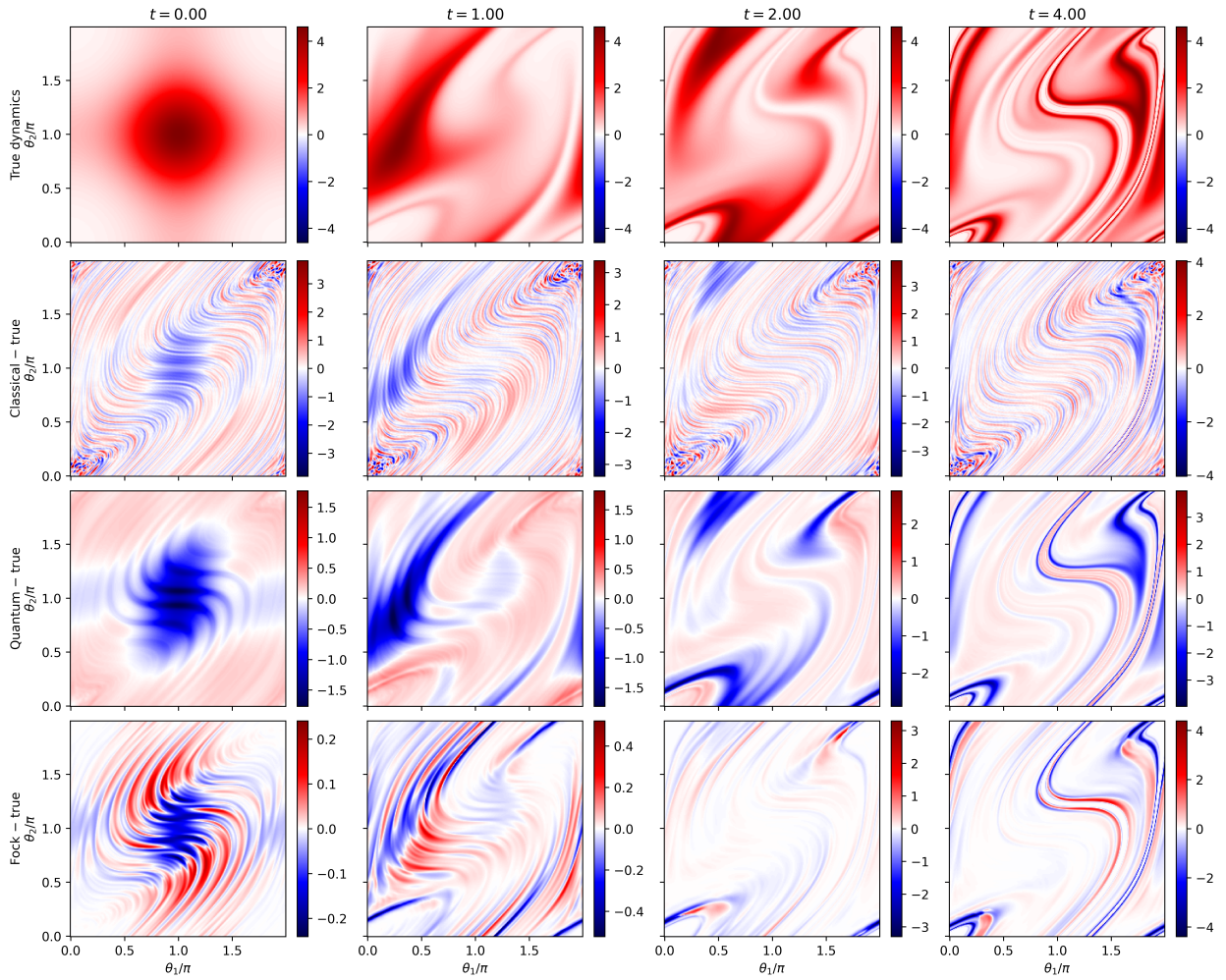


Figure 10: Errors in the classical, quantum mechanical, and Fock space approximations from Fig. 9 (second from top to bottom rows, respectively) relative to the true evolution. The true evolution is plotted in the first row for reference.

weaker than those seen in  $f_{\text{cl}}^{(0)}$  and  $f_{\text{qm}}^{(0)}$ . Moreover, as can be seen from the error plots in Fig. 10, the amplitude of extremal values of  $f^{(0)}$  is reproduced with significantly higher accuracy.

Next, turning to the  $t > 0$  results, a comparison of the top rows of Figs. 7 and 9 clearly illustrates the higher dynamical complexity of the Stepanoff flow over the torus rotation, with the former producing stretching and folding of the initially circular level sets of  $\sigma_{\mu,\kappa}$  versus the rigid translation seen in the latter. All three approximations track the large-scale behavior of  $f_{\text{true}}^{(t)}$  from the true system, although the classical approximation  $f_{\text{cl}}^{(t)}$  continues to be affected by imprinting of eigenfunction the patterns as discussed above for  $t = 0$ . Again,  $f_{\text{Fock}}^{(t)}$  provides the best overall prediction results, particularly for  $t \leq 2$ , demonstrating the benefits of Fock space amplification.

Inspecting the  $t = 2, 4$  results in Figs. 9 and 10, we see that the largest errors in  $f_{\text{Fock}}^{(t)}$  are concentrated in regions such as the vicinity of the fixed point, where the approximation appears to be rounded off (visually “whitened out”) to near-zero values. In separate calculations, we have verified that at such points  $x \in \mathbb{T}^2$  the state vector  $\tilde{F}_{\kappa_{\text{eval}},\tau,n,d,m}(x) \in F(\mathcal{H}_\tau)$  becomes an extremely localized function upon application of  $\Delta_n^*$ . Thus, the forecast  $f_{\text{Fock}}^{(t)}(x)$  is dominated by an exceedingly small number of sampled values  $\sigma_{\mu,\kappa}(x_i^{(t)})$  of the forecast observable. In other words, the approximation  $f_{\text{Fock}}^{(t)}(x)$  at these points appears to be affected by some type of overfitting. In Figs. 9 and 10, the quantum mechanical approximation  $f_{\text{qm}}^{(t)}(x)$  does not seem to be impacted by the same issue. Since  $f_{\text{qm}}^{(t)}$  is essentially an  $n = 1$  version of the Fock space scheme, decreasing  $n$  would be a way of restoring smoothness of the prediction  $f_{\text{Fock}}^{(t)}(x)$  under changes in  $x$ .

Of course, sensitive dependence on initial conditions is a hallmark of complex dynamics, so the fact that  $f_{\text{Fock}}^{(t)}(x)$  appears to have higher sensitivity on  $x$  than other methods is not necessarily a disadvantage of the tensor network scheme. Nonetheless, the presence of the whitened-out regions in Fig. 9 indicates that  $t$ -dependent tuning of  $n$  and/or modification of the quantum observable  $A_{f,\tau,n}$  used for prediction may be beneficial. We comment on possibilities for the latter approach in Section 8.

## 8. Concluding remarks

In this paper, we developed a framework for approximating the statistical evolution of continuous observables of measure-preserving, ergodic dynamical systems based on a combination of techniques from Koopman/transfer operator theory and many-body quantum theory. For this framework, the working hypothesis was that the multiplicative structure of approximate eigenfunctions of Koopman operators contains information about the underlying dynamical system that is not utilized by classical Koopman operator techniques. The principal elements of this scheme are (i) spectral regularization for consistently approximating the skew-adjoint Koopman generator (which is typically unbounded and non-diagonalizable) by a family of skew-adjoint, diagonalizable operators,  $V_\tau$ , on  $L^2(\mu)$ ; (ii) lift of the evolution of observables and probability densities under the dynamics generated by  $V_\tau$  to the setting of a Fock space  $F(\mathcal{H}_\tau)$  generated by a reproducing kernel Hilbert algebra (RKHA) of observables,  $\mathcal{H}_\tau$ . Notable features of this construction are:

1. The lifted Koopman/transfer operators act multiplicatively on the tensor algebra  $T(\mathcal{H}_\tau) \subset F(\mathcal{F}_\tau)$ . This means that their eigenvalues are generative as an additive group, and the corresponding eigenfunctions are generative as a multiplicative group under the tensor product.

2. The RKHA  $\mathcal{H}_\tau$  is simultaneously an RKHS, a coalgebra, and a Banach algebra with respect to the pointwise product of functions. This structure enables a mapping of probability densities on state space into quantum state vectors in the Fock space that project non-trivially to all of its gradings  $\mathcal{H}_\tau^{\otimes n} \subset F(\mathcal{H}_\tau)$ . Moreover, classical observables  $f \in L^\infty$  are mapped into quantum observables  $A_{f,\tau,n}$  acting on the Fock space. The observables  $A_{f,\tau,n}$  are built as smoothed multiplication operators, amplified to act on any of the tensor product spaces  $\mathcal{H}^{\otimes(n+1)}$ ,  $n \in \mathbb{N}$ , via the comultiplication operator  $\Delta: \mathcal{H}_\tau \rightarrow \mathcal{H}_\tau \otimes \mathcal{H}_\tau$  of the RKHA.

3. The lifted system on the Fock space is projected onto finite-dimensional subspaces generated by tensor products of eigenfunctions of  $V_\tau$ . The resulting quantum state evaluation can be expressed as a tree tensor network (Fig. 3), and is positivity preserving and asymptotically consistent in appropriate limits.

Importantly, the tensor network approach provides a route for algebraically building high-dimensional approximation spaces from a modest number of approximate Koopman/transfer operator eigenfunctions.

In broad terms, our approach can be thought of as (i) distributing an initial sharp probability density function  $\varrho \in \mathcal{H}_\tau$  into a linear combination of tensor products  $\xi^{1/n} \otimes \dots \otimes \xi^{1/n} \in \mathcal{H}_\tau^{\otimes n}$  of coarser functions by the  $n$ -th roots of the quantum mechanical state vector  $\xi \propto \varrho^{1/2}$ ; (ii) dynamically evolving each of the factors  $\xi^{1/n}$ ; and (iii) recombining the results using into a sharp, time-evolved quantum state that approximates the evolution of densities under the transfer operator of the dynamical system. Our analysis characterized the convergence properties of the scheme (Proposition 9 and Theorem 12), and its efficacy was assessed with numerical prediction experiments involving an irrational rotation and a Stepanoff flow on  $\mathbb{T}^2$ . In both cases, approximations utilizing the Fock space were found to perform better than conventional subspace projection methods in terms of approximation accuracy, consistent with the working hypothesis, and with the added benefit of being positivity preserving.

In terms of future work, the tensor network approach presented in this paper provides a flexible approximation framework with several possible directions for further development. First, as noted in Remark 1, the scheme based on the  $n$ -th roots  $\xi^{1/n}$  is one of many possibilities of lifting the state vector  $\xi \in \mathcal{H}_\tau$  to the Fock space. From the point of view of asymptotic convergence, it suffices to identify any set of functions  $\xi^{(1)}, \dots, \xi^{(n)}$  whose pointwise product  $\Delta_n^*(\xi^{(1)} \otimes \dots \otimes \xi^{(n)})$  recovers  $\xi$ . Second, the amplification scheme leading to the quantum observables  $A_{f,\tau,n}$  that act on individual gradings  $\mathcal{H}^{\otimes(n+1)}$  could be generalized to yield quantum observables acting on multiple gradings, e.g., through (possibly infinite) linear combinations  $\sum_n c_n A_{f,\tau,n}$ . Exploring these more general schemes would be a fruitful avenue of future work that could potentially improve the performance of the method at large evolution time  $t$  and/or in regions of state space such as fixed points with highly oscillatory eigenfunctions (see Section 7.3). A related research direction would be to characterize the structure of the resulting tree tensor networks (TTNs) using methods from renormalization group theory.

Finally, even though the methods presented in this paper are already beneficial in the context of classical numerical computation, their common mathematical foundation with many-body quantum physics motivates the development of efficient implementations on quantum computing platforms. Here, a challenge stems from the fact that the comultiplication operators  $\Delta$  employed in the scheme are not unitary, and thus cannot be directly implemented using quantum logic gates. Recent work on representing non-unitary operators in tensor networks through orthogonal forms [121] may be a promising way of addressing these challenges. More generally, we are hopeful that the work presented in this paper will stimulate fruitful interactions between the fields of classical dynamics and many-body quantum theory.

## Acknowledgments

Dimitrios Giannakis acknowledges support from the U.S. Department of Defense, Basic Research Office under Vannevar Bush Faculty Fellowship grant N00014-21-1-2946 and the U.S. Office of Naval Research under MURI grant N00014-19-1-242. Mohammad Javad Latifi Jebelli and Michael Montgomery were supported as postdoctoral fellows from these grants. Philipp Pfeffer is supported by the project no. P2018-02-001 "DeepTurb – Deep Learning in and of Turbulence" of the Carl Zeiss Foundation, Germany. Jörg Schumacher is supported by the European Union (ERC, MesoComp, 101052786). Views and opinions expressed are however those of the authors only and do not necessarily reflect those of the European Union or the European Research Council. Neither the European Union nor the granting authority can be held responsible for them.

## Appendix A. Numerical implementation

The numerical schemes described in this paper were implemented in Python. Jupyter notebooks reproducing the results in Figs. 5–10 can be found in the repository <https://dg227.github.io/NLSA>. Our code uses JAX [122] as the main numerical library. We found that JAX's functional programming features, such as composable function transformations and lazy evaluation, lend themselves well to computational

implementation of the operator-theoretic methods in the paper, including eigendecomposition of the regularized generator and evaluation of quantum states. Additional notes on numerical implementation are as follows:

- To solve the generalized eigenvalue problem (34) we used the `eigs` iterative solver from SciPy, using JAX to implement the action of the  $\mathbf{V}_m$  and  $\mathbf{B}_m$  matrices on vectors. To our knowledge, no JAX-native generalized eigenvalue solvers are available in the public domain at the time of writing this article.

- Following solution of (34), our code proceeds by implementing the eigenfunctions  $\tilde{\zeta}_{j,z,\tau,m}$ , the quantum feature maps  $\Xi_{\kappa_{\text{eval}},\tau,d,m}$  and  $\Xi_{\kappa_{\text{eval}},\tau,n,d,m}$ , and the discrete multiplication operators  $\pi_l f$  associated with the prediction observables as Python function objects. The prediction functions  $f_{\text{qm}}^{(t)}$  and  $f_{\text{Fock}}^{(t)}$  are also built as function objects by operating on the implementations of the eigenfunctions, feature maps, and multiplication operators. These computations are lazy, in the sense that no computation of intermediate function values is performed prior to formation of  $f_{\text{qm}}^{(t)}$  and  $f_{\text{Fock}}^{(t)}$ . Once formed, the prediction functions are vectorized (to allow simultaneous evaluation and multiple prediction points), and just-in-time (JIT) compiled using JAX to yield efficient implementations capable of running on hardware accelerators such as GPUs.

- Numerical integrations of the Stepanoff system (58) (providing the “true model” data in Figs. 9 and 10) were obtained using the `Dopri5` solver from the JAX-based `DiffraX` library [123].

---

**Algorithm 1** Eigendecomposition of the regularized generator  $W_\tau$  for the ergodic rotation and Stepanoff flow on  $\mathbb{T}^2$ . `kron` in Step 3 of the algorithm denotes the Kronecker product of two arrays. See Remark 7 regarding application of the function  $\tilde{q}_z^{-1}$  in Step 8.

---

**Input:** Resolvent parameter  $z > 0$ ; RKHA parameters  $p \in (0, 1)$ ,  $\tau > 0$ ; maximal Fourier wavenumber  $J \in \mathbb{N}$ ; number of eigenfrequency pairs  $d \leq ((2J + 1)^2 - 1)/2$ .

**Output:** With  $m = (2J + 1)^2$ : Eigenfrequencies  $\boldsymbol{\omega} = (\omega_0, \dots, \omega_{2d}) \in \mathbb{R}^{2d+1}$ ; generalized eigenvectors  $\mathbf{C} = (\tilde{\mathbf{c}}_0, \dots, \tilde{\mathbf{c}}_{2d+1}) \in \mathbb{C}^{m \times (2d+1)}$ ; Dirichlet energies  $\mathbf{E} = (E_0, \dots, E_{2d}) \in \mathbb{R}^{(2d+1)}$ ; eigenfunctions  $\{\tilde{\zeta}_0, \dots, \tilde{\zeta}_{2d} \in \mathcal{H}_\tau\}$ .

- 1: Form the ordered index set  $\mathcal{J} = \{(j_1, j_2) : j_1, j_2 \in \{-J, \dots, J\}\}$  using lexicographical ordering.
  - 2: Form generator matrix  $\mathbf{V} \in \mathbb{R}^{m \times m} = [V_{rs}]_{r,s \in \{0, \dots, m-1\}}$  using (59) (ergodic rotation) or (60) (Stepanoff flow) for the index set  $\mathcal{J}$ .
  - 3: Compute RKHA weight vector  $\boldsymbol{\lambda} \in \mathbb{R}^m = \mathbf{kron}(\boldsymbol{\lambda}_1, \boldsymbol{\lambda}_1)$ , where  $\boldsymbol{\lambda}_1 = [e^{-\tau|j|^p/2}]_{j \in \{-J, \dots, J\}}$ .
  - 4: Form regularized generator matrix  $\mathbf{V}_{\tau,m} \in \mathbb{R}^{m \times m} = \boldsymbol{\Lambda} \mathbf{V}_m \boldsymbol{\Lambda}$ , where  $\boldsymbol{\Lambda} = \mathbf{diag}(\boldsymbol{\lambda})$ .
  - 5: Form mass matrix  $\mathbf{B} \in \mathbb{R}^{m \times m} = z^2 \mathbf{I}_m - \mathbf{V}_m^T \mathbf{V}_m$ , where  $\mathbf{I}_m$  is the  $m \times m$  identity matrix.
  - 6: Compute  $2d$  eigenvalues  $\beta_1, \dots, \beta_{2d} \in \mathbb{C}$  of largest modulus from the generalized eigenvalue problem (34) and the corresponding eigenvectors  $\tilde{\mathbf{c}}_1, \dots, \tilde{\mathbf{c}}_{2d} \in \mathbb{C}^m$ . Normalize the  $\tilde{\mathbf{c}}_j$  to unit 2-norm.
  - 7: Compute Dirichlet energies  $E_j$  of the eigenvectors  $\tilde{\mathbf{c}}_j$  using (29). Sort  $(\beta_1, \dots, \beta_{2d})$ ,  $(\tilde{\mathbf{c}}_1, \dots, \tilde{\mathbf{c}}_{2d})$ , and  $(E_1, \dots, E_{2d})$  in order of increasing Dirichlet energy  $E_j$ .
  - 8: Compute eigenfrequencies  $\omega_r$  corresponding to  $\beta_r$  using (30).
  - 9: For each eigenvector  $\tilde{\mathbf{c}}_r = (c_{1r}, \dots, c_{mr})^\top$ , form the function  $\zeta_r : \mathbb{T}^2 \rightarrow \mathbb{C}$ , where  $\zeta_r(x) = \sum_{s=1}^m c_{sr} \lambda_s e^{ij_s \cdot x}$  and  $j_s \in \mathcal{J}$ .
  - 10: Set  $\omega_0 = 0$ ,  $\tilde{\mathbf{c}}_0 = [\delta_{j,(0,0)}]_{j \in \mathcal{J}}$ ,  $E_0 = 0$ ,  $\zeta_0(x) = 1$ .
  - 11: **return**  $\boldsymbol{\omega} = (\omega_0, \dots, \omega_{2d})$ ,  $\mathbf{C} = (\tilde{\mathbf{c}}_0, \dots, \tilde{\mathbf{c}}_{2d})$ ,  $\mathbf{E} = (E_0, \dots, E_{2d})$ ,  $\{\zeta_0, \dots, \zeta_{2d}\}$ .
- 

## References

- [1] B. O. Koopman, Hamiltonian systems and transformation in Hilbert space, Proc. Natl. Acad. Sci. 17 (5) (1931) 315–318. doi:10.1073/pnas.17.5.315.
- [2] B. O. Koopman, J. von Neumann, Dynamical systems of continuous spectra, Proc. Natl. Acad. Sci. 18 (3) (1932) 255–263. doi:10.1073/pnas.18.3.255.
- [3] V. Baladi, Positive Transfer Operators and Decay of Correlations, Vol. 16 of Advanced Series in Nonlinear Dynamics, World Scientific, Singapore, 2000.

---

**Algorithm 2** Classical prediction using (61).

---

**Input:** Eigenfrequencies  $\boldsymbol{\omega} \in \mathbb{R}^{2d+1}$ , generalized eigenvectors  $\mathbf{C} \in \mathbb{C}^{m \times (2d+1)}$ , and eigenfunctions  $\{\zeta_0, \dots, \zeta_{2d} \in \mathcal{H}_\tau\}$  from Algorithm 1; column vector of Fourier coefficients  $\hat{\mathbf{f}} \in \mathbb{C}^m$  of prediction observable (ordered according to the index set  $\mathcal{J}$  from Algorithm 1); evolution time  $t \in \mathbb{R}$ ; evaluation point  $x \in \mathbb{T}^2$ .

**Output:** Value  $y = f_{\text{cl}}^{(t)}(x) \in \mathbb{R}$  of classical prediction function.

- 1: Form unitary evolution matrix  $\mathbf{U}^t \in \mathbb{C}^{(2d+1) \times (2d+1)} = \text{diag}([e^{i\omega_j t}]_{j \in \{0, \dots, 2d+1\}})$ .
  - 2: Compute column vector  $\boldsymbol{\zeta} = (\zeta_0(x), \dots, \zeta_{2d}(x))^\top$  of eigenfunction values.
  - 3: **return**  $y = (\mathbf{C}^\dagger \hat{\mathbf{f}})^\top \mathbf{U}^t \boldsymbol{\zeta}$ .
- 

---

**Algorithm 3** Quantum mechanical prediction using (63).

---

**Input:** Eigenfrequencies  $\boldsymbol{\omega} \in \mathbb{R}^{2d+1}$ , generalized eigenvectors  $\mathbf{C} \in \mathbb{C}^{m \times (2d+1)}$ , and eigenfunctions  $\{\zeta_0, \dots, \zeta_{2d} \in \mathcal{H}_\tau\}$  from Algorithm 1; sharpness parameter  $\kappa_{\text{eval}} > 0$  for quantum feature map; values  $\mathbf{f} = (\tilde{f}(x_0^{(l)}), \dots, \tilde{f}(x_{l^2-1}^{(l)})) \in \mathbb{C}^{l^2}$  of prediction observable on  $l \times l$  grid on  $\mathbb{T}^2$ ; evolution time  $t \in \mathbb{R}$ ; evaluation point  $x \in \mathbb{T}^2$ .

**Output:** Value  $y = f_{\text{qm}}^{(t)}(x) \in \mathbb{R}$  of quantum mechanical prediction function.

- 1: Form unitary evolution matrix  $\mathbf{U}^t \in \mathbb{C}^{(2d+1) \times (2d+1)} = \text{diag}([e^{i\omega_j t}]_{j \in \{0, \dots, 2d+1\}})$ .
  - 2: Form matrix  $\mathbf{Z} \in \mathbb{C}^{l^2 \times (2d+1)} = [Z_{ij}]$  of eigenfunction values, where  $Z_{ij} = \zeta_j(x_i^{(l)})$ .
  - 3: Compute column vector  $\boldsymbol{\xi}_{t,x} \in \mathbb{C}^{l^2} = \mathbf{Z} \mathbf{U}^{t\dagger} \mathbf{C}^\dagger \hat{\mathbf{F}}_{\kappa_{\text{eval}}}(x)$  using  $\hat{\mathbf{F}}_{\kappa_{\text{eval}}}$  from Section 7.3.3.
  - 4: Return  $y = \boldsymbol{\xi}_{t,x}^\dagger \mathbf{M} \boldsymbol{\xi}_{t,x} / \boldsymbol{\xi}_{t,x}^\dagger \boldsymbol{\xi}_{t,x}$ .
- 

---

**Algorithm 4** Fock space prediction using (65).

---

**Input:** Eigenfrequencies  $\boldsymbol{\omega} \in \mathbb{R}^{2d+1}$ , generalized eigenvectors  $\mathbf{C} \in \mathbb{C}^{m \times (2d+1)}$ , and eigenfunctions  $\{\zeta_0, \dots, \zeta_{2d} \in \mathcal{H}_\tau\}$  from Algorithm 1; Fock space grading  $n \in \mathbb{N}$ ; sharpness parameter  $\kappa_{\text{eval}} > 0$  for quantum feature map; values  $\mathbf{f} = (\tilde{f}(x_0^{(l)}), \dots, \tilde{f}(x_{l^2-1}^{(l)})) \in \mathbb{C}^{l^2}$  of prediction observable on  $l \times l$  grid on  $\mathbb{T}^2$ ; evolution time  $t \in \mathbb{R}$ ; evaluation point  $x \in \mathbb{T}^2$ .

**Output:** Value  $y = f_{\text{qm}}^{(t)}(x) \in \mathbb{R}$  of Fock space prediction function.

- 1: Form unitary evolution matrix  $\mathbf{U}^t \in \mathbb{C}^{(2d+1) \times (2d+1)} = \text{diag}([e^{i\omega_j t}]_{j \in \{0, \dots, 2d+1\}})$ .
  - 2: Form matrix  $\mathbf{Z} \in \mathbb{C}^{l^2 \times (2d+1)} = [Z_{ij}]$  of eigenfunction values, where  $Z_{ij} = \zeta_j(x_i^{(l)})$ .
  - 3: Compute column vector  $\boldsymbol{\xi}_{n,t,x} \in \mathbb{C}^{l^2} = \mathbf{Z} \mathbf{U}^{t\dagger} \mathbf{C}^\dagger \hat{\mathbf{F}}_{\kappa_{\text{eval}},n}(x)$  using  $\hat{\mathbf{F}}_{\kappa_{\text{eval}},n}$  from Section 7.3.4.
  - 4: Return  $y = \boldsymbol{\xi}_{n,t,x}^\dagger \mathbf{M} \boldsymbol{\xi}_{n,t,x} / \boldsymbol{\xi}_{n,t,x}^\dagger \boldsymbol{\xi}_{n,t,x}$ .
-



- [4] T. Eisner, B. Farkas, M. Haase, R. Nagel, *Operator Theoretic Aspects of Ergodic Theory*, Vol. 272 of Graduate Texts in Mathematics, Springer, Cham, 2015.
- [5] G. Froyland, Computer-assisted bounds for the rate of decay of correlations, *Commun. Math. Phys.* 189 (NN) (1997) 237–257. doi:10.1007/s002200050198.
- [6] M. Dellnitz, O. Junge, On the approximation of complicated dynamical behavior, *SIAM J. Numer. Anal.* 36 (1999) 491. doi:10.1137/S0036142996313002.
- [7] I. Mezić, A. Banaszuk, Comparison of systems with complex behavior: Spectral methods, in: *Proceedings of the 39th IEEE Conference on Decision and Control*, IEEE, Sydney, Australia, 1999, pp. 1224–1231. doi:10.1109/CDC.2000.912022.
- [8] M. Dellnitz, G. Froyland, O. Junge, The algorithms behind GAIO – set oriented numerical methods for dynamical systems, in: B. Fiedler (Ed.), *Ergodic Theory, Analysis, and Efficient Simulation of Dynamical Systems*, Springer, Berlin, Heidelberg, 2001, pp. 145–174. doi:10.1007/978-3-642-56589-2\_7.
- [9] I. Mezić, Spectral properties of dynamical systems, model reduction and decompositions, *Nonlinear Dyn.* 41 (2005) 309–325. doi:10.1007/s11071-005-2824-x.
- [10] S. L. Brunton, M. Budisić, E. Kaiser, J. N. Kutz, Modern Koopman theory for dynamical systems, *SIAM Rev.* 64 (2) (2022) 229–340. doi:10.1137/21M1401243.
- [11] A. Mauroy, I. Mezić, Y. Susuki (Eds.), *The Koopman Operator in Systems and Control*, no. 484 in *Lecture Notes in Control and Information Sciences*, Springer, 2020. doi:10.1007/978-3-030-35713-9.
- [12] S. E. Otto, C. W. Rowley, Koopman operators for estimation and control of dynamical systems, *Annu. Rev. Control Robot. Auton. Syst.* 4 (2021) 59–87. doi:10.1146/annurev-control-071020-010108.
- [13] M. Colbrook, The multiverse of dynamic mode decomposition algorithms, in: *Handbook of Numerical Analysis*, Amsterdam, 2024, p. 88.
- [14] P. J. Schmid, J. L. Sesterhenn, Dynamic mode decomposition of numerical and experimental data, in: *Bull. Amer. Phys. Soc.*, 61st APS meeting, San Antonio, 2008, p. 208.
- [15] P. J. Schmid, Dynamic mode decomposition of numerical and experimental data, *J. Fluid Mech.* 656 (2010) 5–28. doi:10.1017/S0022112010001217.
- [16] C. W. Rowley, I. Mezić, S. Bagheri, P. Schlatter, D. S. Henningson, Spectral analysis of nonlinear flows, *J. Fluid Mech.* 641 (2009) 115–127. doi:10.1017/s0022112009992059.
- [17] M. O. Williams, I. G. Kevrekidis, C. W. Rowley, A data-driven approximation of the Koopman operator: Extending dynamic mode decomposition, *J. Nonlinear Sci.* 25 (6) (2015) 1307–1346. doi:10.1007/s00332-015-9258-5.
- [18] C. Penland, Random forcing and forecasting using principal oscillation pattern analysis, *Mon. Weather Rev.* 117 (10) (1989) 2165–2185.
- [19] H. Arbabi, I. Mezić, Ergodic theory, dynamic mode decomposition and computation of spectral properties of the Koopman operator, *SIAM J. Appl. Dyn. Syst.* 16 (4) (2017) 2096–2126. doi:10.1137/17M1125236.
- [20] S. L. Brunton, B. W. Brunton, J. L. Proctor, E. Kaiser, J. N. Kutz, Chaos as an intermittently forced linear system, *Nat. Commun.* 8 (2017). doi:10.1038/s41467-017-00030-8.
- [21] S. Das, D. Giannakis, Delay-coordinate maps and the spectra of Koopman operators, *J. Stat. Phys.* 175 (6) (2019) 1107–1145. doi:10.1007/s10955-019-02272-w.
- [22] C. R. Constante-Amores, A. J. Linot, M. D. Graham, Enhancing predictive capabilities in data-driven dynamical modeling with automatic differentiation: Koopman and neural ODE approaches, *Chaos* 34 (2024). doi:10.1063/5.0180415.
- [23] Y. Susuki, A. Mauroy, I. Mezić, Koopman resolvent: A Laplace-domain analysis of nonlinear autonomous dynamical systems, *SIAM J. Appl. Dyn. Syst.* 20 (4) (2021) 2013–2036. doi:10.1137/20M1335935.
- [24] M. J. Colbrook, The mpEDMD algorithm for data-driven computations of measure-preserving dynamical systems, *SIAM J. Numer. Anal.* 61 (3) (2023) 1585–1608. doi:10.1137/22M1521407.
- [25] P. J. Badoo, B. Herrmann, B. J. McKeon, J. N. Kutz, S. L. Brunton, Physics-informed dynamic mode decomposition, *Proc. R. Soc. A* 479 (2023). doi:10.1098/rspa.2022.0576.
- [26] G. Froyland, O. Junge, P. Koltai, Estimating long-term behavior of flows without trajectory integration: The infinitesimal generator approach, *SIAM J. Numer. Anal.* 51 (1) (2013) 223–247. doi:10.1137/110819986.
- [27] T. Berry, D. Giannakis, J. Harlim, Nonparametric forecasting of low-dimensional dynamical systems, *Phys. Rev. E* 91 (2015). doi:10.1103/PhysRevE.91.032915.
- [28] D. Giannakis, J. Slawinska, Z. Zhao, Spatiotemporal feature extraction with data-driven Koopman operators, in: D. Storcheus, A. Rostamizadeh, S. Kumar (Eds.), *Proceedings of the 1st International Workshop on Feature Extraction: Modern Questions and Challenges at NIPS 2015*, Vol. 44 of *Proceedings of Machine Learning Research*, PMLR, Montreal, Canada, 2015, pp. 103–115.  
URL <https://proceedings.mlr.press/v44/giannakis15.html>
- [29] D. Giannakis, Data-driven spectral decomposition and forecasting of ergodic dynamical systems, *Appl. Comput. Harmon. Anal.* 47 (2) (2019) 338–396. doi:10.1016/j.acha.2017.09.001.
- [30] D. Giannakis, C. Valva, Consistent spectral approximation of Koopman operators using resolvent compactification, *Nonlinearity* 37 (7) (2024). doi:10.1088/1361-6544/ad4ade.
- [31] D. Giannakis, C. Valva, Differentiable programming for spectral approximation of Koopman operators, in preparation (2024).
- [32] J. A. Rosenfeld, R. Kamalapurkar, B. Russo, T. T. Johnson, Occupation kernels and densely defined Liouville operators for system identification, in: *2019 IEEE 58th Conference on Decision and Control (CDC)*, 2019, pp. 6455–6460. doi:10.1109/CDC40024.2019.9029337.
- [33] J. A. Rosenfeld, R. Kamalapurkar, L. F. Gruss, T. T. Johnson, Dynamic mode decomposition for continuous time systems

- with the Liouville operator, *J. Nonlinear Sci.* 32 (2022). doi:10.1007/s00332-021-09746-w.
- [34] Y. Kawahara, Dynamic mode decomposition with reproducing kernels for Koopman spectral analysis, in: D. D. Lee, M. Sugiyama, U. von Luxburg, I. Guyon, R. Garnett (Eds.), *Advances in Neural Information Processing Systems*, Curran Associates, 2016, pp. 911–919. URL <http://papers.nips.cc/paper/6583-dynamic-mode-decomposition-with-reproducing-kernels-for-koopman-spectral-analysis.pdf>
- [35] S. Das, D. Giannakis, J. Slawinska, Reproducing kernel Hilbert space compactification of unitary evolution groups, *Appl. Comput. Harmon. Anal.* 54 (2021) 75–136. doi:10.1016/j.acha.2021.02.004.
- [36] S. Klus, F. Nüske, S. Peitz, J.-H. Niemann, C. Clementi, C. Schütte, Data-driven approximation of the Koopman generator: Model reduction, system identification, and control, *Phys. D* 406 (2020). doi:10.1016/j.physd.2020.132416.
- [37] V. R. Kostic, P. Novelli, A. Mauer, C. Ciliberto, L. Rosasco, M. Pontil, Learning dynamical systems with Koopman operator regression in reproducing kernel Hilbert spaces, in: S. Koyejo, S. Mohamed, A. Agarwal, D. Belgrave, K. Cho, A. Oh (Eds.), *Advances in Neural Information Processing Systems 35 (NeurIPS 2022)*, 2022, pp. 4017–4031.
- [38] M. Ikeda, I. Ishikawa, C. Schlosser, Koopman and Perron–Frobenius operators on reproducing kernel Banach spaces, *Chaos* 32 (2022). doi:10.1063/5.0094889.
- [39] M. Korda, M. Putinar, I. Mezić, Data-driven spectral analysis of the Koopman operator, *Appl. Comput. Harmon. Anal.* 48 (2) (2020) 599–629. doi:10.1016/j.acha.2018.08.002.
- [40] N. Govindarajan, R. Mohr, S. Chandrasekaran, I. Mezić, On the approximation of Koopman spectra of measure-preserving flows, *SIAM J. Appl. Dyn. Syst.* 20 (1) (2021) 232–261. doi:10.1137/19M1282908.
- [41] M. J. Colbrook, A. Townsend, Rigorous data-driven computation of spectral properties of Koopman operators for dynamical systems, *Commun. Pure Appl. Math.* 77 (2024) 221–283. doi:10.1002/cpa.22125.
- [42] G. Froyland, An analytic framework for identifying finite-time coherent sets in time-dependent dynamical systems, *Phys. D* 250 (2013) 1–19. doi:10.1016/j.physd.2013.01.013.
- [43] G. Froyland, K. Padberg, Almost-invariant sets and invariant manifolds – Connecting probabilistic and geometric descriptions of coherent structures in flows, *Phys. D* 238 (2009) 1507–1523. doi:10.1016/j.physd.2009.03.002.
- [44] C. González-Tokman, A. Quas, A semi-invertible operator Oseledec’s theorem, *Ergod. Theory Dyn. Syst.* 34 (4) (2014) 1230–1272. doi:10.1017/etds.2012.189.
- [45] G. Froyland, Dynamic isoperimetry and the geometry of Lagrangian coherent structures, *Nonlinearity* (2015) 3587–3622. doi:10.1088/0951-7715/28/10/3587.
- [46] G. Froyland, P. Koltai, Detecting the birth and death of finite-time coherent sets, *Commun. Pure Appl. Math.* (2023). doi:10.1002/cpa.22115.
- [47] G. Benenti, G. Casati, S. Montangero, D. L. Shepelyansky, Efficient quantum computing of complex dynamics, *Phys. Rev. Lett.* 87 (2001) 227901. doi:10.1103/PhysRevLett.87.227901.
- [48] B. Kacewicz, Almost optimal solution of initial-value problems by randomized and quantum algorithms, *J. Complex.* 22 (2006) 676–690. doi:10.1016/j.jco.2006.03.001.
- [49] S. K. Leyton, T. J. Osborne, A quantum algorithm to solve nonlinear differential equations (2008). arXiv:0812.4423. URL <https://arxiv.org/abs/0812.4423>
- [50] D. W. Berry, A. M. Childs, A. Ostrander, G. Wang, Quantum algorithm for linear differential equations with exponentially improved dependence on precision, *Commun. Math. Phys.* 356 (2017) 1057–1081. doi:10.1007/s00220-017-3002-y.
- [51] T. J. Elliott, M. Gu, Superior memory efficiency of quantum devices for the simulation of continuous-time stochastic processes, *npj Quantum Inf.* 4 (2018) 18. doi:10.1038/s41534-018-0064-4.
- [52] I. Joseph, Koopman-von Neumann approach to quantum simulation of nonlinear classical dynamics, *Phys. Rev. Research* 2 (2020) 043102. doi:10.1103/PhysRevResearch.2.043102.
- [53] S. Lloyd, G. DePalma, C. Gokler, B. Kiani, Z.-W. Liu, M. Marvian, F. Tennie, T. Palmer, Quantum algorithm for nonlinear differential equations (2020). URL <https://arxiv.org/pdf/2011.06571.pdf>
- [54] O. Kyriienko, A. E. Paine, V. E. Elfving, Solving nonlinear differential equations with differentiable quantum circuits, *Phys. Rev. A* 103 (2021). doi:10.1103/PhysRevA.103.052416.
- [55] A. Kalev, I. Hen, Quantum algorithm for simulating Hamiltonian dynamics with an off-diagonal series expansion, *Quantum* 5 (2021) 426–449. doi:10.22331/q-2021-04-08-426.
- [56] D. Giannakis, A. Ourmazd, P. Pfeffer, J. Schumacher, J. Slawinska, Embedding classical dynamics in a quantum computer, *Phys. Rev. A* 105 (2022). doi:10.1103/PhysRevA.105.052404.
- [57] A. Mezzacapo, M. Sanz, L. Lamata, I. Egusquiza, S. Succi, E. Solano, Quantum simulator for transport phenomena in fluid flows, *Sci. Rep.* 5 (2015) 13153. doi:10.1038/srep13153.
- [58] P. C. S. Costa, S. Jorran, A. Ostrander, Quantum algorithm for simulating the wave equation, *Phys. Rev. A* 99 (2019). doi:10.1103/PhysRevA.99.012323.
- [59] A. Engel, G. Smith, S. E. Parker, Quantum algorithm for the Vlasov equation, *Phys. Rev. A* 100 (2019). doi:10.1103/PhysRevA.100.062315.
- [60] S. Bharadwaj, K. R. Sreenivasan, Quantum computation of fluid dynamics, *Indian Acad. Sci. Conf. Ser.* 3 (1) (2020) 77–96. doi:10.29195/iascs.03.01.0015.
- [61] F. Gaitan, Finding flows of a Navier–Stokes fluid through quantum computing, *npj Quantum Inf.* 6 (2020) 61. doi:10.1038/s41534-020-00291-0.
- [62] I. Y. Dodi, E. A. Startsev, On applications of quantum computing to plasma simulations, *Phys. Plasmas* 28 (2021). doi:10.1063/5.0056974.
- [63] P. Pfeffer, F. Heyder, J. Schumacher, Hybrid quantum-classical reservoir computing of thermal convection flow, *Phys.*

- Rev. Research 4 (2022). doi:10.1103/PhysRevResearch.4.033176.
- [64] P. Pfeffer, F. Heyder, J. Schumacher, Reduced-order modeling of two-dimensional turbulent Rayleigh-Bénard flow by hybrid quantum-classical reservoir computing, *Phys. Rev. Research* 5 (2023). doi:10.1103/PhysRevResearch.5.043242.
- [65] I. Joseph, Y. Shi, M. D. Porter, A. R. Castelli, V. I. Geyko, F. R. Graziani, S. B. Libby, J. L. DuBois, Quantum computing for fusion energy science applications, *Phys. Plasmas* 30 (1) (2023). doi:10.1063/5.0123765.
- [66] S. Bharadwaj, K. R. Sreenivasan, Hybrid algorithms for flow problems, *Proc. Natl. Acad. Sci.* 120 (49) (2023) e2311014120. doi:10.1073/pnas.2311014120.
- [67] F. Tennie, T. N. Palmer, Quantum computers for weather and climate prediction, *Bull. Amer. Math. Soc.* 104 (2) (2023) E488–E500. doi:10.1175/BAMS-D-22-0031.1.
- [68] D. Giannakis, Quantum mechanics and data assimilation, *Phys. Rev. E* 100 (2019). doi:10.1103/PhysRevE.100.032207.
- [69] D. C. Freeman, D. Giannakis, B. Mintz, A. Ourmazd, J. Slawinska, Data assimilation in operator algebras, *Proc. Natl. Acad. Sci.* 120 (8) (2023). doi:10.1073/pnas.2211115120.
- [70] D. C. Freeman, D. Giannakis, J. Slawinska, Quantum mechanics for closure of dynamical systems, *Multiscale Model. Simul.* 22 (1) (2024) 283–333. doi:10.1137/22M1514246.
- [71] R. Orús, Tensor networks for complex quantum systems, *Nat. Rev. Phys.* 1 (2019) 538–550. doi:10.1038/s42254-019-0086-7.
- [72] M. C. Bañuls, Tensor network algorithms: A route map, *Annu. Rev. Condens. Matter Phys.* 14 (2023) 173–91. doi:10.1146/annurev-conmatphys040721-022705.
- [73] R. J. Baxter, Dimers on a rectangular lattice, *J. Math. Phys.* 9 (4) (1968) 650–654. doi:10.1063/1.1664623.
- [74] I. Affleck, T. Kennedy, E. H. Lieb, H. Tasaki, Rigorous results on valence-bond ground states in antiferromagnets, *Phys. Rev. Lett.* 59 (7) (1987) 799–802. doi:10.1103/PhysRevLett.59.799.
- [75] A. Klümper, A. Schadschneider, J. Zittartz, Matrix product ground states for one-dimensional spin-1 quantum antiferromagnets, *Europhys. Lett.* 24 (4) (1993) 293–297. doi:10.1209/0295-5075/24/4/010.
- [76] E. M. Stoudenmire, D. J. Schwab, Supervised learning with tensor networks, in: D. Lee, M. Sugiyama, U. Luxburg, I. Guyon, R. Garnett (Eds.), *Advances in Neural Information Processing Systems* 30 (NeurIPS 2016), 2016, pp. 1–9.
- [77] Z.-Y. Han, J. Wang, H. Fan, L. Wang, P. Zhang, Unsupervised generative modeling using matrix product states, *Phys. Rev. X* 8 (031012) (2018). doi:10.1103/PhysRevX.8.031012.
- [78] S. Das, D. Giannakis, On harmonic Hilbert spaces on compact abelian groups, *J. Fourier Anal. Appl.* 29 (1) (2023) 12. doi:10.1007/s00041-023-09992-4.
- [79] S. Das, D. Giannakis, M. Montgomery, Correction to: On harmonic Hilbert spaces on compact abelian groups, *J. Fourier Anal. Appl.* 29 (6) (2023) 67. doi:10.1007/s00041-023-10043-1.
- [80] D. Giannakis, M. Montgomery, An algebra structure for reproducing kernel Hilbert spaces (2024). arXiv:\protect\vrulewidthOpt\protect\href{http://arxiv.org/abs/2401.01295}{arXiv:2401.01295}.
- [81] D. Lehmann, *Mathematical Methods of Many-Body Quantum Field Theory*, Vol. 436 of *Research Notes in Mathematics*, Chapman & Hall/CRC, Boca Raton, 2004.
- [82] J. C. Oxtoby, Stepanoff flows on the torus, *Proc. Amer. Math. Soc.* 4 (1953) 982–987.
- [83] G. Froyland, D. Giannakis, B. Lintner, M. Pike, J. Slawinska, Spectral analysis of climate dynamics with operator-theoretic approaches, *Nat. Commun.* 12 (2021). doi:10.1038/s41467-021-26357-x.
- [84] C. Schütte, W. Huisinga, P. Deuffhard, Transfer operator approach to conformational dynamics in biomolecular systems, in: B. Fiedler (Ed.), *Ergodic Theory, Analysis, and Efficient Simulation of Dynamical Systems*, Springer-Verlag, Berlin, 2001, pp. 191–223. doi:10.1007/978-3-642-56589-2\_9.
- [85] I. Mezić, Analysis of fluid flows via spectral properties of the Koopman operator, *Annu. Rev. Fluid Mech.* 45 (2013) 357–378. doi:10.1146/annurev-fluid-011212-140652.
- [86] B. W. Brunton, L. A. Johnson, J. G. Ojemann, J. N. Kutz, Extracting spatial-temporal coherent patterns in large-scale neural recordings using dynamic mode decomposition, *J. Neurosci. Methods* 258 (2016) 1–15. doi:10.1016/j.jneumeth.2015.10.010.
- [87] N. Marrouch, J. Slawinska, D. Giannakis, H. L. Read, Data-driven Koopman operator approach for computational neuroscience, *Ann. Math. Artif. Intel.* 88 (2019) 1155–1173. doi:10.1007/s10472-019-09666-2.
- [88] Y. Susuki, I. Mezić, F. Raak, T. Hikihara, Applied Koopman operator theory for power systems technology, *NOLTA* 7 (4) (2016) 430–459. doi:10.1587/nolta.7.430.
- [89] P. Koltai, P. Kunde, A Koopman-Takens theorem: Linear least squares prediction of nonlinear time series (2023). URL <https://arxiv.org/abs/2308.02175>
- [90] P. R. Halmos, *Lectures on Ergodic Theory*, American Mathematical Society, Providence, 1956.
- [91] M. Dellnitz, G. Froyland, S. Sertl, On the isolated spectrum of the Perron-Frobenius operator, *Nonlinearity* 13 (2000) 1171–1188. doi:10.1088/0951-7715/13/4/310.
- [92] C. Blank, D. K. Park, J.-K. K. Rhee, F. Petruccione, Quantum classifier with tailored quantum kernel, *npj Quantum Inf.* 6 (2020) 41. doi:10.1038/s41534-020-0272-6.
- [93] F. Cucker, S. Smale, On the mathematical foundations of learning, *Bull. Amer. Math. Soc.* 39 (1) (2001) 1–49. doi:10.1090/S0273-0979-01-00923-5.
- [94] O. Junge, D. Matthes, B. Schmitzer, Entropic transfer operators (2022). URL <https://arxiv.org/abs/2204.04901>
- [95] D. Giannakis, Delay-coordinate maps, coherence, and approximate spectra of evolution operators, *Res. Math. Sci.* 8 (2021). doi:10.1007/s40687-020-00239-y.
- [96] A. F. M. ter Elst, M. Lemańczyk, On one-parameter Koopman groups, *Ergodic Theory Dyn. Syst.* 37 (2017) 1635–1656. doi:10.1017/etds.2015.111.

- [97] N. Boullé, M. Colbrook, Multiplicative Dynamic Mode Decomposition (2024). URL <https://arxiv.org/pdf/2405.05334>
- [98] S. M. Ulam, Problems in Modern Mathematics, Dover Publications, Mineola, 1964.
- [99] T.-Y. Li, Finite approximation for the Frobenius–Perron operator. a solution to Ulam’s conjecture, *J. Approx. Theory* 17 (2) (1976) 177–186. doi:10.1016/0021-9045(76)90037-X.
- [100] G. Froyland, Ulam’s method for random interval maps, *Nonlinearity* 12 (4) (1999) 1029–1052. doi:10.1088/0951-7715/12/4/318.
- [101] O. Junge, P. Koltai, Discretization of the Frobenius–Perron operator using a sparse Haar tensor basis: The sparse Ulam method, *SIAM J. Numer. Anal.* 47 (2009) 3464–2485. doi:10.1137/080716864.
- [102] M. Takesaki, Theory of Operator Algebras I, Vol. 124 of Encyclopaedia of Mathematical Sciences, Springer, Berlin, 2001.
- [103] D. Mauro, On Koopman–von Neumann waves, *Int. J. Mod. Phys. A* 17 (2002) 1301–1325. doi:10.1142/S0217751X02009680.
- [104] G. Della Riccia, N. Wiener, Wave mechanics in classical phase space, Brownian motion, and quantum theory, *J. Math. Phys.* 7 (8) (1966) 1732–1383. doi:10.1063/1.1705047.
- [105] J. Wilkie, P. Brumer, Quantum-classical correspondence via Liouville dynamics. I. Integrable systems and chaotic spectral decomposition, *Phys. Rev. A* 55 (1) (1997) 27–42. doi:10.1103/PhysRevA.55.27.
- [106] J. Wilkie, P. Brumer, Quantum-classical correspondence via Liouville dynamics. II. Correspondence for chaotic Hamiltonian systems, *Phys. Rev. A* 55 (1) (1997) 43–61. doi:10.1103/PhysRevA.55.43.
- [107] D. I. Bondar, F. Gay-Balmaz, C. Tronci, Koopman wavefunctions and classical–quantum correlation dynamics, *Proc. Roy. Soc. A* 475 (2019) 20180879. doi:10.1098/rspa.2018.0879.
- [108] I. McCulloch, From density-matrix renormalization group to matrix product states, *J. Stat. Mech.* 2007 (2007). doi:10.1088/1742-5468/2007/10/P10014.
- [109] N. Nakatani, G. K.-L. Chan, Efficient tree tensor network states (TTNS) for quantum chemistry: Generalizations of the density matrix renormalization group algorithm, *J. Chem. Phys.* 138 (2013). doi:10.1063/1.4798639.
- [110] V. I. Paulsen, M. Raghupathi, An Introduction to the Theory of Reproducing Kernel Hilbert Spaces, Vol. 152 of Cambridge Studies in Advanced Mathematics, Cambridge University Press, Cambridge, 2016.
- [111] I. Steinwart, A. Christmann, Support Vector Machines, Information Science and Statistics, Springer, New York, 2008.
- [112] W. Rudin, Fourier Analysis on Groups, Dover Publications, Mineola, 2017. doi:10.1002/9781118165621.
- [113] B. K. Sriperumbudur, K. Fukumizu, G. R. Lanckriet, Universality, characteristic kernels and RKHS embedding of measures, *J. Mach. Learn. Res.* 12 (2011) 2389–2410.
- [114] H. G. Feichtinger, Gewichtsfunktionen auf lokalkompakten Gruppen, Österreich. Akad. Wiss. Math.-Natur. Kl. Sitzungsber. II 188 (8–10) (1979) 451–471.
- [115] K. Gröchenig, Weight functions in time-frequency analysis, in: L. Rodino, et al. (Eds.), Pseudodifferential Operators: Partial Differential Equations and Time-Frequency Analysis, Vol. 52 of Fields Inst. Commun., American Mathematical Society, Providence, 2007, pp. 343–366.
- [116] E. Kaniuth, A Course in Commutative Banach Algebras, Vol. 246 of Graduate Texts in Mathematics, Springer Science+Media, 2009.
- [117] F. Chatelin, Spectral Approximation of Linear Operators, Classics in Applied Mathematics, Society for Industrial and Applied Mathematics, Philadelphia, 2011.
- [118] C. R. de Oliveira, Intermediate Spectral Theory and Quantum Dynamics, Vol. 54 of Progress in Mathematical Physics, Birkhäuser, Basel, 2009.
- [119] M. Blank, Egodic averaging with and without invariant measures, *Nonlinearity* 30 (2017) 4649–4664. doi:10.1088/1361-6544/aa8fe8.
- [120] M. Abramowitz, I. A. Stegun, Handbook of Mathematical Functions, United States Department of Commerce, National Bureau of Standards, 1964.
- [121] S.-J. Ran, Encoding of matrix product states into quantum circuits of one- and two-qubit gates, *Phys. Rev. A* 101 (2020). doi:10.1103/PhysRevA.101.032310.
- [122] J. Bradbury, R. Frostig, P. Hawkins, M. J. Johnson, C. Leary, D. Maclaurin, G. Necula, A. Paszke, J. VanderPlas, S. Wanderman-Milne, Q. Zhang, JAX: Composable transformations of Python+NumPy programs (2018). URL <http://github.com/google/jax>
- [123] P. Kidger, On Neural Differential Equations, Ph.D. thesis, University of Oxford (2021).